AUTOMATED PROCESSOR FOR OPTIMIZING TRACTOR OPERATION

PETER WILLIAM LIVERSEDGE LYNE

Submitted in partial fulfilment of the
requirements for the degree of Ph.D.

Department of Agricultural Engineering

University of Natal

1991

ABSTRACT

The agricultural tractor is designed as a general purpose machine and consequently, does not perform all its tasks at maximum efficiency. Various methods of increasing the field performance of these vehicles have been studied.

Traction is one of the main factors limiting the field performance of the modern tractor. The process of developing traction has therefore been investigated by many researchers and although this study has resulted in a better understanding of the mechanics, it has not to any great extent assisted the operator to optimize performance in the field.

It was concluded that in order to solve the problem the operator required a control system to maintain the dynamic load and inflation pressure at optimum levels. Work was carried out to develop and evaluate such a system using the Single Wheel Traction Research Vehicle at the USDA's National Soil Dynamics Laboratory in Auburn, Alabama, USA.

A computer management system was developed to control the dynamic load, net traction and inflation pressure of the test tyre. During a simulated field operation the system was programmed to cycle the tyre over its operating range of dynamic load and inflation pressure while monitoring tractive efficiency. A tractive efficiency response surface was

computed for the particular condition and the surface searched for the dynamic load and inflation pressure levels which resulted in maximum tractive efficiency. The tyre was then controlled and operated at maximum tractive efficiency.

Evaluation showed that within the operating range of the tyre, tractive efficiency varied considerably with dynamic load, inflation pressure, net traction and soil condition. The results indicated that a considerable advantage could be obtained by using such an arrangement on a tractor. The system would automatically maximize the tractive efficiency of the tractor under the particular field conditions and with the particular implement being used.

Implements could be ballasted and the hitch system used to control the weight transfer to ensure maximum tractive efficiency. Systems such as these would result in a significant improvement in the field performance of the machine and a reduction in management time required to optimize the performance of the tractor implement combination.

I wish to certify that the work reported in this thesis is my own original and unaided work except where specific acknowledgement is made. In addition I wish to declare that this thesis has not been submitted for a degree in any other university.

Signed : .....

P.W.L. LYNE

Acknowledgements

The author wishes to record his sincere appreciation for the assistance given by the following:

Professor P. Meiring, Head of the Department of Agricultural Engineering, University of Natal, for his supervision of the work and his encouragement and support during the project.

Dr E.C. Burt, Agricultural Engineer, National Soil Dynamics Laboratory, Auburn, Alabama, USA, for his considerable advice and assistance during the project.

Dr A. C. Bailey and Mr J. D. Jarrell for their assistance during the development of the computer control system.

Dr A C Hansen for his valuable advice and support during the preparation of the document.

The National Soil Dynamics Laboratory, Auburn, Alabama, USA, for the use of their facilities and the Single Wheel Traction Research Vehicle.

Miss J. Whyte and Miss D. Grantham for their assistance in preparing the document.

My wife, Sandra, and children Bruce, Debra and Mark for their understanding, encouragement and patience during this period of study.

TABLE OF CONTENTS

TABLE OF CONTENTS (continued)

LIST OF TABLES

LIST OF FIGURES

1 INTRODUCTION

The agricultural tractor is designed as a general purpose machine and as such is not ideally suited to the execution of all its tasks which include high-speed low-draft operations, low-speed high-draft operations and operations where a significant portion of the power is transmitted through the PTO. The result is a machine which is reasonably efficient for most tasks and inefficient for others. In the past this compromise has been a cost effective solution for the prime mover on the farm, however, steadily increasing costs and lower profit margins have demanded that every effort be made to maximize efficiency under all conditions. Some researchers such as Göhlich (1984) question whether the general purpose nature of the tractor will be applicable in the future and believe that moves should be made towards special purpose vehicles. Others, however, have studied various methods of increasing the field performance and optimizing the efficiency of the standard agricultural tractor.

The overall objective of this research was to identify the most effective route for optimizing the efficiency of tractor operation under a wide range of operating conditions and to develop an appropriate control system to achieve optimum efficiency.

The modern two-wheel drive tractor has a high power to weight ratio and because of traction limitations it is difficult to utilize the available engine power during low speed operations. The inefficient use of engine power has been investigated by a number of researchers and a wide variety of solutions have been put forward (Meiring and Rall, 1979, Lyne, Jacobs and Meiring, 1980, Schrock, Matteson and Thompson, 1982, Jahns, 1983, Grogan, Morris, Searcy, Wiedemann and Stout, 1984, Lyne, Bremner, Hansen, and Meiring, 1988, and Wang and Zoerb, 1988). The work has resulted in various types of indicators being used to assist the operator of a tractor in selecting the appropriate gear ratio and engine speed to ensure reasonable engine loading and a high engine operating efficiency.

Once a high level of engine power is being utilized the second problem that arises is the transmission of the power to the drawbar of the tractor via the traction developed by the drive wheels. High draft is usually achieved with high wheel slip and low efficiency. The constraints related to traction have been investigated by many researchers and an effort has been made to gain a better understanding of traction mechanics, to enable increases in tractive efficiency to be achieved.

Despite the many studies carried out the complexities of traction are such that it is still not fully understood by researchers. Tractive efficiency is a function of a number

of variables including tyre characteristics, soil characteristics, axle load, axle power and net traction requirements. It is thus inevitable that a tractor operator will not be able to achieve a high tractive efficiency in the field with a standard tractor.

Three approaches to solving the traction problem have been adopted in the past. The first has involved the fundamental approach using classical soil mechanics but, the inability to quantify all the parameters has made it impossible to provide rigorous mathematical solutions for traction theory and this is likely to remain the case for the foreseeable future.

The second approach has involved the use of empirical methods to model traction. Various models have been developed by researchers, notably Wismer and Luth (1972), Gee-Clough, McAllister, Pearson and Evernden (1978), Dwyer (1985), Brixius (1987), and Zoz (1987), to assist in the prediction of traction parameters. Although these models have contributed to the understanding of traction mechanics they have proved impractical for the operator to use mainly because of the difficulty in defining soil conditions.

The third approach is the use of the finite element method and this is the most likely method to provide a rigorous solution. Although finite element analysis is an invaluable tool for the designer it is of little assistance to the operator who is unable to quantify his operating parameters.

A solution to the operator's problem requires operator feedback and a control system to maximize efficiency under operating conditions. In the past it was not feasible to measure tractive efficiency directly on a production tractor and wheel slip was used as an indicator of tractive efficiency. Wheel slip meters were developed (Lyne and Meiring, 1977), and today commercial units are available to aid the operator in achieving a high level of tractive efficiency. However, this was only a partial solution because the relationship between slip and tractive efficiency is dependent on soil and tyre behaviour, both of which are difficult to define.

With the availability of electronic draft control systems on commercial tractors and the ability to obtain a measure of the engine power being developed, the measurement of tractive efficiency becomes a viable alternative (Hansen, Meiring and North, 1978 and Lyne et al., 1988). Such an indicator would be a significant improvement on a wheel slip meter and would facilitate the variation of operating parameters to maximize the tractive efficiency.

In theory, an operator could thus optimize tractive efficiency by selecting the traction device, the drawbar load, the dynamic load on the drive wheels and the inflation pressure to ensure the desired efficiency. However, in practice because of the general purpose nature of the tractor and the variation in field conditions, the axle load and

inflation pressure are the only variables and even here there are severe limitations. Firstly axle load or dynamic load is made up of static load which is inconvenient to vary, and weight transfer, which is not easy to determine and varies with implement setting, implement condition, and soil type. Secondly, the inflation pressure is specified at a fixed level by the tractor manufacturer to insure that the tyre is not overloaded when operated at high drawbar pull.

Lyne, Burt and Meiring (1984) postulated that a control system should be developed to monitor tractive efficiency and maintain dynamic load and inflation pressure at optimum levels. Such a system would greatly ease the operators task and enable him to achieve and maintain high levels of tractive efficiency in the field. Czako (1974) examined the uses of central tyre inflation pressure systems on military vehicles, and concluded that these systems offered a definite increase in mobility with a relatively small increase in vehicle complexity. Della-Moretta and Hodges (1986) discussed the potential for use of central tyre inflation pressure systems on logging trucks for reducing maintenance costs of forest haul roads. Ashmore (1986) used a central tyre inflation pressure system on logging trucks in investigations of trafficability and road maintenance of logging roads. Also, hitches for tractors which control weight transfer have been investigated (Yavnai and Wolf, 1979). Therefore, it seems likely that reliable central tyre inflation pressure systems and automatically controlled

weight-transfer hitches can be developed which will permit the selection of the desired dynamic load and inflation pressure.

In this thesis the various models and methods for optimizing the traction of tractors are reviewed with the objective of determining the most effective method of optimizing tractive efficiency. The equipment and procedures to achieve real time control of dynamic load and inflation pressure, and hence to arrive at an optimum efficiency are described in detail. Finally an extensive evaluation of the optimization algorithm is presented. This evaluation involves the simulation of a range of field conditions including, soil type, net traction levels, inflation pressures and dynamic loads.

2 OPTIMIZING TRACTOR TRACTION

A tractor carries out a variety of field operations over a wide range of surface conditions while at the same time it must cause as little damage to the surface as possible and operate at minimum cost. High labour costs and increased work rate requirements have resulted in a gradual increase in the tractor's power to weight ratio. While work rates have increased, efficiency has decreased because of the difficulty of transmitting the extra engine power to the drawbar. Over 20 years ago Gill and Vanden Berg (1967) indicated that the engine power available was in excess of the traction capacity of the traction device and yet the trend has continued.

Dwyer (1982) stated that at the first European Conference of ISTVS, limitations on the design of Agricultural tractors and machines were discussed. It was agreed that one of the main limitations was the inability of these machines to carry out their primary function with maximum efficiency.

One solution to the problem has been the use of front wheel assist to transfer the extra power to the drive wheels. However, this solution is an expensive one and the more cost effective approach would be to use the two wheel drive (2WD) efficiently on tractors of less than 150kW.

To optimize traction a thorough understanding of the mechanics involved is required. An accurate prediction of tractive performance in its widest sense is the ultimate goal for the derivation of traction theories (Janosi, 1962; Gill and Vanden Berg, 1967). The primary objective of any traction theory is to predict firstly, the resultant force components of support and net traction, and secondly, the displacement components of forward velocity, sinkage and skid angle. These force and displacement components are produced by the traction device and limited by soil strength. (Janosi, 1962; Persson, 1969).

Attempts have been made to develop a rigorous traction theory, but the intricate nature of the soil-tyre interface has made this a demanding task which is yet to be accomplished. Consequently, much of the research has been directed towards empirical methods of predicting tractive performance. Although these techniques are not ideal they have provided useful information to the designer and user of traction equipment. They have enabled users to predict traction with a reasonable degree of accuracy and to establish the important parameters influencing tractive efficiency.

Research has been carried out in three main fields, namely agriculture which includes forestry, earth moving equipment and military vehicles. Although the fundamentals of the soil-tyre interface are common, the objectives in the various

fields differ. In crop production systems drawbar pull and tractive efficiency are the most important criteria where firstly, work rate (ha/h) and secondly specific fuel consumption (l/ha) are the two most important operating parameters in quantifying a tractor's performance. The objective of this research will be to improve the performance of a 2WD tractor by maximizing tractive efficiency.

2.1 Traction mechanics

Traction is defined by Gill and Vanden Berg (1967) as the force derived from the interaction between a device and a medium that can be used to facilitate a desired motion over the medium. In this case the traction device is the tractor drive wheel which transforms axle torque to net traction and drawbar pull.

The mechanics of a traction device deal with the interaction between the wheel and the terrain over which the vehicle operates (Yong, Fattah and Skiadas 1984). Even if all the necessary characteristics and properties of the wheel and the soil are known, it is still necessary to determine the relationships of the load on the wheel, the applied torque, the pull, the slip, the sinkage and the soil conditions.

Freitag (1985) states that to conduct an analysis of the machine soil interaction, firstly the soil's response to load

must be expressed, including any changes that result from the loading, secondly the shape, size and intensity of the loading must be described and lastly the desired output of the interaction must be identified. Yong et al. (1984) specified the tractive-soil parameters which control the tyres performance as those shown in Figure 1.

TYRES

- Geometrical configurations and dimension:
  cross-sectional shape, width, diameter and section height
- Structural parameters:
  number and direction of plies, mechanical properties of tyre material composite
- Thermal properties of tyre material composite
- Tread geometrical configurations, thickness, width, shape
- Inflation pressure
- Contact area on rigid surface
- Load deformation/distortion characteristics

SOIL-GROUND-SURFACE

- Flotation:
  Plate, cone and vane-cone penetration test, triaxial test
- Traction:
  Soil strength measured by cone penetrometer and various shear devices such as bevameter, triaxial apparatus, vane-cone rotation, shear plate both rectangular and annular
- Surface cover:
  Vegetation, barren, wetness, soil, etc.

Figure 1 Tractive element-soil parameters (after Yong et al. 1984).

The soils which are encountered vary from sand to clay and are usually classified by the triangular size distribution system shown in Figure 2. The soil can also include slippery layers and vegetation.

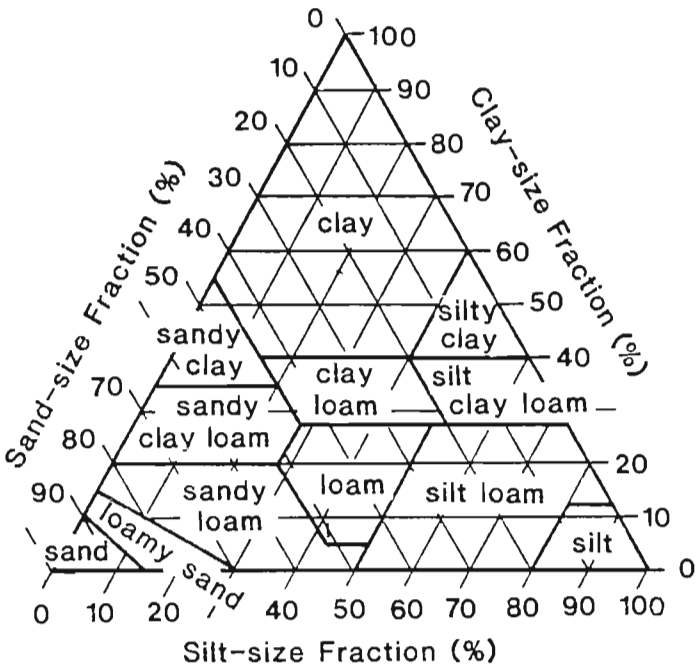

Figure 2 Chart showing percent clay, silt and sand in the soil textural classes of the United States Department of Agriculture (Yong et al. 1984).

The primary problem is that of quantifying the many parameters because the soil is non-homogeneous. It varies from sand to clay and includes varying quantities of air, water, rocks and organic matter. Using a deformable traction device on the above surfaces, which also vary with time, results in an involved system.

As indicated previously the main objective is to relate the vehicle performance in terms of efficiency to those of the soil and vehicle parameters. There have been two main approaches to solving the traction problem. One has involved the fundamental approach, but, the inability to quantify all the parameters has made it impossible to provide rigorous mathematical solutions for a traction theory and this is likely to remain the case for the foreseeable future. In the second approach empirical methods have been used to model traction performance.

2.1.1 Fundamental approach

It is generally accepted that Bekker (1956) was the first researcher to investigate a comprehensive, rigorous and quantitative evaluation of the complete terrain-vehicle system. In Bekker's attempt to develop a comprehensive theory he based the relevant mechanical properties of the soil on the soil shear strength to describe thrust and wheel slip and on the vertical plate penetration test to describe wheel sinkage and rolling resistance. The net traction of a wheel is also generally accepted as being the difference between two primary forces, firstly, the soil thrust or gross tractive effort and secondly the rolling resistance or motion resistance.

The development of the soil thrust is based on the Coulomb-Mickelthwaite criteria of soil failure in shear, which gives the maximum shearing stress (see equation 1) for a particular normal load and this has been used to determine the gross traction or thrust that can be developed by a traction device.

$$F = A\,c + W \tan \phi \qquad \ldots\ldots(1)$$

Where F = shear force

A = area of soil being sheared

c = cohesion

W = normal force

ϕ = internal friction.

The shear strength parameters, cohesion and internal friction are most commonly determined with the use of a triaxial apparatus, translational shear box or the rectangular and annular shear plates as used by Bekker (1956).

Bekker (1956) proposed a more general form of equation (1) given in equation (2), he made use of the fact that the form of soil shear stress-strain curves are similar to the shape of the displacement-natural frequency diagram of an aperiodic damped vibration (see Figure 3).

$$\tau = \left[\frac{c + \tan\phi}{Y}\right] \left[e^{(-k_2 + \sqrt{(k_2^2 - 1)})k_1 j} - e^{(-k_2 - \sqrt{(k_2^2 - 1)})k_1 j}\right]$$

.....(2)

Where τ = shear stress

c = cohesion

ϕ = angle of internal friction

p = normal pressure

Y = number of terms in brackets in equation (2)

k_i = slippage coefficients

j = soil deformation.

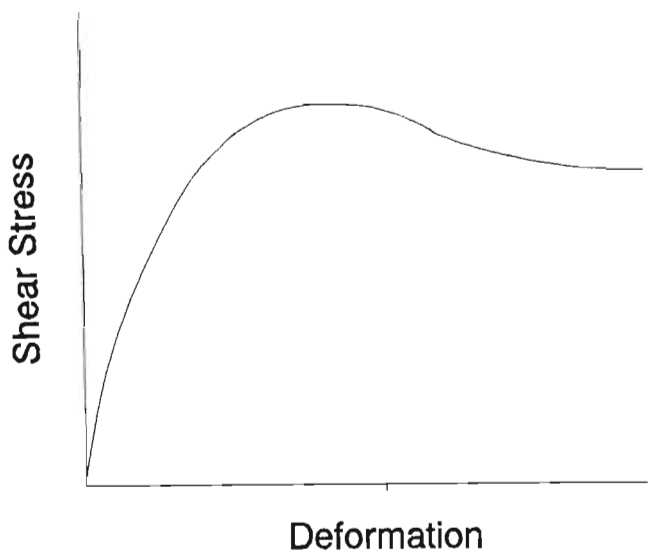

Figure 3 Soil shear stress-strain curve with a "hump" (after Bekker, 1956).

There are many variations of these equations such as those proposed by Janosi and Hanamoto (1961), Taylor and Vanden Berg (1966) and Kacigin and Guskov (1968). Spoor and Godwin

(1979) also pointed out that the shearing characteristics are affected by moisture content and this is not accounted for by the relationships above.

Janosi and Hanamoto (1961) found that in the majority of cases the soil did not exhibit a hump and decay in the stress-strain curve as shown in Figure 3. They felt it was seldom necessary to use an involved equation such as equation (2) and also found that the numerical values of k_i were difficult to determine. They formulated a simpler equation for tangential soil stress which is presented in equation (3). It should be noted that for very large soil deformations the stress described in equation (3) approaches the stress that would be determined by equation (1).

$$\tau = (c + p \tan \phi)(1 - e^{-j/k}) \qquad \ldots\ldots(3)$$

Where k = slip coefficient

p = normal pressure

τ = tangential soil stress

j = soil deformation required to produce the tangential soil stress.

Taylor and Vanden Berg (1966) did not attempt to modify the Coulomb criteria for soil failure. They established the stress-strain relationship based on the deformation as exhibited by the shearing stress-displacement curves and determined a relationship for the maximum soil stress given by equation (4).

$$\tau_{MAX} = c + n_1 \sigma^{(1-n_2)} j^{n_2} \qquad \ldots\ldots(4)$$

Where τ = tangential soil stress

c = cohesion

σ = normal soil stress

j = soil deformation

n_1 and n_2 are system parameters.

Kacigin and Guskov (1968) felt that a hyperbolic function characterised the soil failure pattern more effectively than the aperiodic damped vibration and provided the following equation:

$$\tau = \sigma \left[f_m \left(1 + \frac{a}{\cosh j/K_\tau} \right) \tanh j/K_\tau \right] \qquad \ldots\ldots(5)$$

Where τ = tangential soil stress

σ = normal soil stress

f_m = the ratio of the residual shear strength to the contact stress at large displacements

K_τ = displacement to reach maximum shear stress

a ∝ ratio of the friction coefficients at the peak and residual stresses.

The three constants describe the soil characteristics.

These relationships assume that shearing takes place in a horizontal plane while in practice this is not the case. Measurements made by Burt, Bailey and Wood (1987) of a tyre lug face operating in the soil and shown in Figure 4, illustrate the actual shearing profile.

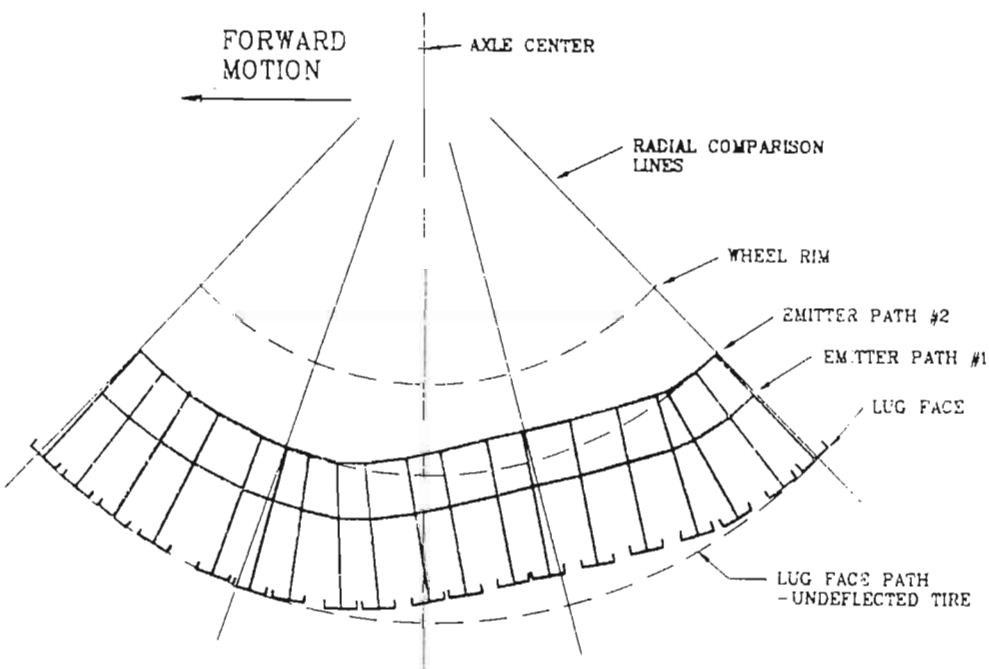

Figure 4 Measured tyre deformation of a tyre operating with a dynamic load of 20kN, an inflation pressure of 110kPa and a net traction ratio of 0,15 (Burt et al. 1987).

Onafeko and Reece (1967) attempted to develop a theory for a rigid wheel in a deformable soil. In an attempt to account for actual shearing profile they postulated the following shear stress equation.

$$\tau = (c+p\tan\phi)\left[1-e^{-r/k((\theta_1-\theta)-(1-s)(\sin\theta_1-\sin\theta))}\right]$$

Where r = rolling radius

k = shear deformation modulus

s = slip

θ = angular coordinate of position on the wheel rim measured from BDC

θ_1 = coordinate of the point where rim and soil surface meet.

Measurements carried out by Onafeko and Reece (1967) to validate the equation showed that it provided better correlation with their results than previous theories. However, they indicated that further research was necessary to improve the ability of the model to describe the relationship between wheel slip and shear stress.

Johnson, Grisso, Nichols and Bailey (1987) reviewed the current methods available to measure the shear strength of agricultural soils. They concluded that the best method, apparatus and technique of shear measurement for agricultural soils had not yet been established. A review was also carried out by Maclaurin (1987) to determine the progress in

modelling, predicting and measuring soil-vehicle performance. He stated that a generally accepted method for describing strength-deformation properties of surface soils has yet to evolve.

These are a few examples of the relationships that have been postulated to describe the shear stress that develops in the soil and some of the difficulties that have been encountered. They illustrate the diversity of thinking that occurs as each researcher attempts to account for the various factors and they show that there is still no generally accepted theory for describing the strength-deformation properties of surface soils.

The second major force in traction is rolling resistance and the mechanics are based on the Bernstein equation shown below.

$$p = kz$$

Where z = sinkage

p = normal pressure

k = function of the soil.

In applying the limit equilibrium approach to the evaluation of the bearing capacity of the loaded plate, Bekker (1956) proposed equation (6) which is a modification of the Bernstein equation. Bekker also gives numerous procedures

using a bevameter to determine numerical values for the coefficients in the equation.

$$p = \left(\frac{k_c}{b} + k_\phi\right) z^n \qquad \ldots\ldots(6)$$

Where z = sinkage

p = normal pressure

k_c = cohesive modulus of sinkage

k_ϕ = frictional modulus of sinkage

n = an exponent reflecting the hyperbolic shape of the sinkage curve.

Bekker (1956), assumed that the rolling resistance of the traction device was the sum of:

(a) The forces required to compact the soil in the vertical direction R_c.

(b) The forces required to bulldoze the soil in the horizontal direction R_b.

(c) The motion resistance due to flexing of the traction device R_t.

Yong et al. (1984) agrees that this is still a valid approach and that the plate model can be used to calculate the vertical compaction if the following assumptions are made:

(a) There are uniform stresses below the traction device.

(b) The sinkage is the same for the plate and traction device.

Using equation (6) and the above assumptions the sinkage Z_0 illustrated in Figure 5 and compaction resistance of a rigid wheel can be written as shown in equation (7).

$$R_c = \frac{bk}{n+1}\left[\frac{3W}{bkd(3-n)}\right]^{(2n+2)/(2n+1)} \qquad \ldots\ldots(7)$$

Where d = wheel diameter

b = Wheel width

$k = (k_c/b + k_\phi)$

W = wheel load

k_c, k_ϕ and n are soil values.

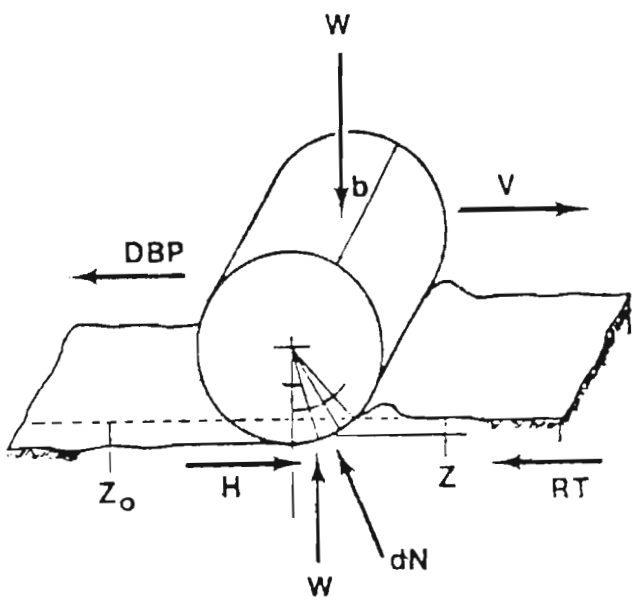

Figure 5 Wheel and plate - soil force system (after Yong et al., 1984).

The application of the plate model to predict the motion resistance of a pneumatic tyre is not accurate since the

model does not physically represent the true deflection of the tyre in the soil. If the tyre is physically idealised as shown in Figure 6 and if the pressure is assumed to be distributed uniformly along the flat contact surface, Yong et al. (1984) showed that the compaction resistance can be represented by the following equation.

$$R_c = \frac{\left[b \left(P_i + P_c \right) \right] 1^{(n+1)/n}}{\left(k_c + b k_\phi \right) (n + 1)}$$

Where b = Wheel width

P_i = tyre inflation pressure

P_c = carcass pressure

k_c, k_ϕ and n are soil values.

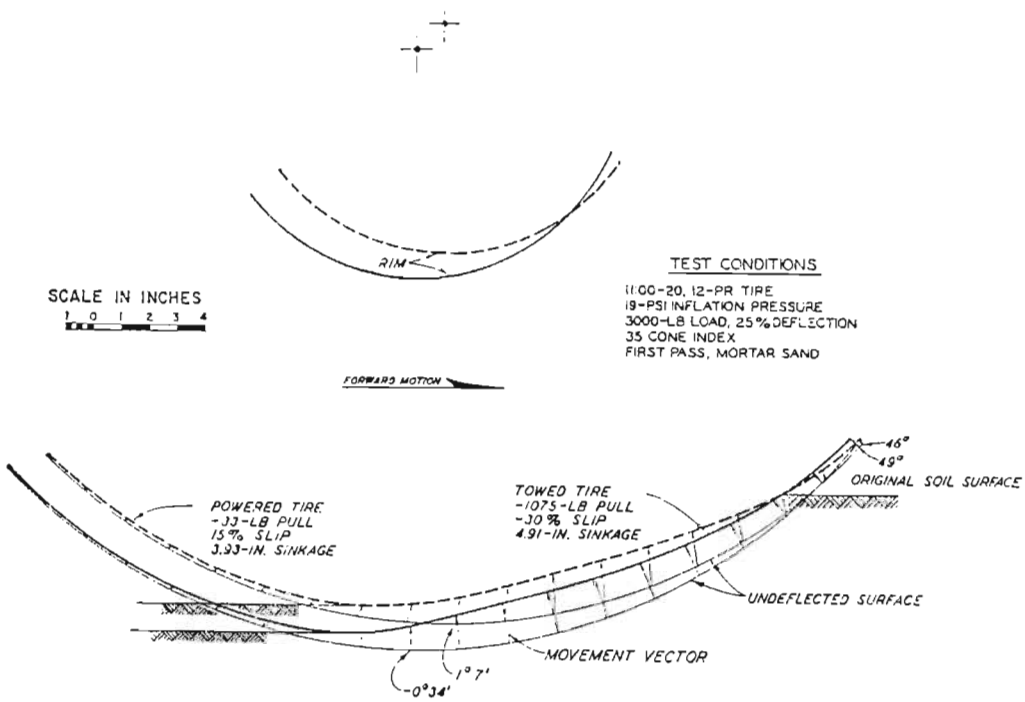

Figure 6 The physical model and actual measurements for a pneumatic tyre (Freitag and Smith, 1966).

It is interesting to note the discrepancy in the soil-tyre profile as measured by Freitag and Smith, (1966) and that measured by Burt et al. (1987) and shown in Figure 3. This again highlights the dilemma in establishing a rigorous theory.

The bulldozing resistance is difficult to separate from the sinkage forces. If it is assumed to be the force required to push the soil mass at sinkage z ahead of the wheel it can be calculated using passive earth pressure theories, as shown below:

$$R_b = \frac{b \sin(\alpha+\phi)}{2 \sin \alpha \cos \phi}\left[2zck_k+\gamma z^2 k_\gamma\right] \qquad \ldots\ldots(9)$$

Where $k_k = (N_c - \tan \phi) \cos^2\phi$

$k_\gamma = (2N\gamma/\tan\phi+1)\cos^2\phi$

$\alpha = \cos^{-1}(1-2z/d)$

z = wheel sinkage

Nc , $N\gamma$ = bearing capacityfactors

γ = soil density

Where no soil displacement takes place in front of the wheel equation (9) will overestimate the real values.

Motion resistance due to flexing of the tyre is dependent on many factors such as;

(a) tyre stiffness,

(b) tread design,

(c) soil-tyre relative stiffness, and

(d) inflation pressure.

The resistance can be measured on a hard surface and will yield an upper value for the tyre, this was evaluated by Bekker (1960) as:

$$R_t = W\mu/IPr^f$$

Where μ = empirical constant

f = empirical constant

IPr = inflation pressure.

The total motion resistance RR is the sum of the individual components:

$$RR = R_c + R_b + R_t$$

Again, there are many variations of the pressure sinkage relationships which emphasise the diversity of thinking.

At this stage it should be noted that Bekker (1956) warned that the refinements of a rigorous solution might not lead to significant practical gains. Experimental results however, have shown that significant performance differences are related to variables which are not accounted for by present theory (Burt, Lyne, Meiring and Keen, 1983; Lyne and Burt,

(1989). Improved solutions are therefore necessary and this has been more closely approached by the recent use of the finite element method.

Perumpral, Liljedahl, and Perloff (1971) first used the finite element technique to predict traction forces. This work was followed by Yong and Fattah (1976) using a rigid wheel. Yong, Fattah and Boonsinsuk (1978) developed the technique further to take into account tyre flexibility. This work required X-ray photographic techniques to determine the terrain responses and displacement boundary conditions. This approach is of limited practical value as these conditions would have to be determined for each field condition.

Yong (1985) described the use of energy transfer methods in conjunction with the finite element method to model the traction process. Again the soil and tyre properties and the boundary conditions play an important role in the success of the technique.

Plackett (1985) states that although a major disadvantage of numerical methods is not being able to describe the mechanical properties of the soil adequately, one advantage is that they are able to predict the state of stress of the entire soil body after the passage of a wheel.

In an effort to describe the soil-wheel interface more accurately, Burt and Bailey (1985) and Burt, Wood and Bailey (1987) developed a sonic digitizer system to measure the stresses at the tyre-soil interface for a pneumatic tyre. This system enables researchers to measure directly the boundary conditions for the soil-tyre interface with a standard agricultural tyre and will improve the quantitative inputs required by numerical method techniques.

Accurate measurements were made of the magnitude and directions of the normal and tangential stress by Burt et al. (1987) using the sonic system. The system was also applied by Wood and Burt (1987) to measure the thrust and motion resistance of a standard pneumatic tyre. The stresses were affected by both inflation pressure and dynamic load and the thrust ratios varied across the lug width for different soil and operating conditions, again indicating that assumptions made by researchers still require refinements to describe the traction process accurately.

With the latest measuring techniques and the use of numerical methods researchers are obtaining a better understanding of the soil-tyre interface. However, a limitation of these methods is that, to predict the required forces, data are required which cannot be obtained realistically in a practical situation. This limitation has lead to the development of the scientifically less satisfactory, but easier to use empirical methods.

2.1.2 Empirical approach

Freitag (1966) initiated a method based on dimensional analysis to relate the various soil and tyre parameters and one of his aims was to reduce the number of variables and to use the relatively simple method of soil penetration resistance to quantify the soil parameters.

Turnage (1972a) further improved the relationships and he developed the clay mobility number provided below to predict each of the following four tyre performance coefficients;

(a) motion resistance / load,

(b) pull / load,

(c) sinkage / diameter, and

(d) torque / load * rolling radius.

$$\text{Mobility number} = \frac{Cbd}{W}\sqrt{\frac{\delta}{h}}\,\frac{1}{(1+\frac{b}{2d})}$$

Where C = cone index

b = unloaded tyre section width

d = tyre diameter

W = dynamic load

δ = tyre deflection

h = tyre section height.

Wismer and Luth (1972) produced the well known prediction equations by using a simplified mobility number C_n referred to as a wheel numeric for use in agriculture.

$$C_n = CIbd/W$$

Where CI = average cone index over the top 150mm of soil depth

b = unloaded tyre section width

d = tyre diameter

W = dynamic load.

Wismer and Luth (1972) used the following set of dimensionless ratios:

$$\frac{TF}{W}, \frac{P}{W}, \frac{Q}{rW} = f\left(\frac{CI\ bd}{W}, \frac{b}{d}, \frac{r}{d}, s\right)$$

Where TF = towing force or motion resistance

P = pull

Q = axle torque

r = rolling radius

s = wheel slip or travel reduction.

They used similitude methods of experimental analysis to establish three dependent-variable relationships provided in equations (10) and (11).

$$TF = \left(\frac{1,2}{C_n} + 0,04\right)W \qquad \ldots\ldots(10)$$

Where TF = towed force

C_n = wheel numeric

W = dynamic load.

$$F = \left[0,75\ (1 - e^{-0,3C_n s})\right] W \qquad \ldots\ldots(11)$$

Where F = gross tractive effort developed by the wheel

s = wheel slip.

The net traction (P) is the difference between the gross tractive effort and the towed force.

$$P = F - TF$$

These equations were limited by a number of assumptions such as a fixed dynamic load and although they did not provide accurate performance prediction they were widely used as a quick and easy procedure to determine vehicle performance. They went a long way to solving the problem of optimizing performance on the farm. Otterman (1985) showed that the Wismer and Luth (1972) system could be calibrated for a particular soil condition by working backwards to compute CI from vehicle performance. It then provided very good estimates of performance if other operating parameters were varied.

Clark (1984) accounted for the difficulty in obtaining a representative cone index by introducing constants C_1 - C_4 which would vary with soil types and would be determined experimentally from a series of field tests. The more generalized form of the model for towed force and gross traction is given below:

$$TF = W\left[\frac{C_1}{C_n} + C_2\right]$$

$$F = W\left[C_3\left(1 - e^{-\left(C_4\right) C_n s}\right)\right]$$

Where TF = towed force

C_n = wheel numeric

W = dynamic load

F = gross tractive effort

s = wheel slip.

Many refinements have been made to these methods to broaden their scope and to improve the accuracy of the prediction. Dwyer, Comely and Evernden (1975) used the Turnage (1972b) mobility number to examine experimental results obtained with agricultural tyres and produced a handbook of agricultural tyre performance (Dwyer, Evernden and McAllister, 1976).

Gee-Clough et al. (1978) re-examined the work of Dwyer et al. (1975) using an empirical approach and proposed that:

$$C_T = (C_T)_{max} (1 - e^{-ks})$$

Where Ct = coefficient of traction

$(C_t)_{max}$ = maximum value of C_t

k = a rate constant

s = wheel slip.

There is a fundamental difference between the approach taken by Wismer and Luth (1972) who used the classical method of predicting the gross traction and motion resistance separately and Dwyer et al. (1975) who predicted the net traction directly from the mobility number.

The work by Wismer and Luth (1972) assumes a fixed dynamic load. In an effort to account for the real situation of varying dynamic load on log-skidder tyres, Ashmore, Burt and Turner (1987) substituted the dimensionless term W/W_r, for the b/d and r/d terms of Wismer and Luth (1972). W_r is the rated load for the tyre at a particular inflation pressure and this effectively removed the restriction of tyre dimension and deflection.

Tests were carried out by Ashmore et al. (1987) where they used a range of dynamic loads and inflation pressures to

determine the equation below. The equation was used to predict the net traction in terms of travel reduction, dynamic load, cone index, rated load and tyre size.

$$P = \left[0,47\left(1-e^{0,2\,C_n s}\right)+0,38\left(\frac{W}{W_R}\right)-\left(\frac{0,22}{C_n}+0,2\right)\right]$$

Where P = pull

C_n = wheel numeric

s = wheel slip

W = dynamic load.

Figure 7 shows a comparison of the prediction from the above equation and from the Wismer and Luth equation. It can be seen that using assumptions to simplify a model as in the case of Wismer and Luth (1972), can lead to erroneous results.

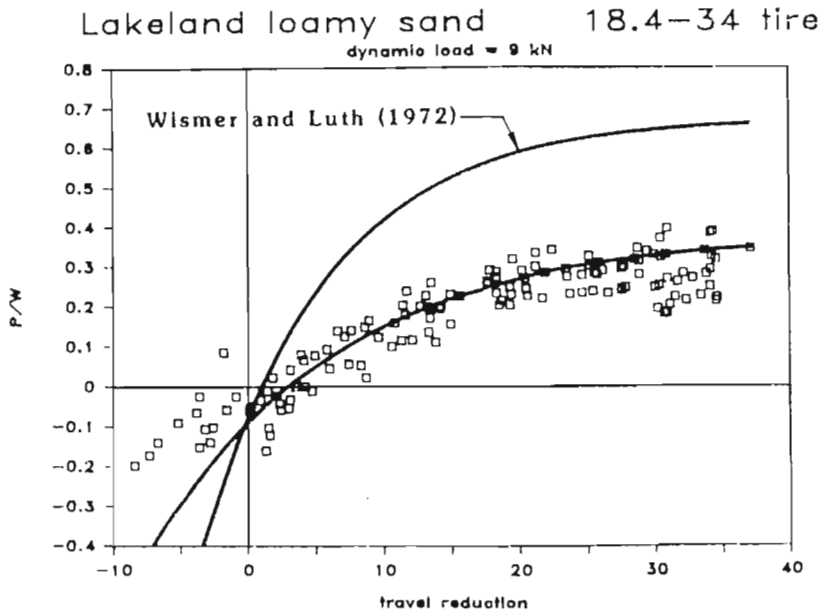

Figure 7 Normalised net traction versus travel reduction for an 18.4-34 log-skidder tyre on a Lakeland sandy loam at an inflation pressure of 172kPa (after Ashmore et al., 1987).

The Wismer and Luth equations were also refined by Brixius (1987) who introduced the following dimensionless ratios;

(a) torque ratio Q/rW,

(b) motion resistance ratio M/W, and

(c) deflection ratio δ/h.

These ratios were formulated to improve the description of the soil-wheel system. A mobility number B_n shown below was developed to include tyre deflection.

$$B_n = C_n \left(\frac{1+5\frac{\delta}{h}}{1+3\frac{b}{d}} \right)$$

Where C_n = wheel numeric

δ = loaded tyre deflection

b = section width

d = unloaded diameter

h = section height.

Brixius (1987) used curve fitting techniques with results of over 2500 tyre tests conducted in separate experiments by four different institutions (see Table 1). This resulted in an updated pull equation provided below.

$$P = W \left[0,88 \left(1 - e^{-0,18_n} \right) \left(1 - e^{-7,5s} \right) - \left(\frac{1,0}{B_n} + \frac{0,5s}{\sqrt{B_n}} \right) \right] \quad \text{.....(12)}$$

Where P = pull

W = dynamic load

s = slip.

Predicted versus measured values of pull ratio (P/W) at 20% wheel slip for the tests described in Table 1 are shown in Figure 8.

Table 1 Range of field test variables of data used for the curve fitting to determine the prediction equation (12) (after Brixius, 1987).

		C_n		δ/h		b/d	
Source	Test Vehicle	Min	Max	Min	Max	Min	Max
WES	Military Vehicles Tracking wheel data at 20% slip	7	94	0,165	0,250	0,261	0,870
NIAE	2WD Agric. Tractor Data at 20% slip	4	58	0,161	0,239	0,220	0,306
TACOM	6 x 6 Military Truck Data from 0-90% slip	6	26	0,104	0,240	0,293	0,293
DEERE	2WD Agric. Tractor Data from 0-60% slip	4	95	0,088	0,305	0,250	0,581

Brixius (1987) also gives recommendations on how equation (12) should be adjusted to account for its use with radial-ply tyres, although he warns that further analysis to improve the model is needed. This is one of the few techniques which recognises the well documented difference in performance between cross-ply and radial-ply tyres.

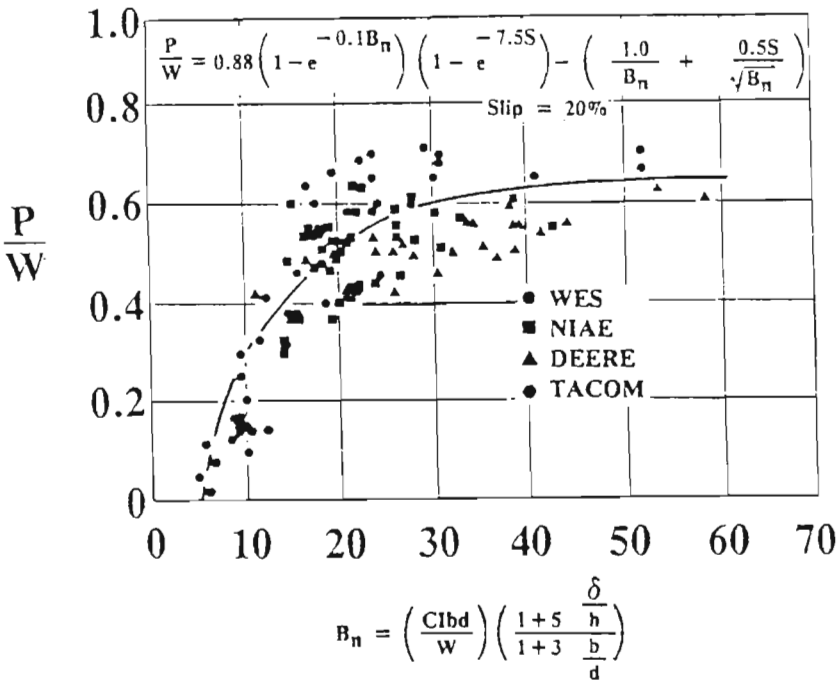

Figure 8 Predicted versus observed values of pull ratio (Brixius, 1987).

An interesting approach by Kaumbutho, Rosenberg, Burkhardt and Srivastava (1987) made use of bond graphs to model the tractor dynamics. They felt this technique would enable them to compare variables more easily than using the traditional mathematical models. Their traction component of the model also relied on the Wismer and Luth (1972) equations and they found that during tests wheel slip was predicted with a 36% error and drawbar pull with a 7% error.

The empirical methods have provided a convenient means of predicting performance and they have served a useful purpose for users of traction equipment. However, the fundamentals of traction mechanics should be studied further to attain a better understanding of the

mechanics involved. Having said this, it is also imperative that an effort be made to maximize present day performance. At present, a traction device is designed for general conditions and maximum performance can only be achieved by optimizing the parameters, and a very effective method of achieving this would be by having real time control of certain operational variables.

2.2 Optimizing tractive efficiency

In practice, for a given set of conditions an operator does not have control over many of the variables affecting the tractive efficiency of his tractor. The traction device is fixed by the available vehicle, the soil condition is fixed by the field being prepared and the net traction is fixed by the operation being performed. This leaves the operator with the option of varying the load being carried by the drive wheel and its inflation pressure. Traditionally the operator has varied the static load and relied on the weight transfer to achieve an acceptable dynamic load. The inflation pressure is normally set to the tractor manufacturers recommended level to ensure safe loading of the tyre.

Various techniques have been developed to assist the operator in selecting the optimum parameters. Dwyer et al. (1975) and Dwyer et al. (1976) produced a handbook to assist operators in their selection of the correct tyre size for their

specific soil conditions. The handbook also gives predicted performance at different axle loadings, inflation pressures and travel reduction levels for various classes of surface condition. Drawbar pull levels are also furnished for the different conditions to enable the operator to match the implement to the tractor.

Zoz (1972), produced a tractor drawbar performance predictor to help operators to match implements to tractors. Tyre performance data were used to predict tractor performance for the three hitch configurations and for surface conditions varying from soft or sandy soil to concrete. The predictor chart was updated by Zoz (1987) where he provided a template to operate in a standard computer spreadsheet. Although the system is easy to use its main limitations are that engine loading is not taken into account and it assumes fixed weight transfer coefficients for the three hitch types which in practice vary considerably.

A curve representing the tyre load per unit of available axle power to achieve maximum efficiency was developed by Gee-Clough, Pearson and McAllister (1982) using the empirical equations postulated by Gee-Clough et al. (1978). A further curve for the required wheel slip to ensure maximum tractive efficiency was provided to assist in the selection of ballast and wheel slip levels.

Evans, Clark and Manor (1989) developed a traction prediction and ballast selection system using the traction equations presented by Brixius (1987) and an equation solving programme. However, the model was only validated for bare soil conditions.

The above procedures are of benefit to operators in enabling them to improve tractive performance. However, they assume that firstly, the pull that the implement requires can be predicted, secondly, that the soil can be classified correctly and lastly that a reliable measurement of the wheel slip that develops can be obtained.

In spite of the various operator aids that have been developed, results show that tractors are still not being used effectively (Meiring and Rall, 1979; Lyne et al. 1980; Meiring, Walker, Hansen and Lyne 1985; Meiring, Rennie, Hansen and Lyne, 1987). During farm visits in Lancaster County, Nebraska, Wertz and Grisso (1988) carried out a survey of forty tractor owners to determine how effectively tractor tyres were being ballasted and inflated. Seventy percent of the owners used dual wheels at all times on their primary tractor. Inflation pressures varied from 34 to 207kPa and only 50% of the two wheel drive tractors had optimum ballast.

To complicate matters there are differences in the definition of zero wheel slip. Most researchers rely on the ASAE method

of determining zero wheel slip on a hard surface whereas Dwyer et al. (1976) define zero wheel slip as the zero net traction point under field conditions in their tyre handbook.

In an effort to further improve the systems, Clark and Vande Linda (1986) developed a rapid ballast system to facilitate the task of loading the tractor wheels correctly. The objective was to predict the required ballast and pump a liquid into tanks on the tractor from a station reservoir. The idea has merit, but the procedure is cumbersome and is therefore not a practical solution for the farmer.

Zhang and Perumpral (1987) developed a slip control mechanism which varied the transmission ratio to control wheel slip at optimum levels. The Wismer and Luth (1972) relationships were used as the basis to determine the optimum wheel slip levels for the control system.

Further systems were developed. Zhang, Liljedahl and Miles, (1984) varied wheel speed and Chancellor and Zhang (1987) varied either the draught control or the implement depth gauge wheel to maintain the wheel slip within a predetermined range. This was similar to a combined slip and draft control system developed by Ismail, Singh and Gee-Clough (1981), which also varied the draft control to maintain a fixed slip level. The above systems showed improved efficiency during trials, however the problem of determining the required wheel slip still exists.

A major criticism of this work is that Zhang et al. (1984) and Zhang and Perumpral (1987) were adjusting the vehicle performance and Ismail et al. (1981) and Chancellor and Zhang (1987) were adjusting implement depth to optimize traction. It is imperative that the speed and depth of operation be fixed by the tillage requirements and other parameters be varied to optimize traction. One has to be very careful that depth is not varied to the detriment of crop yield and profitability. Further, these same researchers were using wheel slip to optimize tractive efficiency when the wheel slip level providing maximum efficiency is difficult to determine. While using sophisticated control systems, tractive efficiency should be used as the control variable.

It has been shown that weight is the most important factor affecting tractive performance (Dwyer, 1985) and that inflation pressure also plays a significant role (Yong, Boonsinsuk and Fattah, 1980; Burt et al. 1983; Charles, 1983; Lyne, et al. 1984). If it were feasible to vary the dynamic load and inflation pressure in the field, by controlling a weight transfer hitch and using a central inflation system to maximize tractive efficiency under the particular conditions, a significant improvement in field performance could be achieved. Such a system would have to ensure that the tractor and tyre remained within their specified load limits.

It was therefore decided to develop and test a system that would determine the tractive efficiency response for the

particular operating conditions and operate the tyre under the dynamic load and inflation pressure levels which would give the maximum tractive efficiency for the specific conditions.

2.3 Tractive efficiency response model

The normal procedure to determine a response surface would be to collect data with tractive efficiency as the independent variable and dynamic load and inflation pressure as the dependent variables and carry out a regression analysis with the data to determine the surface model. However, in order for such a system to succeed in practice it would be necessary to have a general model which could be used under all conditions and to determine the coefficients for the model during field operations.

The method used to postulate a general model involved investigating measured data to determine whether it was feasible to use a general model which would give a good fit under all conditions. One set of data was published by Burt, et al. (1983) and another unpublished set measured at the NTML (1984) were used for the exercise. A tractive efficiency response surface was plotted through the measured points (see Figure 9) of each of 12 different data sets and the surfaces were examined.

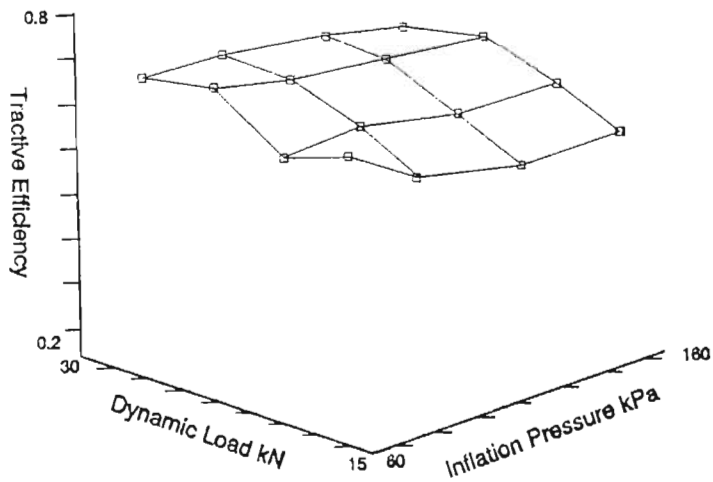

Figure 9 An example of a surface drawn through the data published by Burt et al. (1983).

The surfaces were all segments of a smooth convex shape which could be represented accurately by a full second order linear model of the form shown below:

$$TE = A(0) + A(1)IPr + A(2)IPr^2 + A(3)DL + A(4)DL^2 + A(5)IPr.DL \quad \ldots\ldots(13)$$

Where TE = tractive efficiency

IPr = inflation pressure

DL = dynamic load

A(i) = regression coefficients.

The above model was selected to represent the tractive efficiency response surface for all conditions. A system was developed to evaluate the concept of automatic control of DL and IPr and the suitability of the above model. The abbreviations used for tractive efficiency, inflation pressure and dynamic load will be utilized during the remainder of the document.

3 REAL TIME CONTROL OF DYNAMIC LOAD AND INFLATION PRESSURE

To maintain maximum tractive efficiency of a vehicle during an operation, a system was required to optimize the dynamic load and the inflation pressure of the drive wheels in real time. To ensure operator safety and acceptable tyre life the system would have to maintain the dynamic load and inflation pressure levels within the specified operating range of the tyre. To achieve these requirements a programme was formulated to develop and evaluate such a system using the USDA's Single Wheel Traction Research Vehicle (SWTRV) described by Burt, Reaves, Bailey and Pickering (1980). The SWTRV operated in soil bins thereby enabling the evaluation of such a system to be carried out under strictly controlled conditions. This control would have been difficult to achieve in the field.

Lyne, Burt and Jarrell (1983) added computer control to the existing controls on the SWTRV to implement a real time control programme. The SWTRV is a powerful machine of considerable weight and extreme care had to be taken with the control programme to ensure complete safety to the operators and the machine while under computer control. The system would have to detect and cater for any type of malfunction.

An optimization algorithm to maximize tractive efficiency (TE) was added to the control system. An experiment was then

planned to examine the algorithm's ability to locate the optimum dynamic load and inflation pressure while simulating a field operation (Lyne and Burt, 1989). Soil type, surface preparation and net traction (NT) levels were varied to cover the range of conditions expected in the field.

3.1 Single wheel traction research vehicle

The single wheel traction research vehicle shown in Figures 10 and 11 was a soil bin vehicle with diesel-hydraulic power. It was equipped with electro-hydraulic servo controls to vary the speed of the vehicle along the bin, the angular velocity of the test wheel and the vertical load on the test wheel (Burt, et al. 1980).

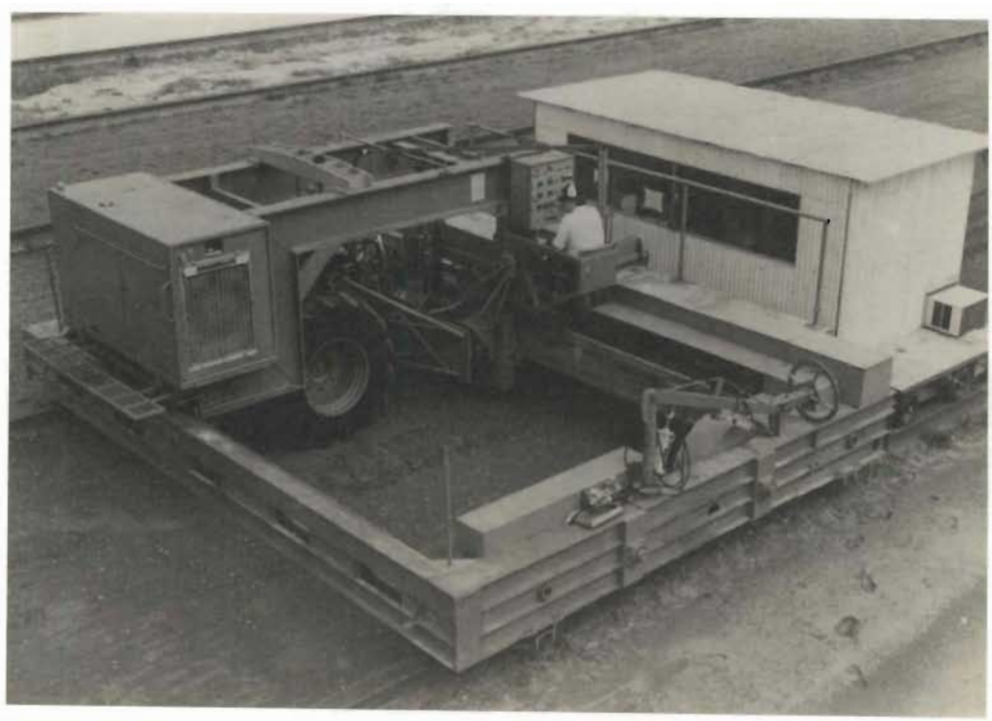

Figure 10 Single wheel traction research vehicle.

The test wheel was secured in a framework which was mounted within a superstructure. The superstructure could traverse across the width of the bin within the car structure. The car structure travelled the length of the soil bin on rails along the side of the soil bin. This enabled the test tyre to be run in a number of lanes down the length of the soil bin.

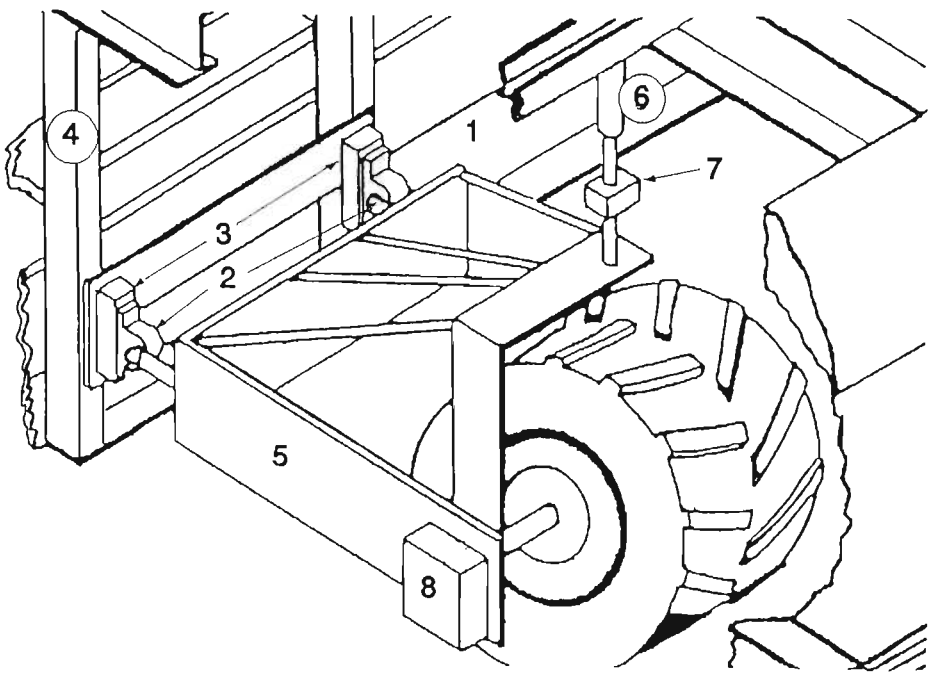

1	Car structure	2	Pivots
3	2D Dynamometers	4	Superstructure
5	Test wheel framework	6	Vertical loading system
7	Vertical load cell	8	Test wheel drive

Figure 11 Wheel frame work on the single wheel traction research vehicle (after Burt, et al. 1980).

The forces generated by the test wheel were transmitted to the superstructure through pivots and a two dimensional dynamometer system at the rear of the test wheel framework (see Figure 11). The vertical load on the test tyre was applied through a hydraulic cylinder in series with a load cell mounted vertically above the test wheel. This enabled all the external forces on the test tyre to be measured. A hydraulic motor drove the test wheel through a torque meter which in conjunction with a shaft encoder gave the torque and speed signals for the test wheel.

3.2 Vehicle drive and control system

A schematic of the drive and control system for the SWTRV is shown in Figure 12. The diesel engine drove two separate hydraulic pumps. One was used to control the vertical load on the test tyre and maintain the tyre framework in a horizontal plane and the second to drive the SWTRV down the bin and power the test wheel.

Each system was controlled by a closed loop analogue controller with a constant or ramp set point which could be selected by the vehicle operator. The system gave the operator the capability of selecting the set points for normal load on the test tyre, the angular velocity of the

test tyre and the forward velocity of the vehicle. A potentiometer was used to adjust the set points for each parameter. The operator was also able to set a ramp between two set points to vary the selected variable linearly at a selected rate.

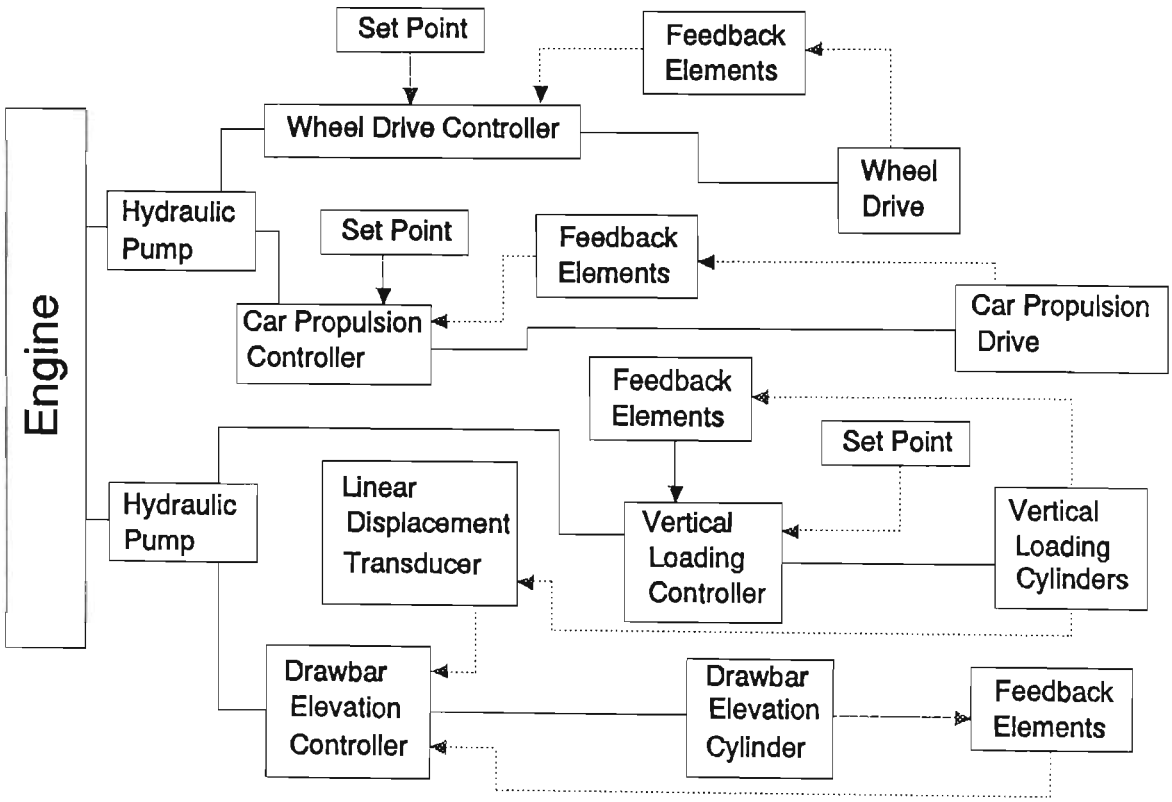

Figure 12 Block diagram for the SWTRV drive and control systems (after Burt, Reaves, and Taylor, 1977).

A displacement transducer was used to monitor the vertical movement of the tyre during operation. This movement was used as a feedback to the framework controller to maintain the framework in a horizontal plane. This ensured that the

external forces on the framework remained in three orthogonal planes.

3.3 Instrumentation and data acquisition

Strain gauge type load cells were used in the two dimensional dynamometer system for measuring the vertical and longitudinal forces transmitted from the test wheel framework to the superstructure. A strain gauge type pressure cell for measuring the tyre inflation pressure was mounted on the superstructure. The pressure cell was coupled to the tyre via a flexible hose and swivel coupling similar to the system described by Czako (1974). The test wheel torque meter was also of the strain gauge type. Shaft encoders producing a frequency output for measuring the tyre car velocity and the test wheel angular velocity were mounted on a fifth wheel running on the soil bin rail and on the test wheel drive respectively. These transducers were coupled via cables to a data acquisition system housed in an enclosed instrument car trailed by the SWTRV (see Figure 10).

The data acquisition system consisted of a Modcomp Classic II/15 mini computer with a real time multi-tasking operating system. The computer was interfaced to a high speed analogue input subsystem for measuring the analogue signals from the SWTRV. Figure 13 is a block diagram of the data acquisition system used.

The strain gauge signals from the load cells and pressure transducer were processed by strain gauge amplifiers and linked to the computer via the A/D subsystem. The frequency outputs from the shaft encoders on the test wheel and fifth wheel were conditioned by process controllers and also coupled to the computer via the A/D subsystem.

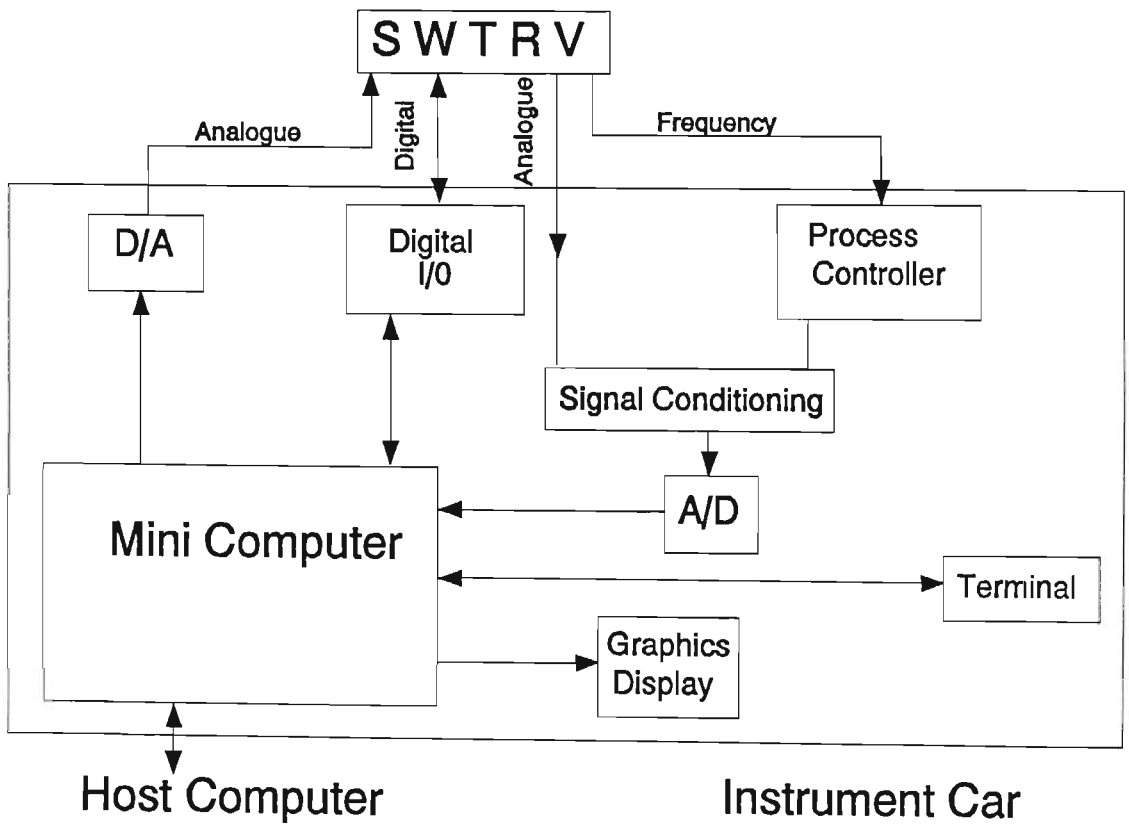

Figure 13 Block diagram of the data acquisition and control system.

A D/A system transmitted display signals such as travel reduction, dynamic load and net traction for the SWTRV operator. The display signals activated analogue meters to provide the SWTRV operator with visual feedback of the

process variables. Analogue signals were also transmitted to the closed loop control systems for the test wheel. A digital I/O system transmitted and received digital signals between the two vehicles, which included, start and stop control signals, computer integrity signals and inflation pressure control valve signals.

The computer was equipped with only 512kb of RAM to store programmes and to buffer the data during a test run and hence it was necessary to be cautious not to over extend a test run. The various programmes used, were stored on an on-line host computer (see Figure 13) and down-loaded as required. At the end of a test run the data were displayed graphically and examined before being down-loaded to the host computer for storage and subsequent processing.

The sequence outlined below was used to calibrate and scale the data acquisition system during the project. At the start of each test day the electronics and hydraulics were warmed up to operating temperature. The diesel engine driving the SWTRV was then switched off and all hydraulic circuits left in an unloaded condition. The data acquisition programme permitted the manual selection of the parameters required during the particular test and the adjustment of the gains of the amplifiers to ensure that the maximum resolution of the A/D converters was used. The transducer signals were measured in the unloaded condition to obtain the zero bias and remeasured with calibration resistors switched into the

circuit. These data were used to compute regression equations relating measured voltages to engineering units.

The bias was remeasured before each test run to account for any offset that might have occurred.

The data acquisition routine cycled through the selected channels and the distance travelled down the bin was used as the criterion for data storage, in preference to a time based criteria. This insured that the frequency of data storage was independent of vehicle speed and data points were saved for each 50mm distance travelled in the soil. The measured data were also used as the feedback information for the control programme.

3.4 Computer control system

A conventional analogue closed loop system as indicated by the solid lines in Figure 14, provided the control for the vertical load on the tyre (normal load), the angular velocity of the tyre and the forward velocity of the test car at the set point levels. The set points were obtained from the potentiometers controlled by the operator. This equipment was mounted on the SWTRV and enabled it to be controlled manually and if required, to operate independently of the instrument car.

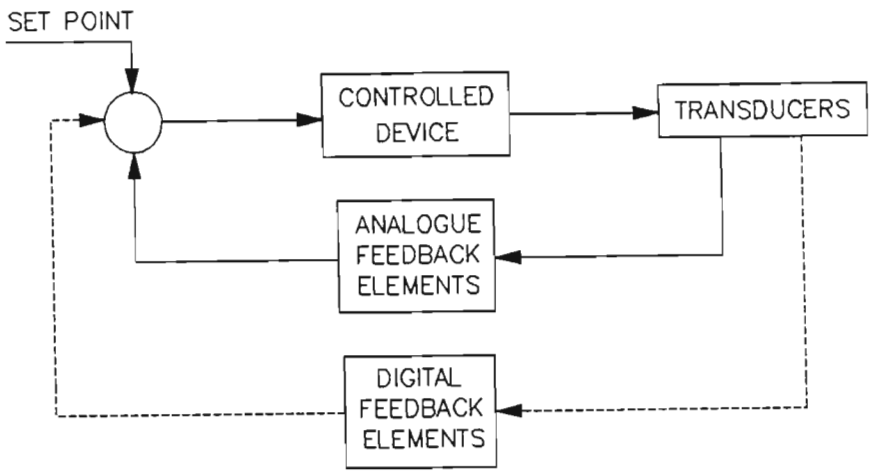

Figure 14 Schematic of the analogue control system used by the SWTRV and the digital control elements (after Lyne, et al. 1983).

Various options for implementing computer control were considered and the following features were believed to be important and were incorporated in the system:

(a) The computer control system should allow the SWTRV to operate independently of the instrument car. It was necessary to separate the SWTRV and the instrument car to move the vehicles from one bin to another. It was also necessary to operate the SWTRV independently during maintenance and development work.

(b) The existing minicomputer in the instrument car should carry out the control function in addition to the existing data acquisition function.

(c) The operator of the SWTRV should have overriding control and be able to switch computer control in and out of operation. The operator was in an ideal position to monitor the vehicle operation and to detect any abnormal operation which would require the automatic control programme to be terminated.

(d) A system should monitor the integrity of the computer and transducer signals and provide a controlled shut-down if any malfunction was detected.

The existing control system was therefore left intact and the dashed line elements illustrated in Figure 14 were added to achieve computer control. The control was accomplished by incorporating a proportional-integral-differential (PID) control algorithm into the data acquisition programme. The control signals were then transmitted via the digital-to-analogue outputs provided on the computer to continually update the set points in the existing analogue control circuits to ensure the necessary control.

The control algorithm is summarized in Figure 15. The programme was written to prompt the operator for the required inputs. Once the required control parameters had been selected the programme cycled the computer through the data acquisition routines, computed the dynamic load, net traction, and travel reduction and carried out the necessary control.

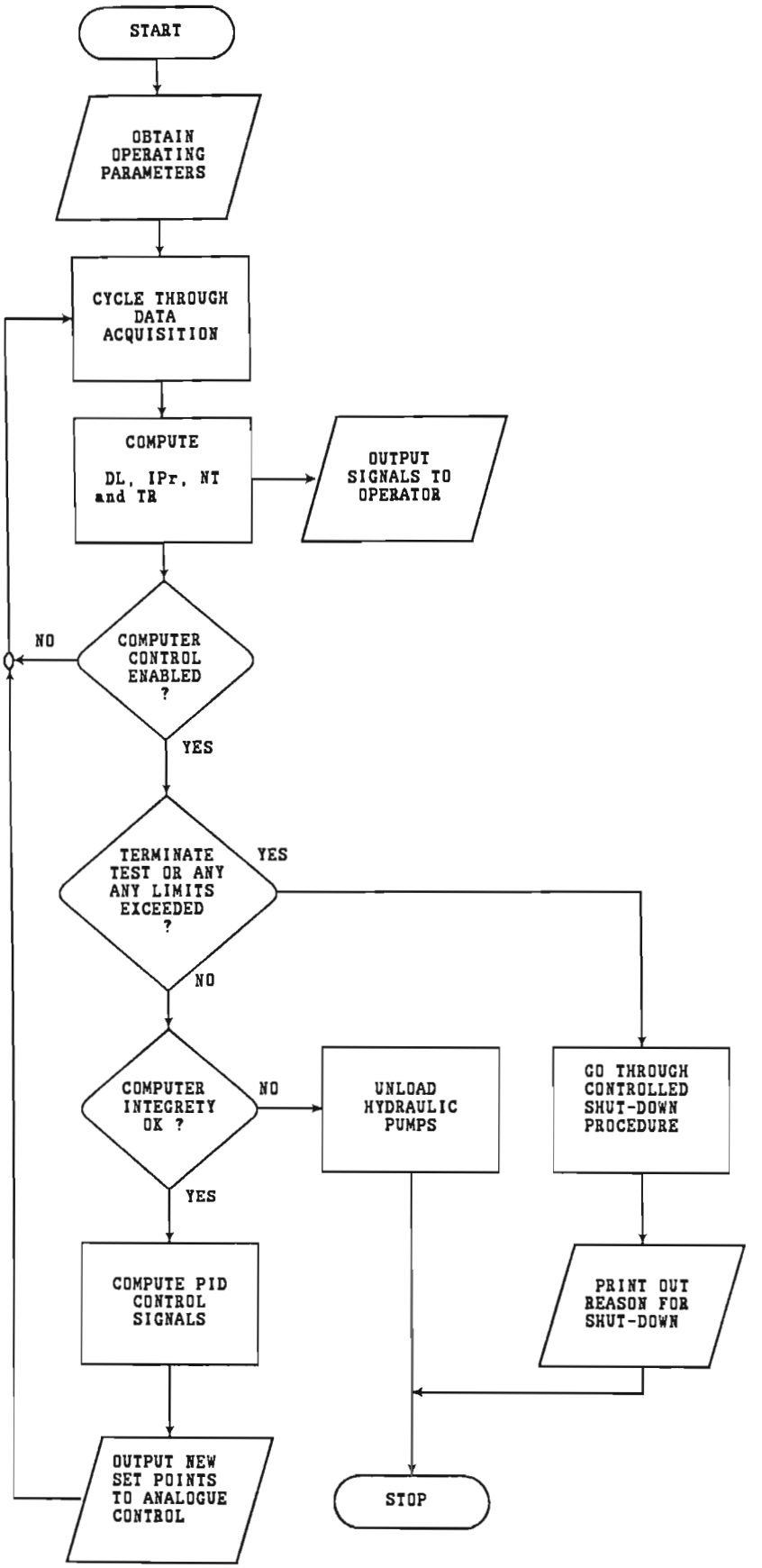

Figure 15 Summarized control algorithm.

A test was run using two operators. One was seated on the SWTRV (see Figure 10) and controlled the test by operating the vehicle and the second, the computer operator, was in the instrument car. At the start of a test the computer operator initiated the control programme and was prompted for the control variables such as tyre load and inflation pressure limits and the net traction required.

Once the inputs were complete the programme cycled through the data acquisition routines to compute the operating variables such as dynamic load, net traction and travel reduction and transmitted these to analogue meters on the SWTRV operator panel. The SWTRV operator then started the SWTRV and manually varied the controls to bring the vehicle up to speed and to get the operating parameters as close to the set points as possible. Once the vehicle speed, dynamic load and inflation pressure were close to their target values control was enabled. The control programme then adjusted the set points to the target values and indicated via a printout once the targets had been attained.

The operators then waited until the vehicle reached the test area and depressed the Data switch to initiate the optimization routine which is discussed in section 3.5. If the SWTRV operator believed that anything was abnormal he could activate the Stop switch to terminate the test. This aborted the programme and the SWTRV was brought to a stop by going through a controlled shut-down procedure.

Certain limits on the measured parameters were checked and if any of these limits were exceeded the programme was aborted and again the SWTRV was stopped by a controlled shut-down procedure. The reason for this check was two fold, firstly, any failure of the transducers or electronics and secondly, inadequate functioning of the control algorithm would have resulted in abnormal parameter values and these values were used to detect system failure. In these cases a printout was produced indicating the reason for the shut-down. The shut-down procedure involved computing a linear ramp to reduce the current levels of dynamic load, test wheel velocity and vehicle velocity to zero in approximately two seconds.

The above procedure did not cater for a computer malfunction and a separate method was devised that checked for this malfunction and then if necessary used the emergency shut-down system built into the SWTRV. This system used a relay which kept the hydraulic pumps in operation and if the relay was released by either a loss of power or the activation of an emergency switch the hydraulic pumps were automatically unloaded. The computer was programmed to generate a fixed frequency which was monitored by an electronic circuit on the SWTRV and if this frequency deviated while computer control was enabled the pump relay was automatically released and the SWTRV brought to a halt.

3.5 Optimization algorithm

As already indicated a key objective of the work was to establish the dynamic load and inflation pressure which would enable maximum tractive efficiency to be attained during a specific operation. The method used to accomplish this involved mapping the tractive efficiency response surface over the dynamic load-inflation pressure range of the tyre. The response surface was computed by using a multiple regression technique and the maximum tractive efficiency point was identified by searching the surface for its maximum point.

Sufficient data were required to compute a representative tractive efficiency response surface and a control sequence was developed to step the tyre through its dynamic load and inflation pressure range to achieve this. A number of factors influenced the design of the system and these are outlined below:

(a) The maximum tractive efficiency point was to be established as quickly as possible. It was important to complete the optimization process before any changes occurred in the operating conditions. This could be a problem during on farm operations if optimization was a lengthy process.

(b) Hydraulic systems which would vary the dynamic load were inherently faster acting than air inflation systems.

This meant that it was possible to vary the dynamic load over its operating range at a faster rate than the inflation pressure could be varied over its range.

(c) The pressure differential between the air in the reservoir of the tyre inflation system and that in the tyre was much greater than that between the air in the tyre and the atmosphere. This meant that the pumping rate of the tyre was about twice the leak rate or the rate at which the tyre could be deflated by exhausting the air in the tyre.

(d) The test had to be started at a load which would ensure sufficient traction to be developed for the net traction selected for the test.

(e) The minimum dynamic load required to obtain the desired net traction in the soil condition had to be established during each particular test.

(f) The system had to be flexible enough to enable the operator to vary as many parameters as possible.

(g) The wheel slip was limited to a maximum of 25%. This was commonly considered a reasonable maximum limit because maximum tractive efficiency would not occur at wheel slip levels above this level.

Certain variables listed below had to be initialized at the beginning of a test run:

(a) The net traction required for the particular test.

(b) The maximum rate at which the dynamic load was varied, DL RATE.

(c) The number of steps, NU STEP, to cover the operating range of the tyre.

The DL RATE was set as a variable to facilitate runs to determine the maximum DL RATE that could be achieved without compromising the stability of the system. The number of steps was set as a variable to minimize the time taken to determine the response surface while acquiring sufficient data to compute a representative surface.

To conserve soil bin area, and with the exception of the first test in a lane, each test run was started on a used test zone to enable the initial target to be attained before the SWTRV reached the current test zone. The computer programme monitored the operating parameters and once the initial target had been reached, this information was displayed to the SWTRV operator who waited for the test zone to be reached before initiating the data acquisition cycle and optimization routine.

A schematic of the procedure used is shown in Figure 16 where:

IPr min is the minimum inflation pressure of the tyre, selected by the operator and normally determined by the tyre specifications.

IPr max is the maximum inflation pressure of the tyre, selected by the operator and normally determined by the tyre specifications.

DL min is the lowest dynamic load expected on a tractor fitted with this particular tyre and is fixed by the tractor mass.

DL max is the maximum dynamic load at any inflation pressure, normally within the recommended inflation pressure range. This is calculated by using the maximum recommended static load at that pressure and the dynamic weight transfer as determined by the procedures provided in ASAE Data D230.4 (ASAE Standards, 1988).

TE max is the point identified by a search of the response surface as the dynamic load-inflation pressure combination resulting in maximum tractive efficiency.

A flow chart and discussion of the control programme is presented in Appendix A.

The operating parameters IPr min, IPr max and DL min were used as variables in the algorithm to enable researchers to investigate the tyre's performance outside the recommended tyre ranges.

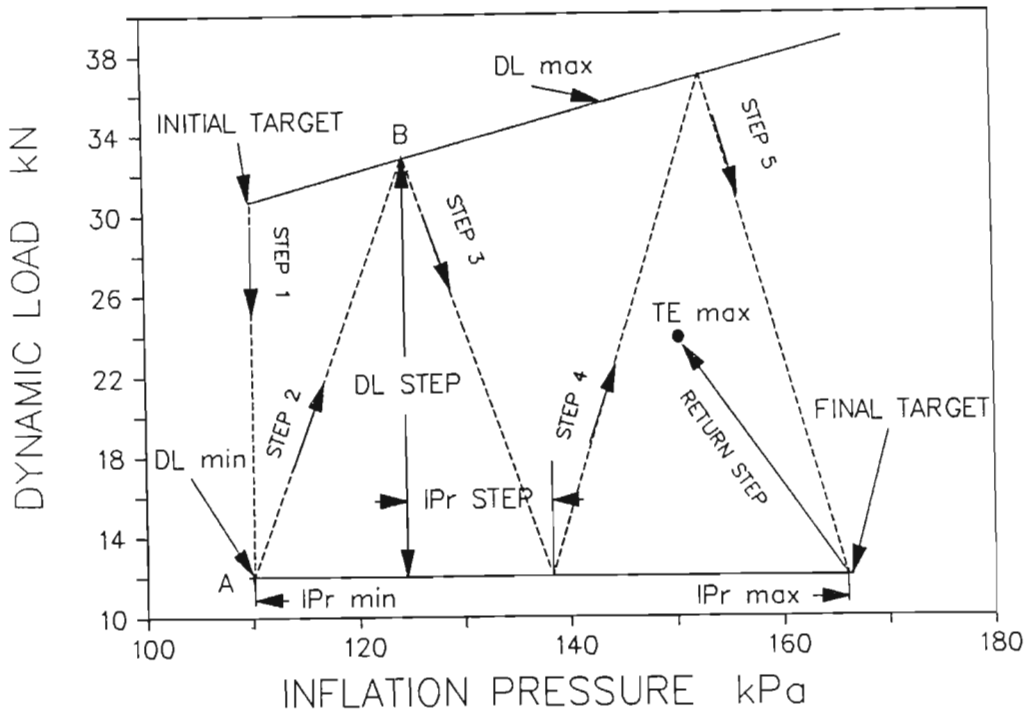

Figure 16 Optimization procedure for determining maximum tractive efficiency point (after Lyne and Burt, 1989).

The initial target was set at the lowest pressure, IPr min because it was faster to increase inflation pressure than decrease it. The initial target was also set at the maximum dynamic load DL max at the inflation pressure IPr min, this was to ensure that the required traction could be achieved without excessive wheel slip (see Figure 16).

The maximum wheel slip limit was achieved by arranging that during step 1 the inflation pressure was held constant and the dynamic load was reduced to the point where a limiting factor of either DL min or 25% wheel slip was reached. This determined the minimum dynamic load to be used for the

particular run and enabled the net traction to be achieved without excessive wheel slip. If the dynamic load at this point was greater than the DL min initially selected DL min was reset to the current value.

From this point, A in Figure 16 to the final target the inflation pressure was gradually increased to IPr max while the dynamic load was cycled between DL min and DL max. It was arranged in this manner because the dynamic load could be varied at a much faster rate than the inflation pressure could be varied. Data were collected while the tyre was operating between the initial target and final target.

The inflation pressure step IPr STEP from point A to point B and dynamic load step DL STEP between the same points for step 2 illustrated in Figure 16 were then computed. The DL RATE (rate at which DL was varied) and the PUMP RATE (rate at which inflation pressure was increased) were determined so that the tyre would move directly from point A to point B. It was desirable that this occur as rapidly as possible while remaining within the limits selected by the operator.

The remainder of the steps were completed in a similar fashion. A typical run with five steps as shown in Figure 16 took approximately 20s to complete. This depended on the net traction required during the test and the soil conditions which determined the DL min that was reached before step 1 was terminated.

Once the final target had been reached the tractive efficiency response surface was computed from the data collected during the cycling procedure. A complete second order linear model of the form presented earlier in equation (13) was used to represent the response surface. The tractive efficiency, inflation pressure and dynamic load data were used to determine the coefficients for the model. Standard matrix algebra procedures was employed to solve for the coefficients of the normal equations to minimize the sum of squares of the residuals.

To minimize the processing time required to solve for the coefficients, the matrix and vector comprising the number of points, sums, sums of squares and sums of products were filled during the data acquisition cycle as each set of readings were taken. This resulted in a significant saving of between three and four seconds in CPU processing time depending on the length of the test run.

Once the last step was complete, the matrix was inverted and the coefficients determined yielding the tractive efficiency response surface for the particular conditions. This step required approximately 100ms of processing time.

The maximum value of tractive efficiency for this surface over the range of the data was determined using the direct search method of Hooke and Jeeves which is a ridge seeking,

hill-climbing routine (Siddall, 1982). Further details of this technique are presented in Appendix C.

The dynamic load and inflation pressure conditions for this optimum efficiency were then automatically applied to the tyre providing the return step illustrated in Figure 16 in order to acquire steady-state data at TE MAX. The data were stored and used at a later stage to quantify the accuracy of the TE MAX determined from the regression surface.

A suitable procedure for varying dynamic load and inflation pressure in real time to arrive at a maximum tractive efficiency via regression modelling and a direct search algorithm had been established. The next step was to evaluate the procedure over a realistic range of operating conditions.

4 EVALUATION OF OPTIMIZATION ALGORITHM

It was necessary to develop a procedure to validate the control and optimization system under conditions simulating those which would be encountered during field operations. The tyre was subjected to a practical range of dynamic loads, inflation pressures, net traction levels and soil conditions.

4.1 Test specification

The general purpose nature of the tractor means that there are no absolute specifications for the various operating parameters. These parameters include the dynamic load on the drive wheels, the tyre inflation pressures, the draught requirements of implements and the soil conditions on which the tractor operates. For the evaluating process to be realistic certain assumptions had to be made in the selection of these parameters.

4.1.1 Tyre, dynamic load and inflation pressure

The main criteria that were applied in the evaluation were firstly, that the tyre should be a common size, and secondly, that the dynamic load on the drive wheel and tyre inflation pressure should vary over the range that could be expected

during field operations. At the same time care was taken not to operate the tyre beyond the dynamic load-inflation pressure limits specified by the Tire and Rim Association Inc., USA (1988).

A radial ply 18.4R34 tyre was selected as being a very common drive wheel size in use on agricultural tractors. The Tire and Rim Association Inc. specify safe inflation pressure limits at various static loads for the tyre as shown in Table 2.

Table 2 Static tyre load and inflation pressure limits for an 18.4R34 Radial ply tyre used as a single wheel (after the Tire and Rim Association Inc. of the USA, 1988).

Load limits (kN) at various inflation pressures (kPa)					
kPa	110	124	138	152	166
kN	23,5	25,3	26,7	28,2	29,4

The pressure limits shown in Table 2 apply to the static load on a tyre, However, to simulate the conditions on a tractor the expected weight transfer and resulting dynamic load on the drive wheel had to be determined. The dynamic load on the drive wheels was equal to the soil reaction (W_r), shown

in Figure 17 and equation (14) and was calculated by using the tractor dimensions and the line of pull of the implement. Figure 17 illustrates the forces which determine the dynamic load on the drive wheels.

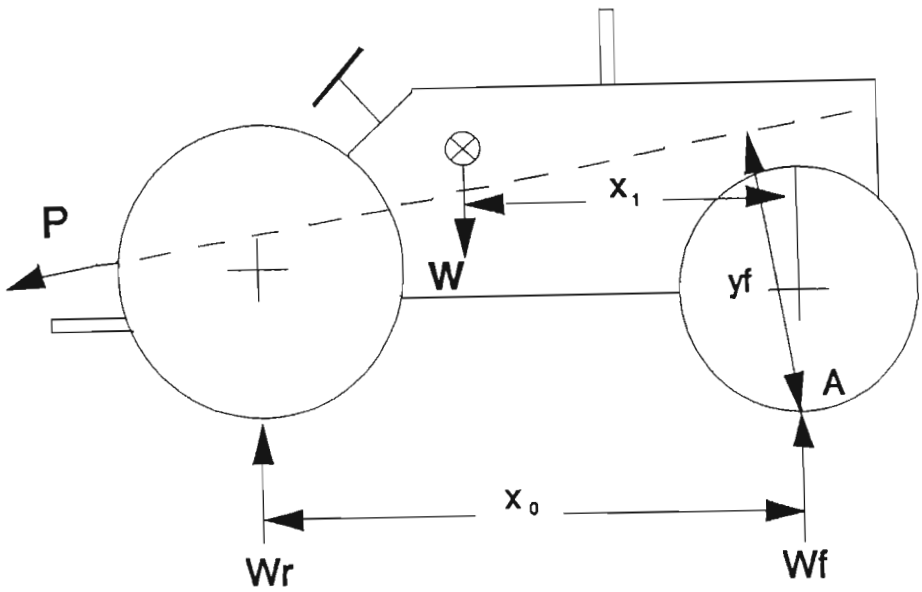

Figure 17 External forces on a tractor implement system which control weight transfer.

$$W_r = \frac{P\, y_f + W\, x_1}{x_0} \qquad \text{.....(14)}$$

Where W = static weight of the tractor

P = pull of the implement.

The line of pull depended on many factors such as the type of implement and hitch system, the state of repair and adjustment of the implement and the soil properties. It was thus not possible to fix an absolute maximum level of dynamic

load that would be reached during field operations at various levels of static load. Consequently estimates were made to determine the practical levels of dynamic load that would be encountered. The specifications of a Massey Ferguson 298 were chosen and used to compute the expected dynamic load on the drive wheels. This particular model was selected because it was a popular tractor and it used the 18.4R34 tyre as standard in a 2WD configuration with single wheels on each drive axle.

In order to determine the maximum expected dynamic load the predictor charts in ASAE Data D230.4 (ASAE Standards, 1988) were used to determine the pull and the weight transfer. In using the predictor charts the following assumptions were made:

(a) The tractor would operate on firm soil conditions, this would result in high levels of pull and weight transfer.
(b) The tractor would operate at a design wheel slip of 9% for firm conditions to give maximum tractive efficiency.
(c) The tractor would be hitched to a fully mounted implement to give maximum weight transfer.
(d) The tractor would operate at 6km/h. This is the lowest speed that should be used to transmit maximum engine power to the drive wheels and develop a high pull without stressing the transmission.

The Massey Ferguson 298 had an axle power of 56.6kW, a static rear axle load of 23.8kN and a total tractor weight of 35.42kN. The predictor chart was then used to determine the drawbar pull for this tractor if the rear wheels were ballasted to each of the static loads provided in Table 2. By using a dynamic weight transfer coefficient of 0,65 for a mounted implement the dynamic load for the wheels in each case were calculated, providing the values provided in Table 3.

Table 3 Weight transfer and dynamic load at 6km/h and at maximum drawbar power for a range of static rear axle forces (SRAF) on a Massey Ferguson 298 tractor fitted with 18.4R34 tyres.

IPr kPa	Max. Load kN	SRAF kN	Pull kN	Weight Transfer kN	Dynamic Load kN
110	23,5	47,0	23,2	15,1	31,0
124	25,3	50,6	24,9	16,2	33,4
138	26,7	53,4	26,3	17,1	35,3
152	28,2	56,4	27,8	18,1	37,2
166	29,4	58,8	29,0	18,8	38,8

The resultant dynamic load-inflation pressure range is summarized in Figure 18 and shows the maximum permitted load on the tyre over the selected inflation pressure range. The minimum load is fixed by equation (14) with the pull equal to zero. The specified operating range of the tyre in terms of the maximum dynamic load at any inflation pressure had thus

been defined. At any stage during the evaluation, the optimization algorithm ensured that the dynamic load-inflation pressure combination was within this operating range.

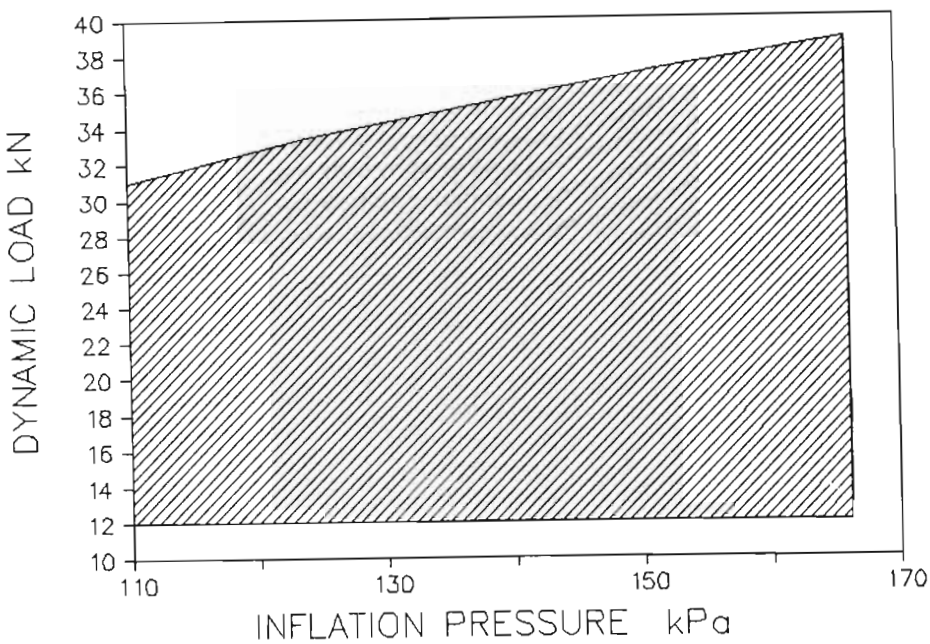

Figure 18 The dynamic load-inflation pressure operating area of a 18.4R34 radial ply tyre.

4.1.2 Net traction and soil conditions

The selection of net traction was based on the dynamic load that the tyre was to be subjected to. Results published by Burt et al. (1983) indicated that a high tractive efficiency was obtained at traction ratios of between 0,3 and 0,4 and Dwyer (1984) stated that maximum tractive efficiency occurred at a traction ratio of 0,4. It was therefore deduced that

maximum efficiency for the high dynamic loads would occur at a net traction in the region of 12kN. To provide for a reasonable operating range, levels of net traction varying from 3kN to 12kN were selected as desirable for the experiment. In practice this would cover the drawbar requirements of the medium to high draft implements used with the Massey Ferguson 298 tractor, and also correspond to the range where a high tractive efficiency would be of most concern to the operator.

The soil types and their preparations were selected to cover as wide a range of conditions that a tractor was likely to encounter in the field. The evaluation runs were carried out on the indoor soil bins at the USDA's National Soil Dynamics Laboratory. The indoor bins were used to assist in maintaining stable soil parameters during the evaluation programme.

The two soil types that were chosen, were a Decatur clay loam and a Norfolk sandy loam. Each soil was prepared initially in a firm condition and subsequently in a loose condition, this preparation was referred to as a soil fitting. The soil contained a compacted layer to simulate a hard pan at a depth of approximately 350mm. The firm soil received additional compaction near the soil surface to simulate a field which had been ploughed to a depth of 250mm and subsequently disced. The loose soil was completely loose between the hard pan and the soil surface. The soil moisture content and bulk

density characteristics are presented in Table 4. The cone penetrometer index-depth curves for the four soil conditions are presented in Appendix D.

Table 4 Soil characteristics of the four soil conditions used for the system evaluation (after Lyne and Burt, 1989).

Soil Type	Prepared Condition	Depth (mm)	Mean Moisture Content %	Mean Bulk Density gm/cc	Mean Cone Index mPa
Norfolk	Firm	10	6,7	1,2	0,01
		90	7,4	1,6	0,4
		140	-	-	1,5(a)
		320	7,4	1,8	1,9(b)
Norfolk	Loose	40	7,1	1,3	0,05
		320	7,5	1,6	0,7
		375	-	-	1,7(b)
Decatur	Firm	10	11,1	1,1	0,05
		90	12,9	1,5	1,7(a)
		270	12,3	1,6	2,5(b)
Decatur	Loose	30	11,7	1,1	0,05
		300	12,4	1,6	1,0
		360	-	-	2,3(b)

(a) A cone index peak due to soil preparation.

(b) Peak cone index within the simulated hardpan.

4.2 Experimental procedure and data capture

The advantage of using a soil bin was that uniform conditions could be obtained within the bin, however, there was only a limited area of soil available. Therefore, there had to be a compromise between the length of a test run and the range of individual tests. In the test design it was necessary to limit the length of each run while still collecting sufficient data to produce a representative tractive efficiency surface and to cover as wide a range of test conditions as possible. Once these conditions had been determined, test zones in the soil bins were allocated and the sequence of events within each test set out.

The main factors affecting the length of the runs were:

(a) The speed at which the SWTRV travelled in the soil bin.

(b) The rate at which the dynamic load was varied.

(c) The net traction selected.

(d) The number of steps used during the optimization routine.

(e) The time taken to move from the final step to the maximum tractive efficiency point.

Burt and Lyne (1985) showed that between the speeds of 0,1 and 0,6 m/s the forward velocity of a tyre had no significant influence on its tractive efficiency. A practical minimum speed for the SWTRV was 0,15 m/s and to limit the rate at

which the soil bin area was used up this speed was selected for the tests.

Trial runs indicated that at a dynamic load ramp of 1,5 kN/s the optimization routine ran smoothly, but, if it was increased above this value there was a noticeable jerk as the routine changed from one step to the next. This DL RATE was thus used as the default value in the programme.

At the higher net traction levels and as the dynamic load was reduced it did not take as long as with the low net traction levels to reach the minimum dynamic load (DL MIN) necessary to limit wheel slip to 25%. This resulted in shorter runs at the higher net traction levels.

It was found that selecting more than five steps in the routine caused a data buffer overflow problem. Using five steps still provided good coverage of the tyre operating area and as will be shown later a good fit for the response surface was generated by the data. The time taken to move from the end of the optimization routine to the optimum tractive efficiency point varied considerably during trial runs and depended on the relative position of the final target and the estimated TE MAX point. The average distance for the trial runs was 14m and this was then selected as an optimum bin length required for a test run.

It was considered necessary that the range of tests should include the following:

(a) Four levels of net traction, the four points would show trends that occurred as the net traction varied from a low level of 3kN to a high level of 12kN.

(b) Three replications at each net traction level randomly located in the soil bin to account for any variation in soil condition.

(c) A zero net traction test to determine the rolling radius of the wheel as a function of dynamic load, inflation pressure and soil type. Spare test areas were set aside to rerun any aborted tests. Any vacant soil area was used to investigate tyre operation beyond the specified operating range. This range of tests resulted in a minimum requirement of 13 test zones in each selected soil treatment. With a test run length of 14m three tests could be fitted into the length of the bin. The width of the bin was sufficient to enable five separate lanes to be used, thus giving a total of fifteen test zones with two spare test zones.

The resulting layout for the Norfolk sandy loam in a loose condition and the test code key used throughout the tests are shown in Table 5. The other three test plans are presented in Appendix E. The SWTRV operated from South to North with the centre of the first lane being 1,27m from the West side and each subsequent lane being 0,84m to the east of the previous lane.

Table 5 Test plan and code for the Norfolk sandy loam in a loose condition.

Soil: Norfolk sandy loam Fitting: Loose North				
Lane				
1 (1,27m)	2 (2,11m)	3 (2,95m)	4 (3,78m)	5 (4,62m)
S11RR1	S1206P	S1306P	S14032	S15033
S11062	S12093	S13122	S14123	S15063
S11091	S12121	S13031	S14092	S15061
South				

Test Code				
Fitting	Soil	Lane	NT	Rep
F S	1 2	1 2 3 4 5	03 06 09 12	1 2 3 P

The soil fitting F in Table 5 referred to the firm condition and S the loose or soft condition. Soil 1 denoted the Norfolk sandy loam and soil 2 the Decatur clay loam. The net traction (NT) varied from 3kN to 12kN in steps of 3kN and RR was used to designate a rolling radius test as shown in the top left corner of the layout in Table 5. There were 3 replications (Rep 1, 2 and 3) at each net traction level. If a problem occurred during a test it was repeated in a spare zone. The suffix P was used to designate a run beyond the extended range.

The tests were carried out sequentially along each of the lanes 1 to 5. The sequence for each test is outlined as follows:

(a) Once the soil had been prepared it was covered with a plastic sheet to prevent evaporation and then left overnight.

(b) The optimization tests were started and completed in one session the following day to reduce moisture changes to a minimum.

(c) The soil bin was then re-covered and the soil parameters measured on the third day.

The optimization programme was loaded and each test run individually. At the end of each test a data summary including means, standard deviations and a graphic display was produced so that the results could be visually evaluated for any possible errors. If everything appeared normal the

data were archived and the next test run commenced, with each lane being completed before the next was started. If a test was aborted the next available test zone was allocated for a re-run.

The sequence of tests for the four soil conditions were firm clay, loose clay, firm sand and loose sand. The transducer signals were recorded and then used to compute the following variables: dynamic load, net traction, axle torque, ground speed, angular velocity, inflation pressure, tractive efficiency and the distance travelled after control and data acquisition were initiated. As an example the results of a 6kN test (test F14061) in the firm sand condition are presented in Figure 19, showing the change in dynamic load and inflation pressure during the optimization cycle.

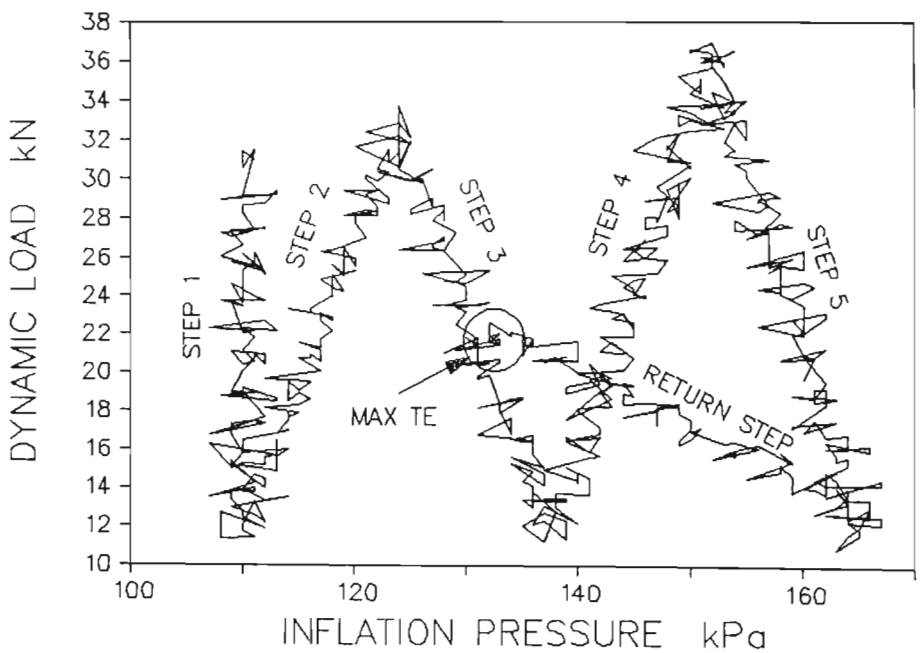

Figure 19 Dynamic load and inflation pressure variation during a test run.

Steps 1 to 5 were the data collection steps after which the tractive efficiency response surface was computed and the maximum tractive efficiency point found. Figure 19 shows the return step to the maximum tractive efficiency point.

An example of a test is shown in Figure 20 where the net traction and forward velocity of the test wheel were controlled at levels of 6kN and 0,15 m/s respectively. Figure 20 shows the variation of net traction and forward velocity for a typical run where the mean and standard deviation of the net traction was 6,021 kN and 0,455 respectively and the mean and standard deviation of the velocity was 0,15 m/s and 0,002 respectively. These indicate that the control system performed well during the test and this was confirmed by Lyne et al. (1987).

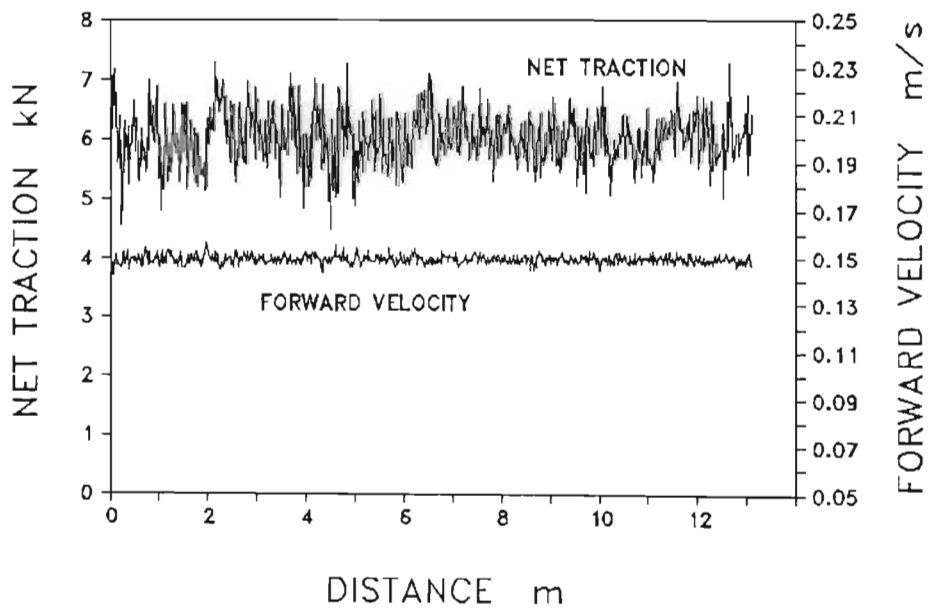

Figure 20 Net traction and forward velocity during a test run.

5 RESULTS AND DISCUSSION

The success of the optimization system that was developed depended on the ability of the general model, presented in section 2.3 on page 43 by equation (13), to provide a good estimate of the actual tractive efficiency response surface. This was validated by examining the actual surfaces determined during each run. The significance of the results was also investigated to estimate the value of the system.

5.1 Validation of the model

An analysis was carried out to validate the model used for the tractive efficiency response surface. Since tractive efficiency is a ratio represented by:

$$TE = \frac{\text{Forward velocity} * \text{Net traction}}{\text{Wheel angular velocity} * \text{Input torque}}$$

any noise that was present in the electronic signals representing the variables, forward velocity, net traction, input torque and angular velocity of the test wheel caused tractive efficiency to reflect an even greater noise. As an illustration, the variation in tractive efficiency that was measured for the three replications of the 3kN tests in the firm sand condition (F13031, F14032 and F15033) are shown in

Figure 21, replication 1, replication 2 and replication 3 respectively. The noise on the signals caused individual data of tractive efficiency to in some cases be greater than 1, this was however only random noise about the mean tractive efficiency. The overall variation in tractive efficiency and thus in the estimated tractive efficiency was the tractive efficiency response to the controlled change in dynamic load and inflation pressure during the test run.

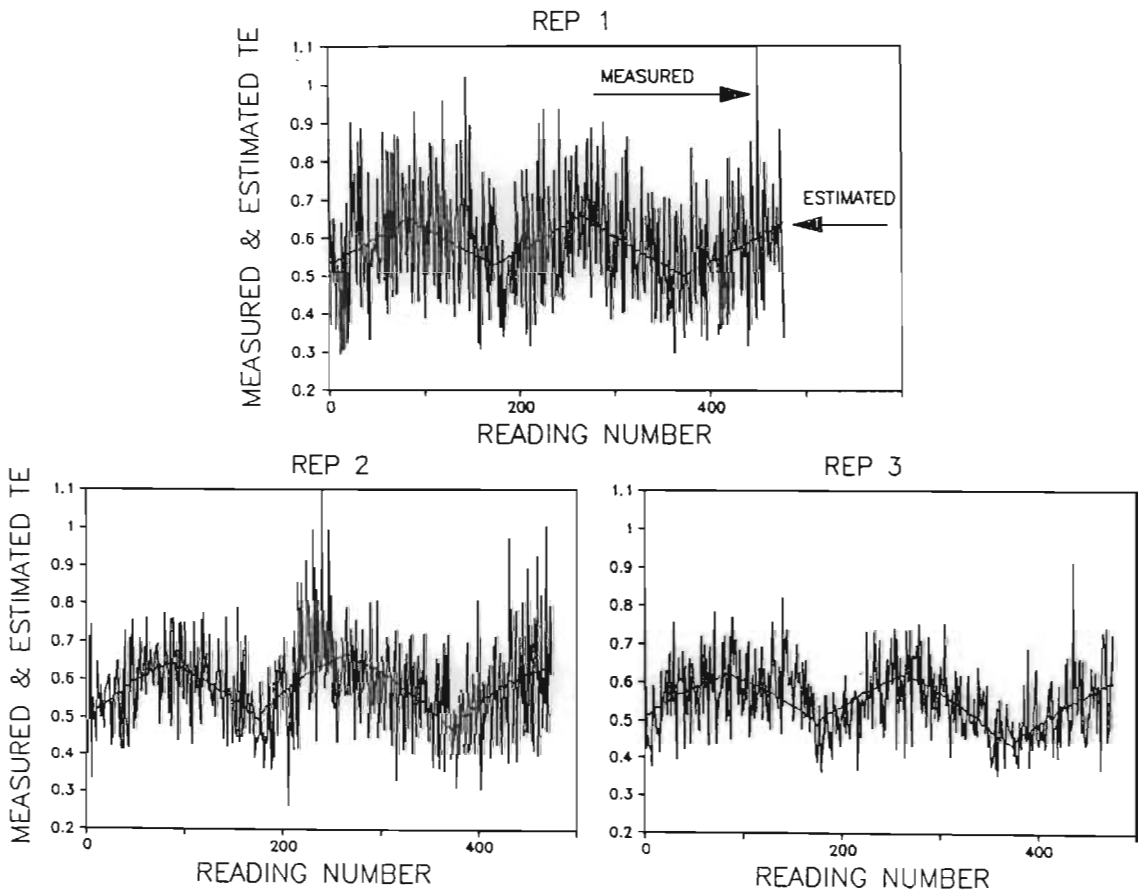

Figure 21 Measured tractive efficiency and the estimated tractive efficiency determined from the coefficients computed during an optimization routine for three replications carried out on a firm sand with a net traction of 3kN.

As the tractive efficiency surface described by equation (13) is relatively flat, the statistical correlation produced is relatively low and this was further affected by the noise. An analysis of variance of the model on the measured tractive efficiency for replication 1 in Figure 21 is shown in Table 6, and illustrates the low R-squared value and the large sum of squares for the error.

Table 6 Analysis of variance for the full regression of the model on measured tractive efficiency for run F13031.

Source	Sum of Squares	DF	Mean Square	F-Ratio	F 1%
Model	0,783461	5	0,156692	8,35164	< 3
Error	8,85559	472	0,0187618		
Total (Corr.)	9,63905	477			

R-squared = 0,0812798 Std error of est. = 0,136974

In order to determine the most appropriate method of reducing the variations shown in Figure 21 the tractive efficiency data were smoothed using a simple moving average of 5, 10 and 15 points respectively on either side of the target value to produce the curves shown in Figure 22 for the same three replications in Figure 21.

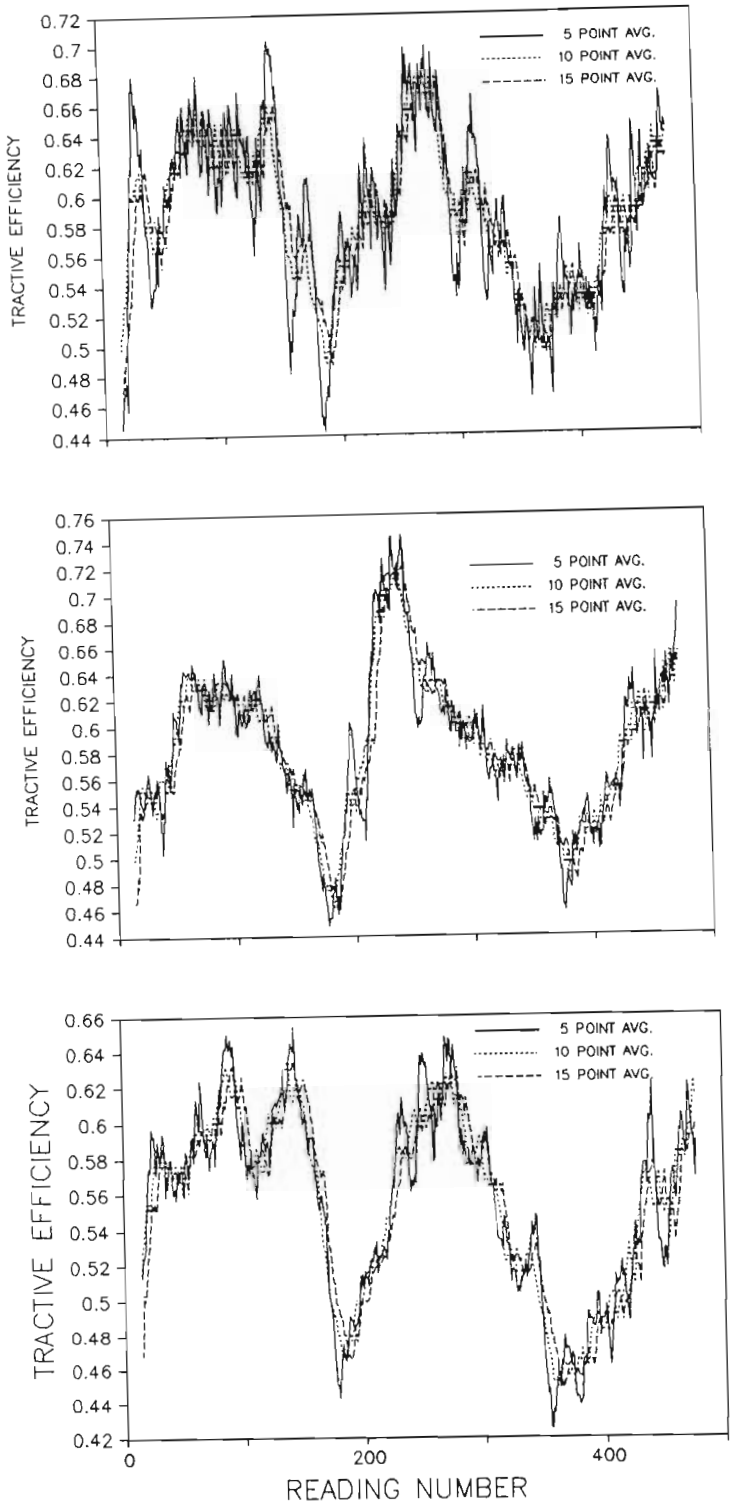

Figure 22 The 5pt, 10pt and 15pt moving average of tractive efficiency determined during an optimization routine carried out on a firm sand with a net traction of 3kN.

The difference between the measured tractive efficiency and the 15 point moving average for replication 1 in Figure 21 was plotted in Figure 23. The mean tractive efficiency and the variation of dynamic load during the cycle were also included in Figure 23. The deviations between the actual readings and the moving average are random and normally distributed about the mean and are not affected by the changing dynamic load. The normal distribution of the deviations justifies the use of a simple moving average as a smoothing technique.

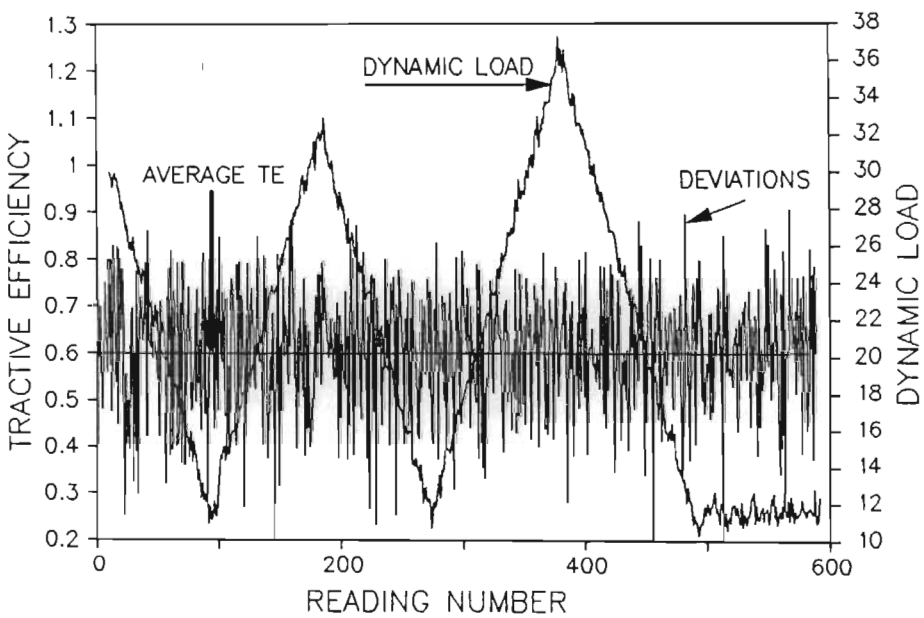

Figure 23 The distribution of the measured tractive efficiency about the average tractive efficiency and the dynamic load versus reading number for a firm sand with a net traction of 3kN.

The 15 point (31 term) simple average provided the highest level of smoothing and at the same time followed the tractive efficiency trend. A multiple regression was therefore carried out with the 15 point data and the analysis of variance is shown in Table 7. In spite of the low slope of the response surface a much improved statistical fit was obtained. The R-squared value increased from 0,08 to over 0,76 and the F ratio was highly significant at the 99% level.

Table 7 Analysis of variance for the full regression of the model on the smoothed tractive efficiency data determined during an optimization routine carried out on a firm sand with a net traction of 3kN.

Source	Sum of Squares	DF	Mean Square	F-Ratio	F 1%
Model	0,683702	5	0,136740	301,539	< 3
Error	0,214040	472	0,000453476		
Total (Corr.)	0,897743	477			

R-squared = 0,761579 Std error of est. = 0,021295

The estimated tractive efficiency using the coefficients determined during the optimization routine while running the soil bin tests, is plotted in Figure 24. Included in Figure 24 are the tractive efficiency estimated from the coefficients determined from the regression on the smoothed data, and the smoothed data. As can be seen the two estimates are very close and only deviate slightly from the

15 point data. The largest difference between the two estimates is 2% of the reading with the average being less than 1½%. These results show that the model provided an excellent representation of the measured data.

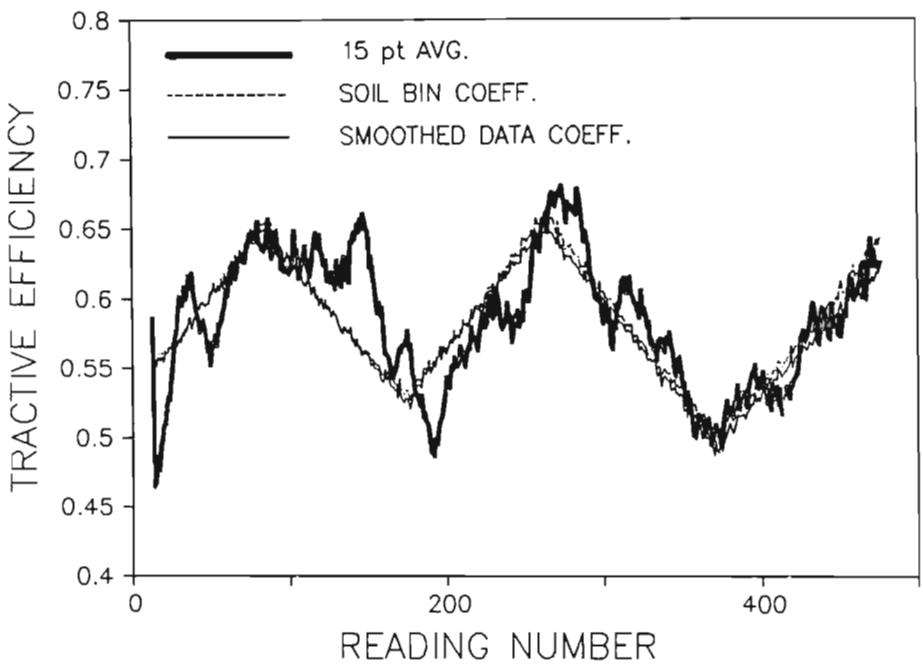

Figure 24 The 15 point moving average data and the tractive efficiency estimated from the measured data and the smoothed data for the optimization routine carried out on a firm sand with a net traction of 3kN.

Figure 25 shows three replications superimposed on each other for both a firm sand 3kN and a loose clay 12kN run. The curves are of estimated tractive efficiency versus, reading number. This highlights the small variation between replications and the large difference between the two sets

of tests as the dynamic load and inflation pressure varied during the cycle.

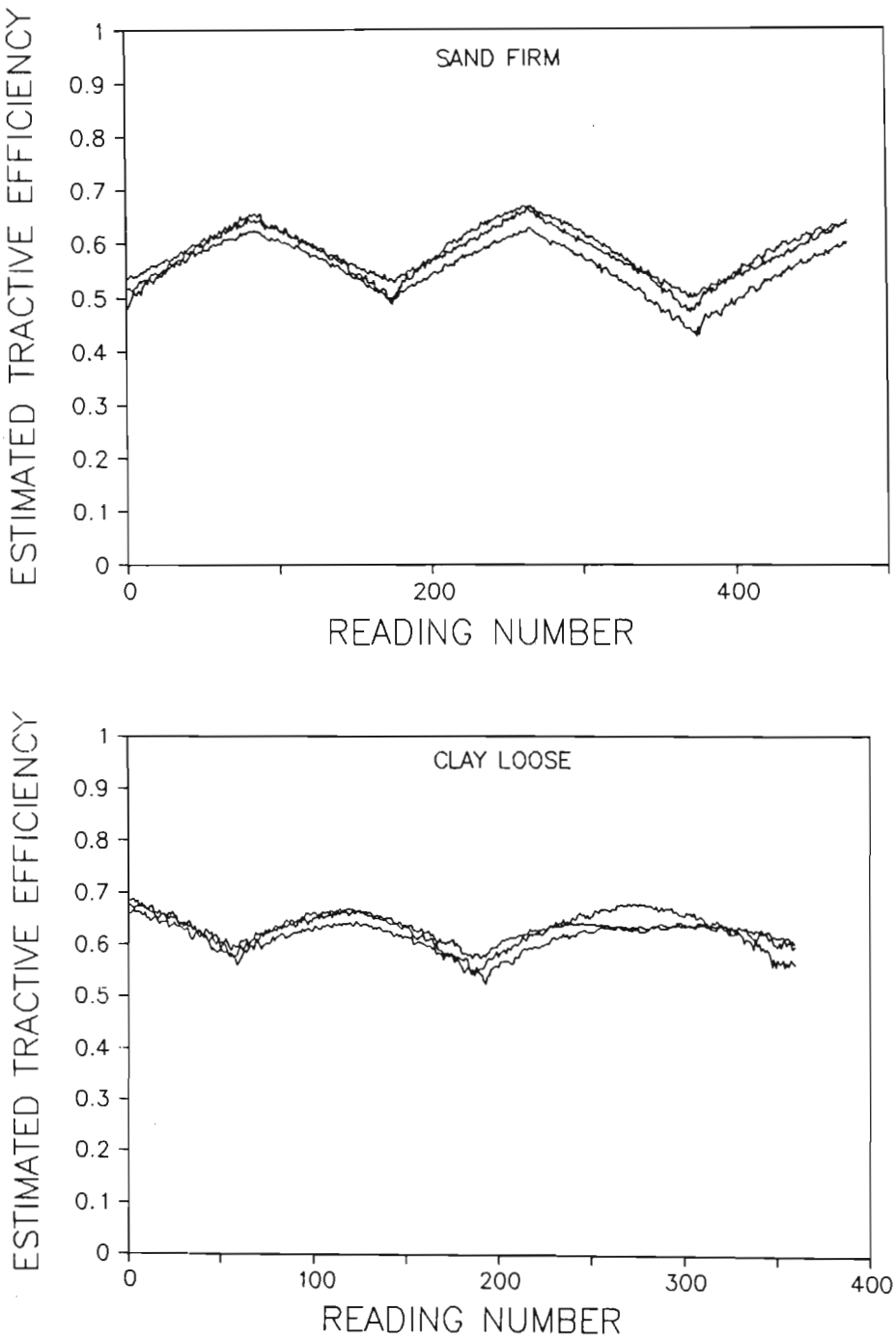

Figure 25 Replications of estimated tractive efficiency with reading number for a 3kN run in a firm sand and a 12kN run in a loose clay.

Two further aspects of the data that were investigated were:

(a) The variation in maximum tractive efficiency between the three replications.

(b) The differences in the maximum tractive efficiency determined from the response surface during the optimization routine and the actual measured tractive efficiency. Both sets of tractive efficiency were measured at the dynamic load-inflation pressure levels for the estimated maximum tractive efficiency point.

The details for the sandy loam soil are illustrated in Figure 26 and a summary of the data is presented in Appendix F.

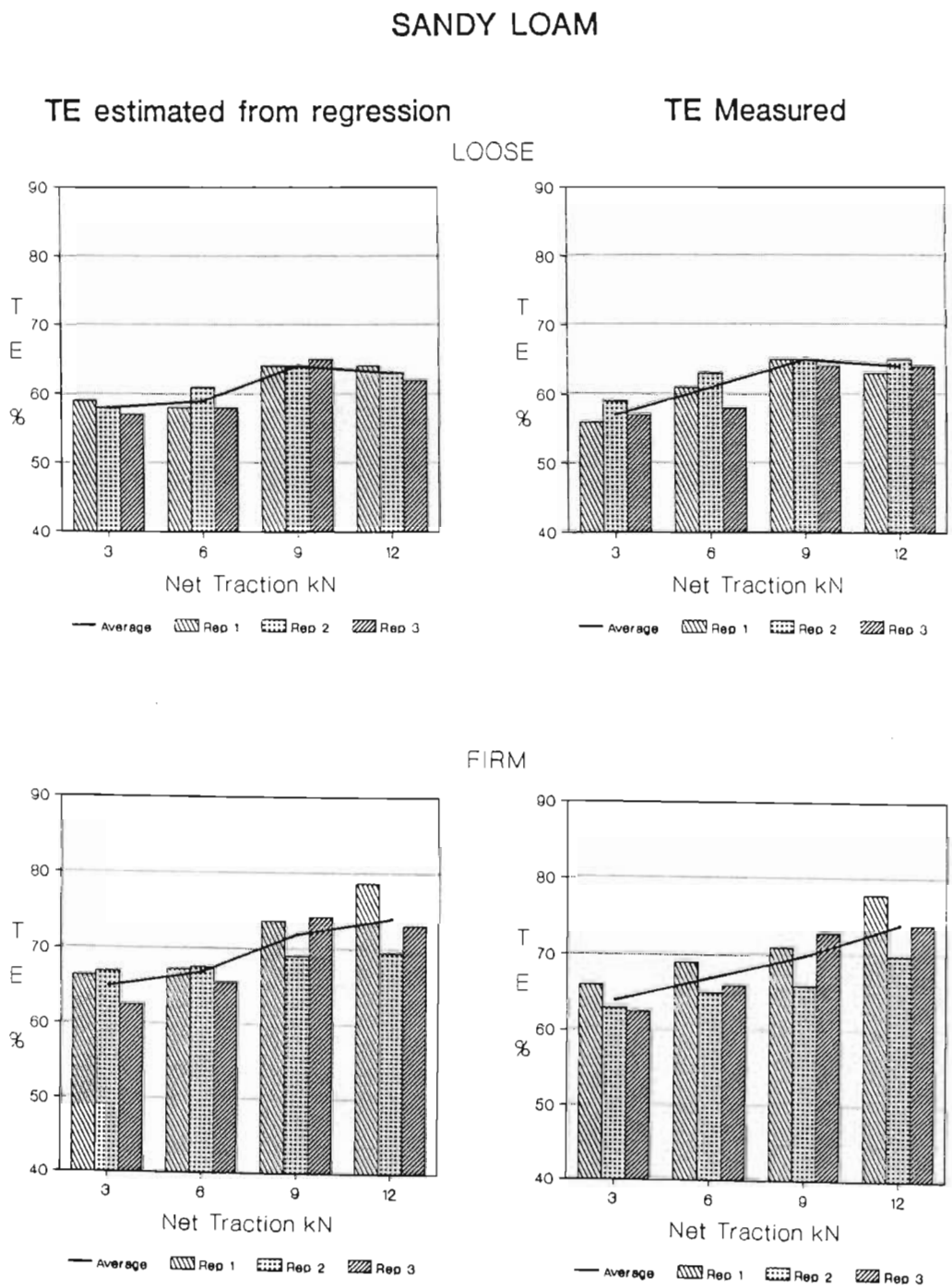

Figure 26 Maximum tractive efficiency and tractive efficiency measured at the maximum tractive efficiency point for each replication in the Norfolk sandy loam.

A difference of 5% occurred between the maximum tractive efficiency and measured tractive efficiency at the 3kN net traction level in the loose sand (replication 1). This was caused by an increase in travel reduction at the end of the optimization routine in the first replication (See Figure 27).

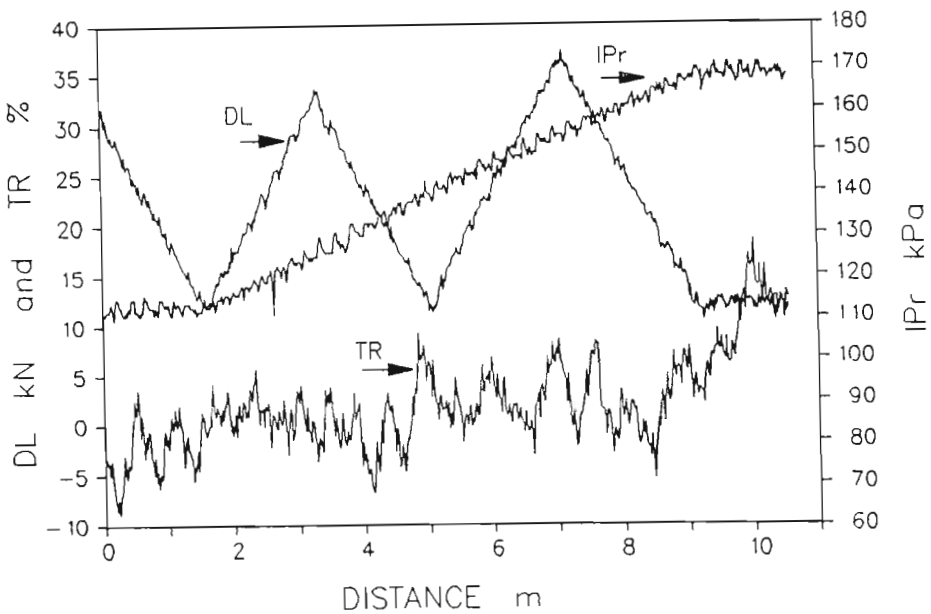

Figure 27 Dynamic load, inflation pressure and travel reduction versus distance travelled in the soil bin during a 3kN net traction test in the loose sand loam.

Figure 27 illustrates how the travel reduction varied with dynamic load and how it gradually increased as the inflation pressure was increased during the optimization routine. At a distance of 8,9m from the start of the test the travel reduction reached its highest level during the test, this coincided with maximum tractive efficiency. However, at this

stage the control system had been accelerating the wheel to maintain net traction as the inflation pressure was increased and dynamic load was decreased. The control system did not react quickly enough to maintain the wheel velocity constant once the dynamic load and inflation pressure had reached their targets at the maximum tractive efficiency point. The wheel slip kept increasing hence giving an unusually low, measured tractive efficiency for that particular test.

It can be seen in Figure 27 that at a distance of 10m the travel reduction had started to reduce. I concluded that if the test had continued the travel reduction would have decreased to the level reached at the 8,5m distance and tractive efficiency would have increased to the estimated level.

This problem highlighted a limitation with the optimization algorithm. In retrospect the algorithm should have started with a high inflation pressure to determine DL MIN and then reduced the pressure during the routine to ensure sufficient traction at all times. Because of the low leak rates this procedure would have meant longer test runs. Furthermore the problem had only occurred with the above run. Therefore the decision was made not to change the test procedure.

The differences in the maximum tractive efficiency determined from the response surface during the optimization routine and the actual measured tractive efficiency for the clay soil are

presented in Figure 28. A summary of this data is also provided in Appendix F.

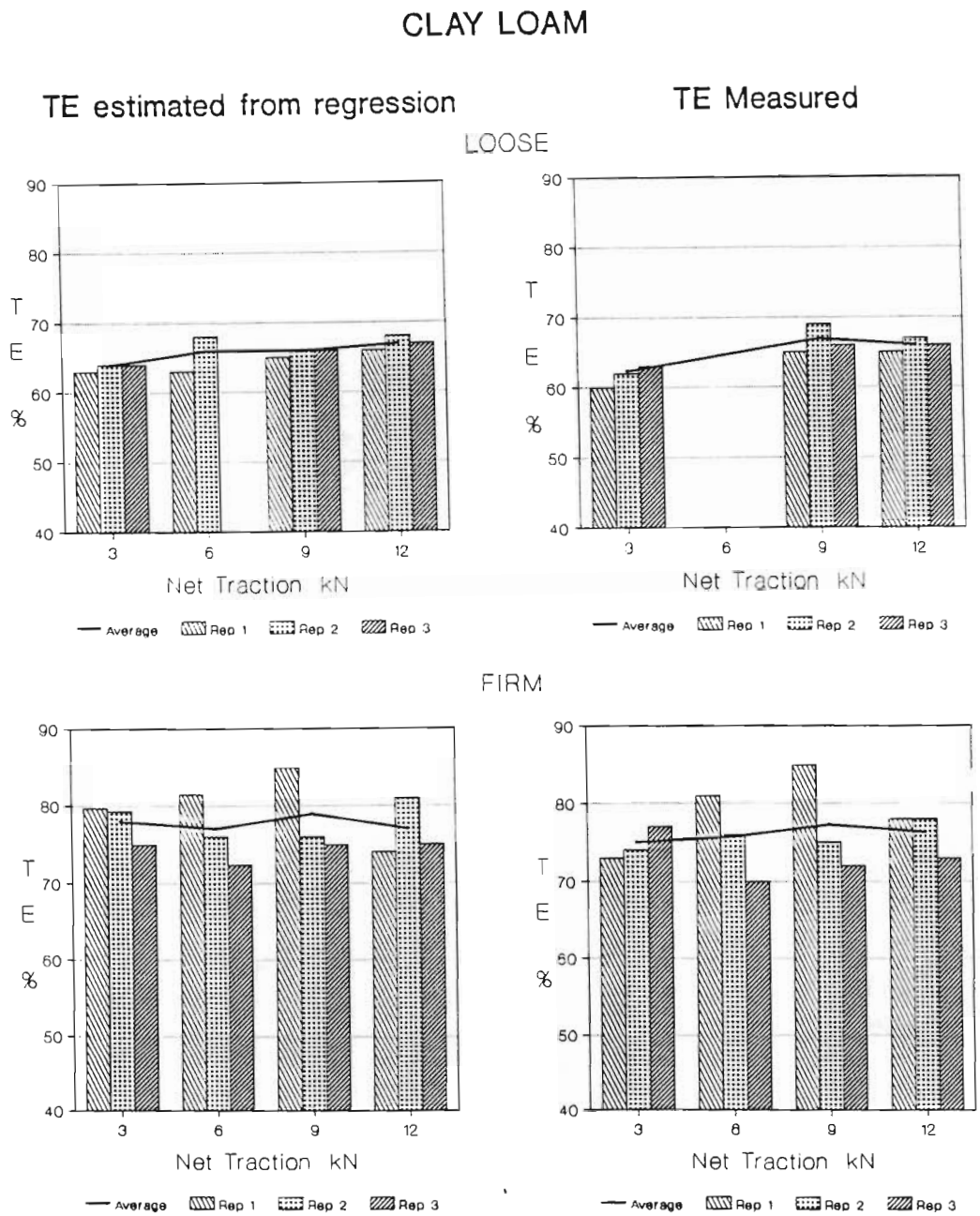

Figure 28 Maximum tractive efficiency and tractive efficiency measured at the maximum tractive efficiency point for each replication in the Decatur clay loam.

During the tests in the loose clay loam problems were encountered with the 6kN setting of net traction. This was caused by a logic error in the control programme which only became evident in this particular test. The control system did not return the tyre to the maximum tractive efficiency point and data were therefore not measured at this point. This fault also caused three tests to be aborted before maximum tractive efficiency was located which meant that two replications of the 6kN routine were only partially completed before all test areas were used. Therefore it was not possible to complete the test. Nevertheless it was concluded that the remaining tests provided sufficient results to be able to determine the trends and relative differences.

The differences between the replications are small and there is very good agreement between the estimated tractive efficiency and measured tractive efficiency. The one exception is the first replication at the 3kN level in the firm clay. Here the estimated maximum tractive efficiency was 80% and the value measured at that point was only 73%. Investigation showed that dynamic load had varied severely during the search process and had caused this discrepancy to occur.

This variation of dynamic load is illustrated in Figure 29. Once the final target had been reached at a distance of 9,2m

the control cycle was paused while the model coefficients were computed and the search routine executed. Although the duration of the pause was for less than a second, in some cases it caused instability when control was restored. In most cases this did not cause any difficulty, but, at the low net traction levels the tractive efficiency was extremely sensitive to dynamic load. The reason for this was that the minimum dynamic load of 12kN was relatively high for a net traction of 3kN.

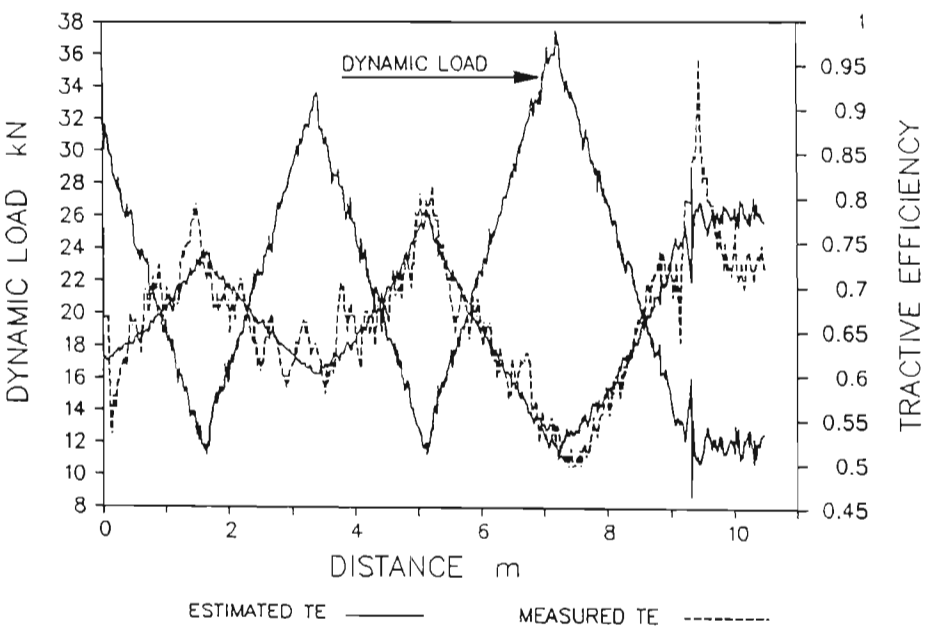

Figure 29 The dynamic load, estimated tractive efficiency and the measured tractive efficiency for a 3kN net traction test in a firm clay soil.

Figure 29 also shows that although the tractive efficiency varied substantially once control was restored it soon became steady and was beginning to increase when the test was

terminated. It was concluded that if the test had been extended the tractive efficiency would have increased to the estimated level.

The differences between the average of the three replications of maximum tractive efficiency and measured tractive efficiency for the loose sandy loam soil are presented in Figure 30. Again, there is good agreement between the estimated maximum tractive efficiency and the measured tractive efficiency with the maximum difference of 2,8% between the two occurring at 6kN net traction.

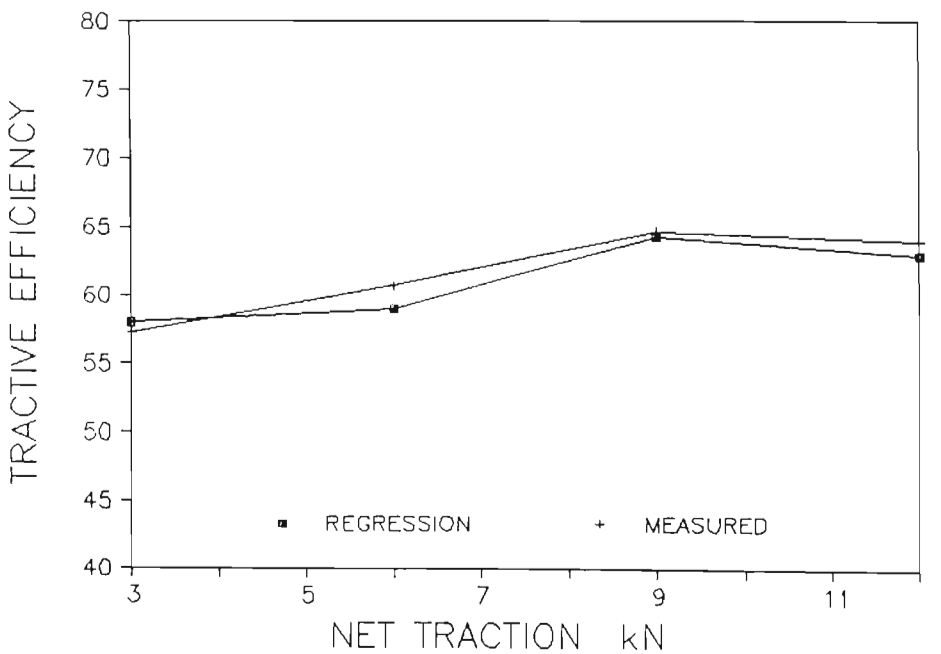

Figure 30 The average maximum regression tractive efficiency and the average maximum measured tractive efficiency for the Norfolk sandy loam in a loose condition.

Under the firm sandy conditions (see Figure 31) the differences were slightly greater being 3,3% at 9kN net traction. These differences were, however, significantly smaller than the differences between the tractive efficiencies measured at the various net traction levels.

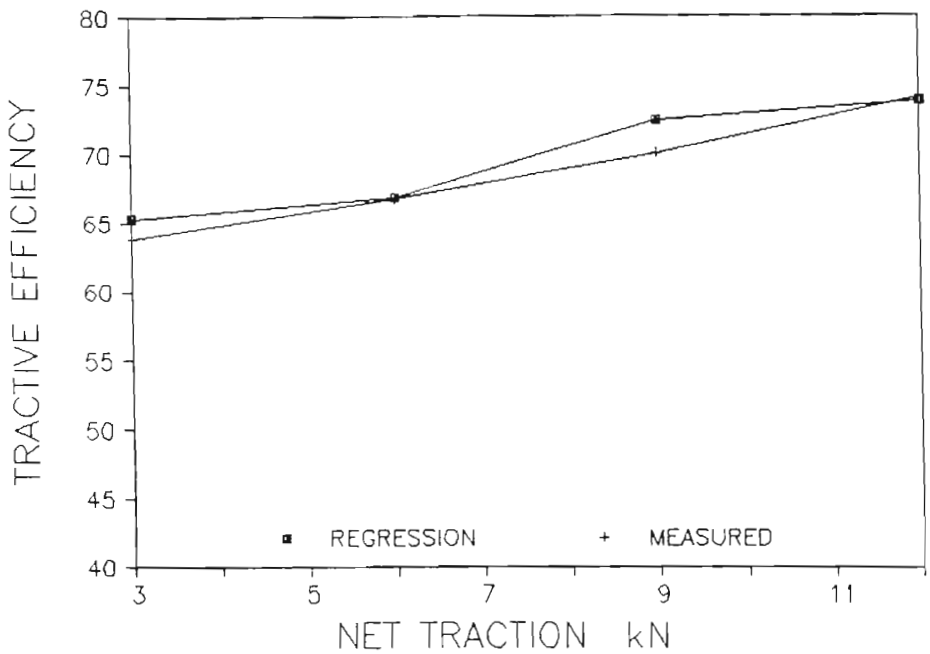

Figure 31 The average maximum regression tractive efficiency and the average maximum measured tractive efficiency for the Norfolk sandy loam in a firm condition.

The differences between the average of the three replications of maximum tractive efficiency and measured tractive efficiency for the loose clay loam soil are presented in Figure 32.

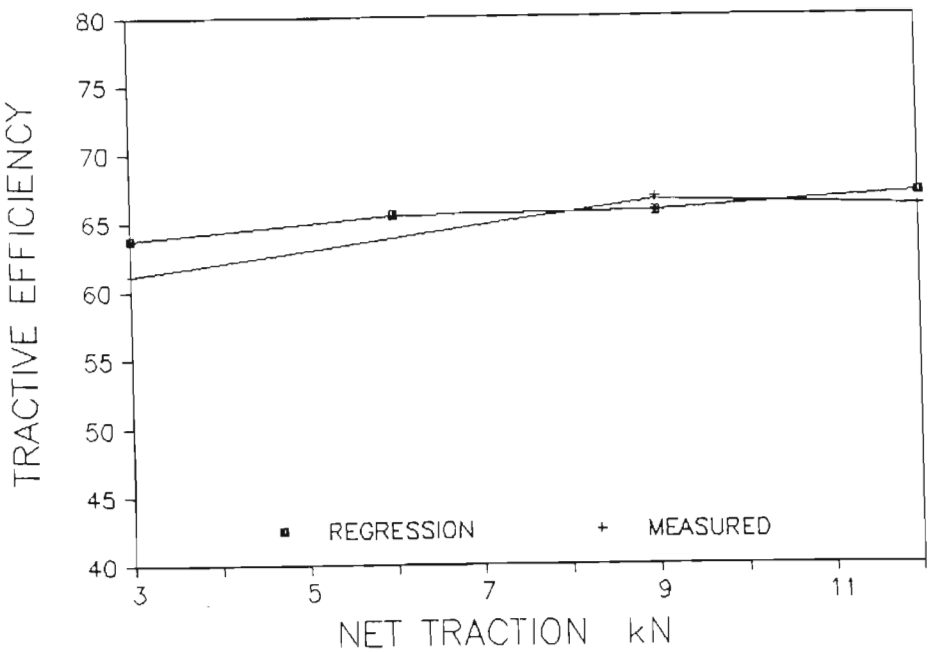

Figure 32 The average maximum regression tractive efficiency and the average maximum measured tractive efficiency for the Decatur clay loam in a loose condition.

The differences between the average of the three replications of maximum tractive efficiency and measured tractive efficiency for the firm clay loam soil are presented in Figure 33. It can be seen that at the 3kN level a large difference of 4% occurred between the estimated and measured tractive efficiency values. This difference resulted from the complication illustrated in Figure 29. The other differences were small with a maximum of 1,7% at the 9kN net traction level.

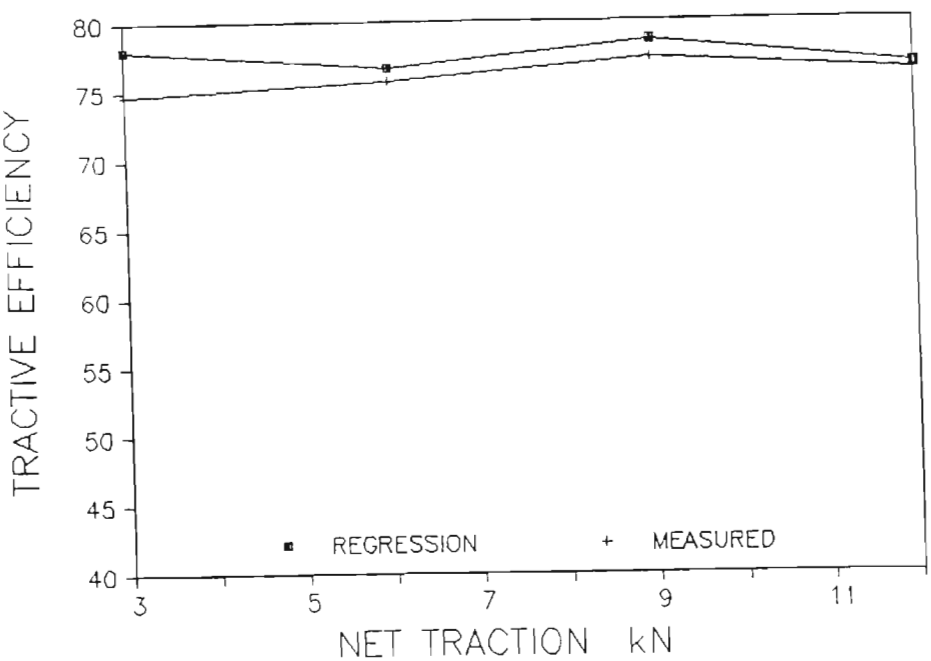

Figure 33 The average maximum regression tractive efficiency and the average maximum measured tractive efficiency for the Decatur clay loam in a firm condition.

From these results it was concluded that with very few exceptions caused by problems that were subsequently rectified, the system functioned exactly as was intended and that the model used to represent the tractive efficiency response surface provide results that were in excellent agreement with the values measured at the estimated maximum tractive efficiency point.

5.2 Optimization of tractive efficiency

To obtain an indication of how the tractive efficiency response surfaces varied with dynamic load and inflation pressure the response surfaces as represented by the model were generated from the measured data. Figure 34 presents typical contours of constant tractive efficiency for the Decatur clay loam soil in a loose condition with the tyre operating at 6kN net traction. These results show that tractive efficiency for the loose soil condition varied from 55% to 63% over the operating range of the tyre with the maximum occurring at an inflation pressure of 140kPa and at a dynamic load of 17kN.

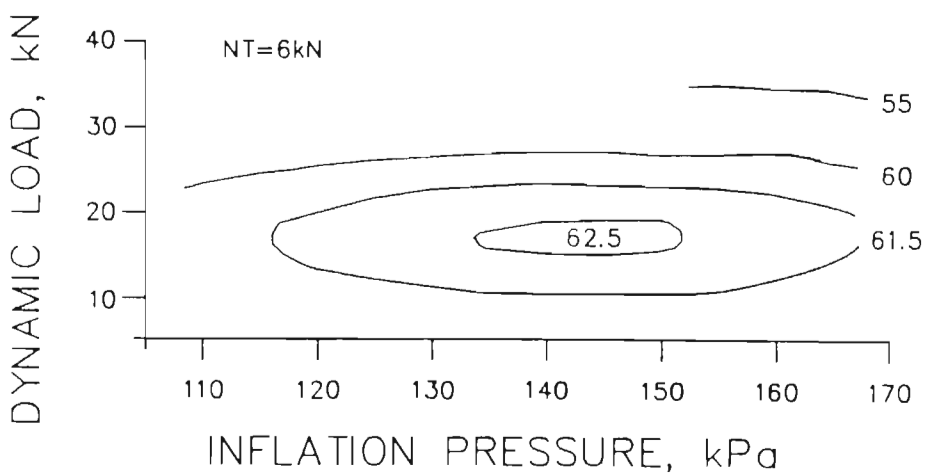

Figure 34 Contours on the tractive efficiency surface for Decatur clay loam soil in a loose condition for 6kN net traction (Lyne and Burt, 1989).

The shape of the surface varied substantially with soil type, soil condition and net traction. Contours from the tractive efficiency surface for a tyre operating at 3kN net traction on a Norfolk sandy loam in a loose condition are shown in Figure 35. The optimum tractive efficiency of 59,8% occurred at an inflation pressure of 118kPa and a dynamic load of 11kN. The minimum tractive efficiency for the results shown in Figure 35 is 38%. These results illustrate that the tractive efficiency surface is fairly uniform and flat, but highly dependent on small changes in soil condition and on the level of net traction demanded from the tyre.

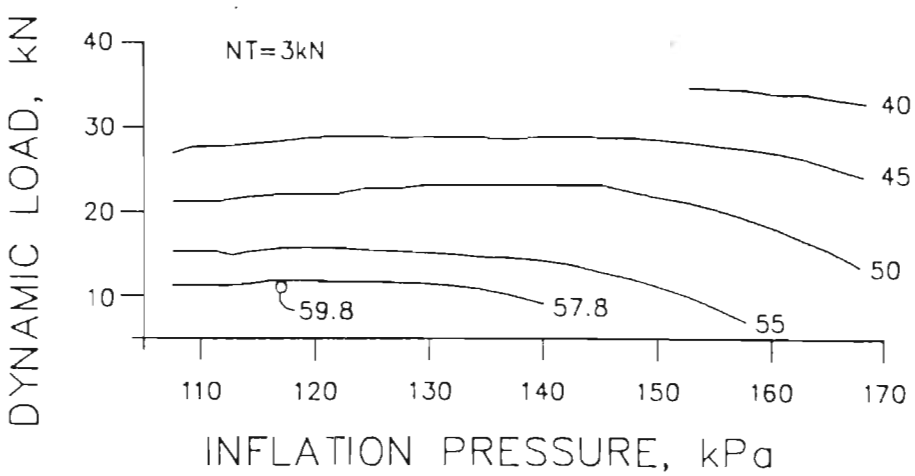

Figure 35 Contours on the tractive efficiency surface for Norfolk sandy loam soil in a loose condition for 3kN net traction (Lyne and Burt, 1989).

Figure 36 illustrates the dynamic load and inflation pressure inputs for a tyre operating at a constant net traction of 9kN on firm Norfolk sandy loam soil. The slip necessary for the

development of the 9kN net traction is also shown in Figure 36. These results indicated that at low dynamic load, slip was high in order to maintain the net traction level. When dynamic load was high, the slip was low. Under these conditions, the optimum tractive efficiency occurred at 30kN dynamic load, at 166kPa inflation pressure, and at a slip of 14%. Therefore, minimum slip is not a reliable criterion for determining the point of optimum tractive efficiency.

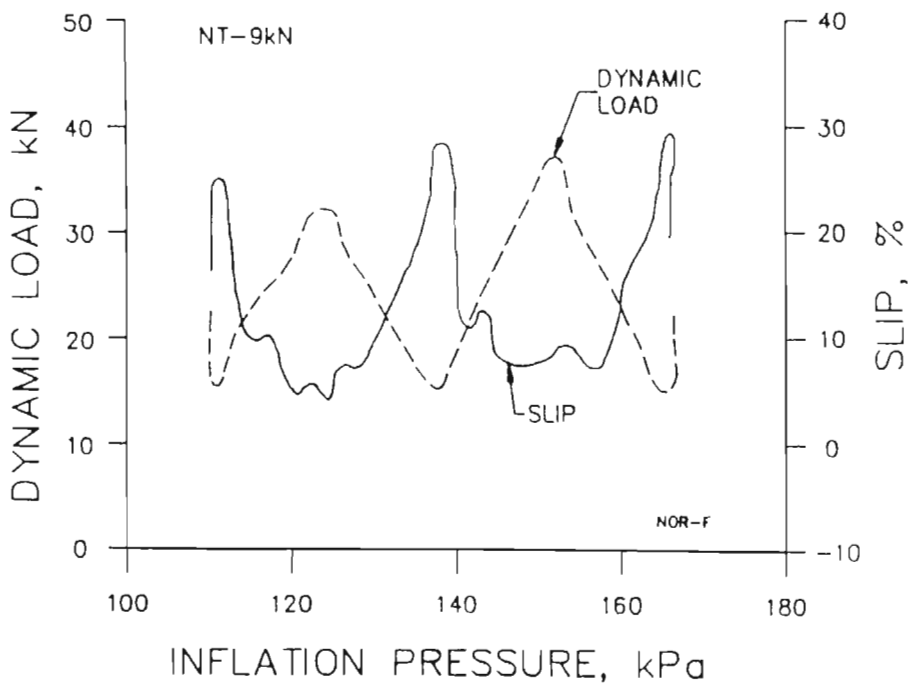

Figure 36 The dynamic load and slip versus inflation pressure on Norfolk sandy loam soil in a firm condition for 9kN net traction (Lyne and Burt, 1989).

If a practical system for optimizing tractive efficiency becomes commercially available, it should select the optimum

based on actual measured values of tractive efficiency rather than selecting values based on slip as many other systems have done.

Figures 37a and 37b present the minimum and the optimum tractive efficiency values that were determined on the Norfolk sandy loam soil over the net traction range of 3 to 12kN for the loose and firm soil conditions, respectively. The benefits from optimizing tractive efficiency by selecting the best combination of dynamic load and inflation pressure will depend on the levels of dynamic load and inflation pressure that would have been selected had the optimization procedure not been used. There is very little published data indicating typical levels of tractive efficiency developed on farms, therefore, the actual benefits are difficult to determine. Personal experience indicates that farmers generally operate at low tractive efficiency levels.

Figure 37a shows that for this loose soil condition, the difference between optimum and minimum tractive efficiency varied from 9% to 19%, depending on the net traction level that was required. Figure 37b shows that on the firm soil condition, the difference between optimum and minimum tractive efficiency varied from 10% to 22%.

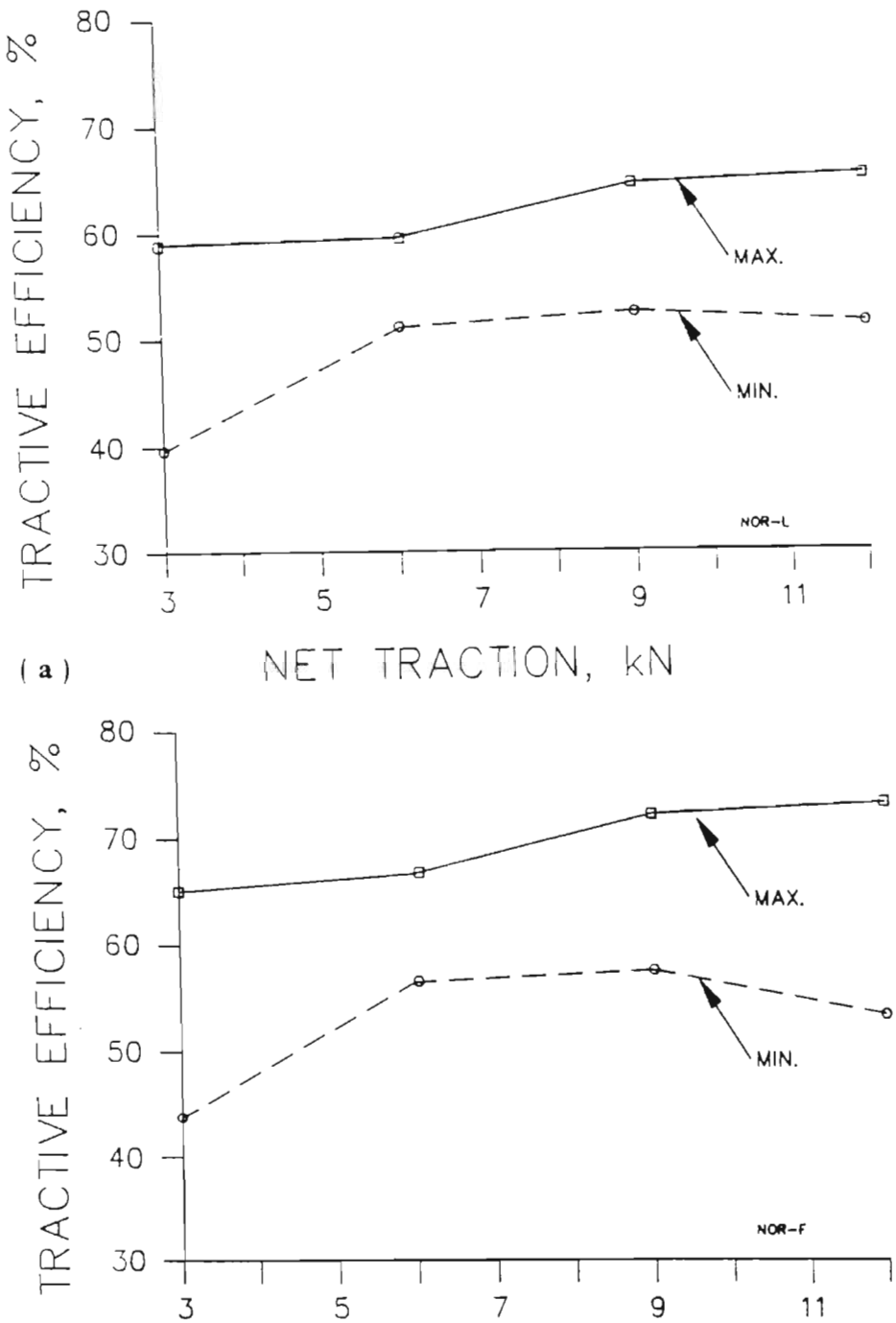

Figure 37 Minimum and optimum tractive efficiency versus net traction for loose (a) and firm (b) Norfolk sandy soil (Lyne and Burt, 1989).

Figure 38 presents results similar to those of Figure 37 except for Decatur clay loam soil. Figure 38a shows that for a loose Decatur clay loam soil, the difference between optimum and minimum tractive efficiency varied between 10% and 27%, depending on the net traction. For the firm soil, Figure 38b, this difference varied between 11% and 30%.

The overall curve shapes for the Norfolk soil in Figures 37a and 37b and for the Decatur soil in Figures 38a and 38b are the same. The tractive efficiencies for the firm soils were higher than for the loose soils. Also, the differences between optimum and minimum tractive efficiency followed the same pattern with the largest difference occurring at 3kN and the smallest difference occurring at 6kN net traction. There is a clear indication that these similarities signify that soil type has a stronger influence on tractive efficiency than does soil condition.

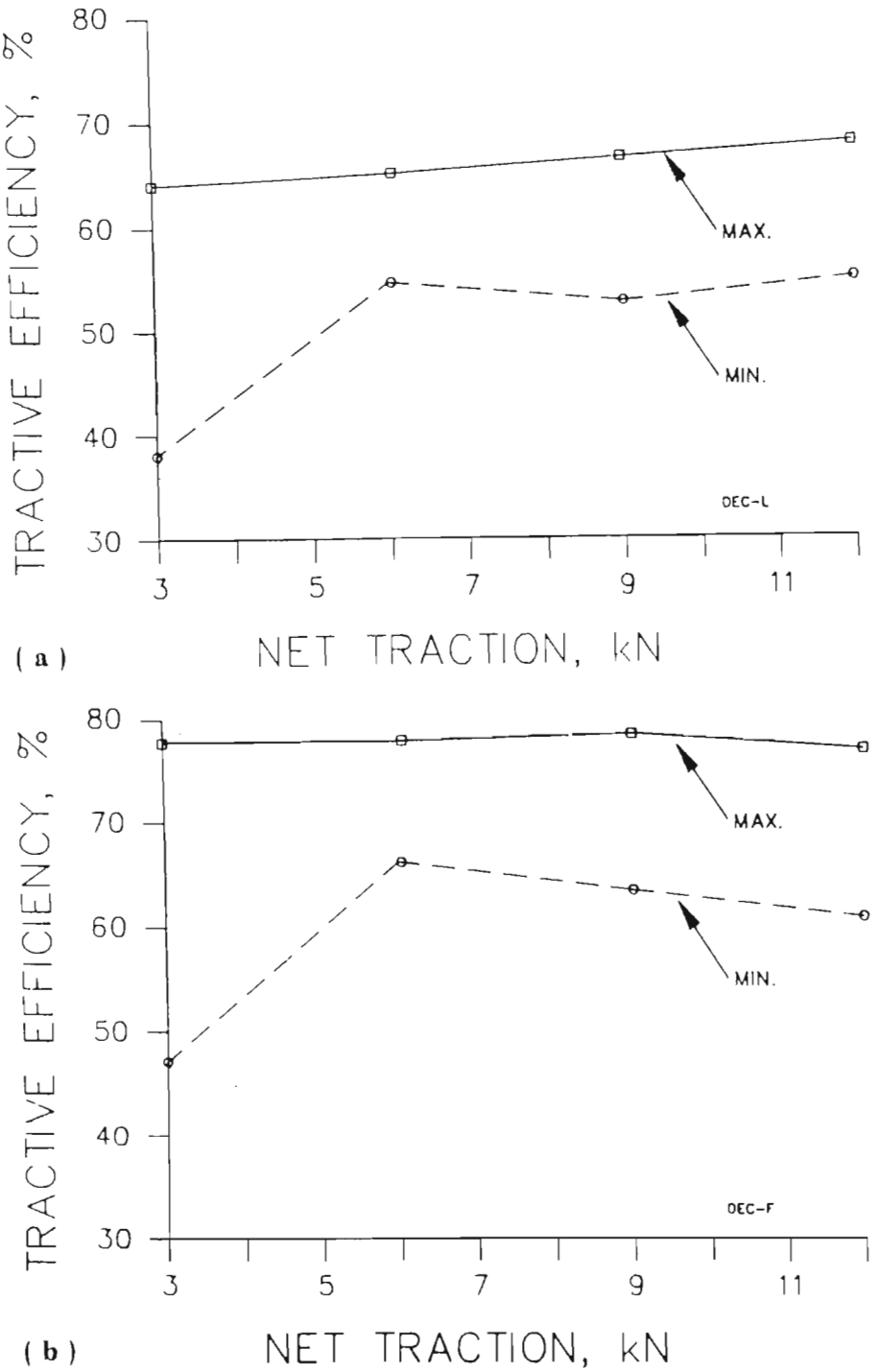

Figure 38 Minimum and optimum tractive efficiency versus net traction for loose (a) and firm (b) Decatur clay soil (Lyne and Burt, 1989).

For each of the soil conditions tested, the greatest difference between optimum and minimum tractive efficiency occurred at 3kN net traction. The lowest tractive efficiency was always at the 3kN net traction level. This low efficiency was the result of operating the tyre at 3kN net traction and at a high level of dynamic load. The energy used in flexing the tyre and compacting the soil under these conditions formed a significant part of the total input power. Also, the output power was quite low since the net traction demand was only 3kN. Therefore, the resulting tractive efficiency was low. These conditions occur, for example, during row crop cultivation. The optimization system should provide a significant improvement in tractive efficiency under such conditions.

There was a tendency on most soil conditions tested, for the optimum tractive efficiency to increase with increasing net traction and, consequently, with higher levels of output power. This tendency may have been the result of minimizing the overall role of rolling resistance by operating at high output power. In cases where tractive efficiency increases with increasing net traction the current trend in machinery management of increasing tractor speed and reducing implement draft is therefore questionable.

Figure 39 shows the dynamic load which was selected for optimum tractive efficiency for each of the net traction levels, soil types and soil conditions tested. Optimum tractive efficiency values for these conditions are presented earlier in Figures 37 and 38. The dynamic load for optimum tractive efficiency increased almost linearly with net traction level up to 9kN net traction.

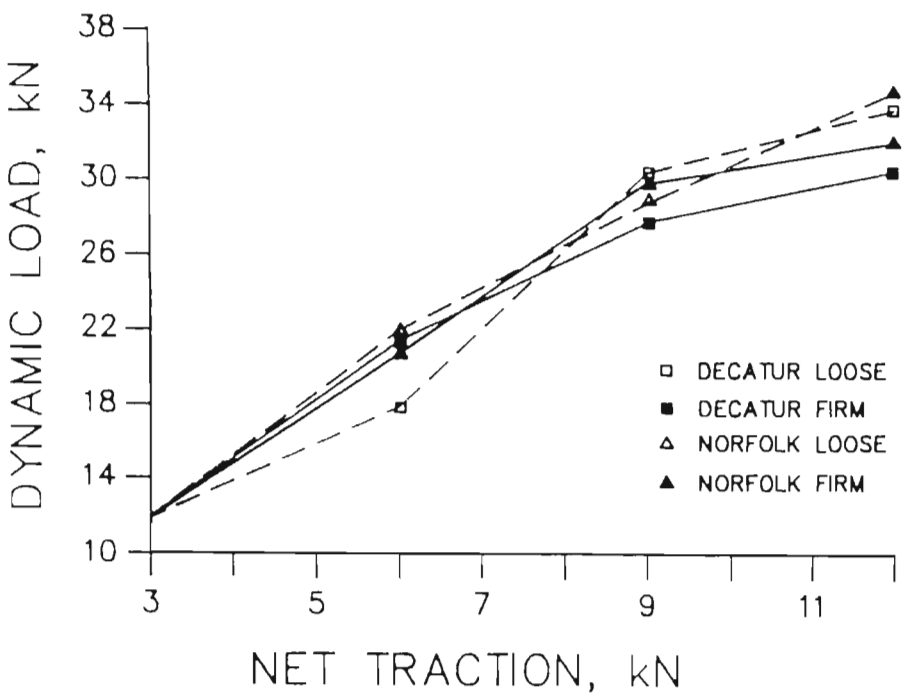

Figure 39 The dynamic load for optimum tractive efficiency for each net traction level and soil condition (Lyne and Burt, 1989).

At 12kN net traction, the dynamic load required for optimum tractive efficiency deviated from the linear trend and was

lower in proportion to the dynamic load than at the lower net traction levels. One explanation for the non-linear trend could be that soil compaction may have reached a maximum at about the 30kN dynamic load level and at 9kN net traction. Hence further increases in dynamic load and net traction did not require a proportional increase in energy for soil compaction.

The inflation pressure for optimum tractive efficiency for each of the net traction levels, soil types and soil conditions tested are presented in Figure 40. At 9kN net traction, the inflation pressure for optimum tractive efficiency differed greatly for the two soil types, with the Decatur soil requiring 166kPa as compared to 110 and 128kPa for the Norfolk soil. At 12kN net traction, the Norfolk soil required the greatest inflation pressure for optimum tractive efficiency. These differences perhaps reflect the division of energy for soil compaction and tyre flexure for the two soil types. It should be noted that the optimum tractive efficiency at a particular level of net traction is sensitive to the combination of dynamic load and inflation pressure. However, at a constant level of dynamic load, tractive efficiency is not highly responsive to inflation pressure as shown in Figures 34 and 35.

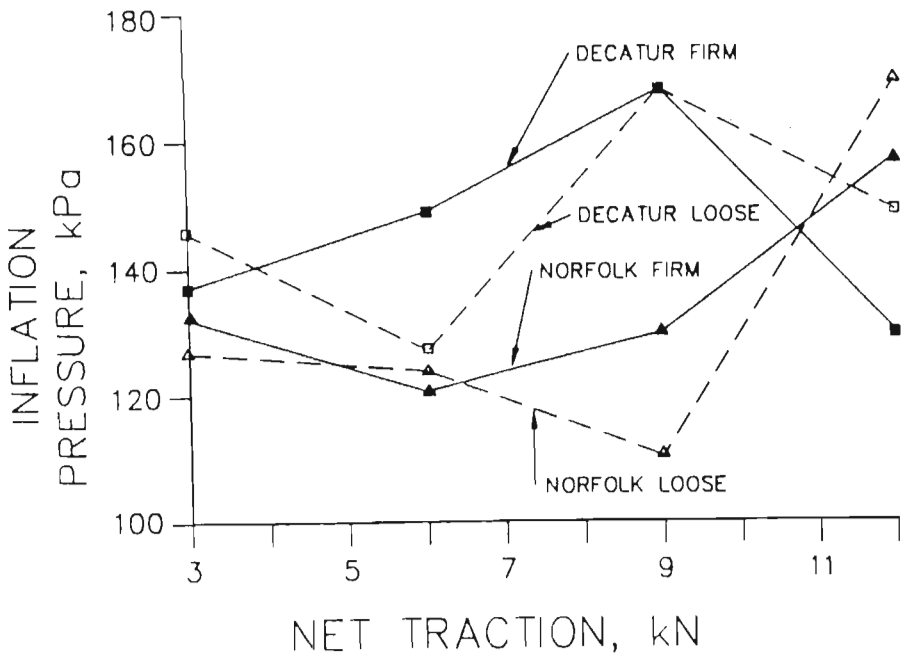

Figure 40 The inflation pressure for optimum tractive efficiency for each net traction level and soil condition (Lyne and Burt, 1989).

The tests provided a comprehensive set of data which were collected under strictly controlled conditions and covered a wide range of operating conditions. It was the first time that performance data had been measured where both dynamic load and inflation pressure were varied over their operating ranges at various net traction levels. The data are lodged with the Department of Agricultural Engineering at the University of Natal in Pietermaritzburg, South Africa, and are available on disk in an ASCII format. These data provided an ideal opportunity to examine the measured results

and compare the optimum operating parameters with some of those recommended by other researchers with particular reference to traction ratio and wheel slip.

5.3 Traction Ratio and Wheel Slip

After studying a large amount of data Dwyer (1984) stated that maximum tractive efficiency occurred at a traction ratio of 0,4 over a surprisingly wide range of tyre and soil conditions. He used this ratio to calculate the optimum ballast for tractors, however, Figure 41 shows that as the operating conditions vary, the traction ratio at maximum efficiency varies from 0,25 to 0,383.

The minimum static weight of the simulated tractor and thus the DL MIN used in the tests was 12kN. The 12kN resulted in a ballast which was higher than the optimum required for the 3kN net traction level and therefore resulted in the low

traction ratio for the 3kN tests. This would also be true for a tractor operating at low net traction levels.

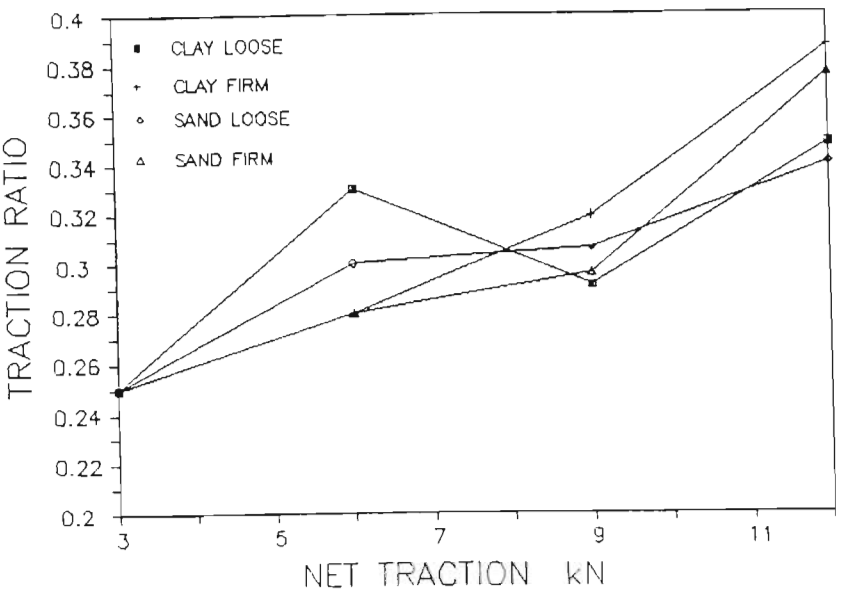

Figure 41 Variation of traction ratio at maximum tractive efficiency for four different net traction and soil conditions.

The difference in tractive efficiency obtained at the peak of the tractive efficiency response surface and that obtained at a traction ratio of 0,4 is shown in Figure 42. Although in some cases the differences are small it must be remembered that Taylor (1980) estimated that a difference of one percent in tractive efficiency would save the U.S.A. farmers between 284 and 302 billion litres of fuel annually.

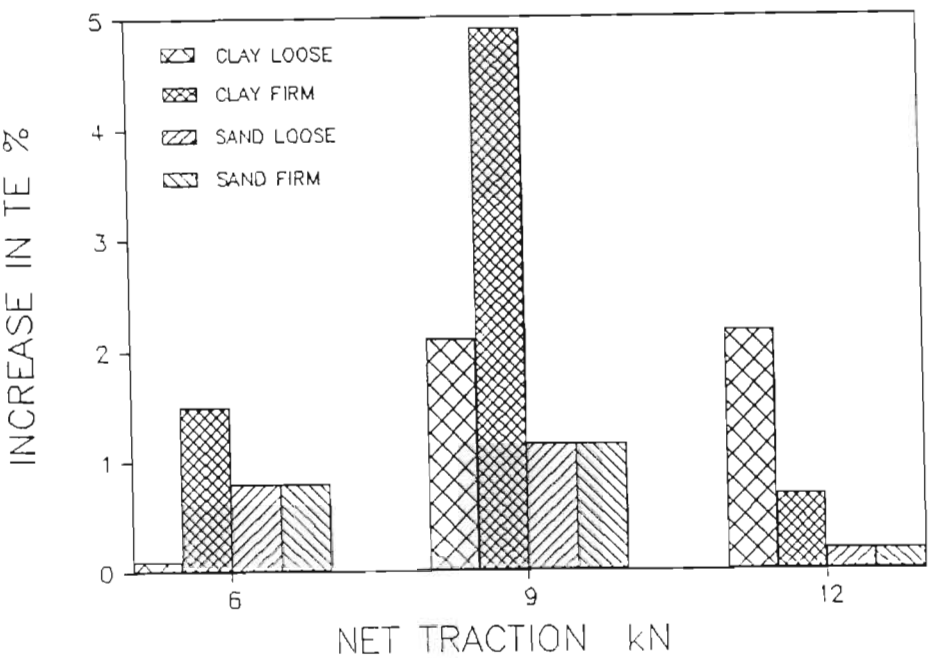

Figure 42 The increase in tractive efficiency obtained by changing the traction ratio from 0,4 to the optimum for four soils and net traction levels.

The wheel slip levels at maximum tractive efficiency were measured at each net traction level and soil condition. These values are provided in Figure 43 and indicate that the optimum wheel slip varies with net traction in a particular soil condition. This shows that linking a wheel slip level to a soil condition would not result in optimum efficiency, and strengthens the case for an automatic control system to be used to optimize tractive efficiency.

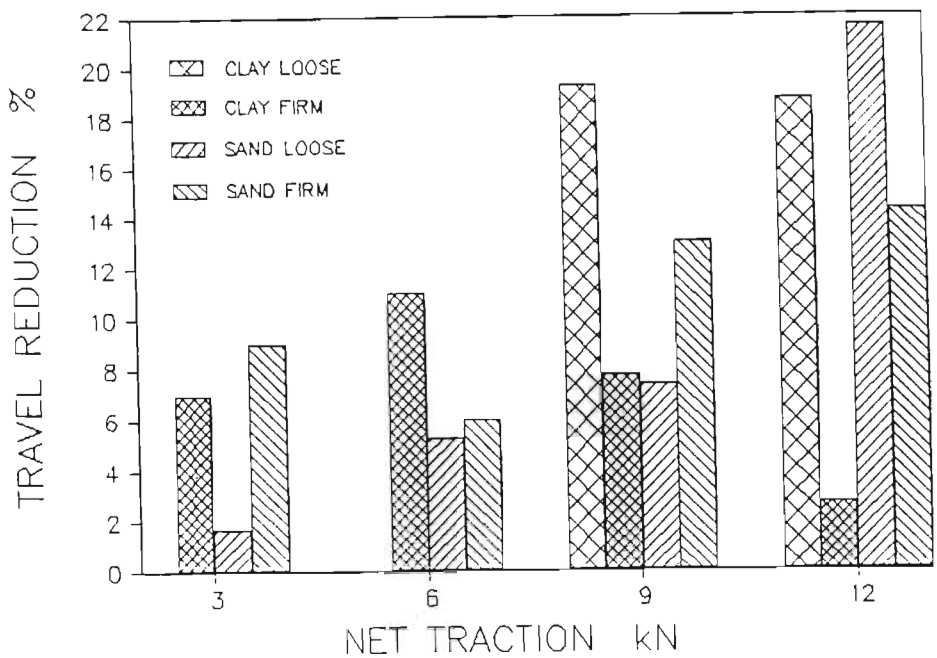

Figure 43 Travel reduction at maximum tractive efficiency, at various net traction levels and various soil conditions.

These results illustrate the tremendous potential of the system developed in this research. Fitted to a tractor it would greatly reduce the management effort required and the inconvenience necessary to improve tractive efficiency. I believe that it is only a matter of time before manufacturers recognise the benefits that such a system would provide and incorporate similar systems on production tractors. I further believe that if farmers were aware of the benefits that could be obtained they would demand such a system on their future tractors.

The safety features programmed into the control system functioned perfectly. A few problems did occur which caused limits to be exceeded and these resulted in a orderly shut-down of the SWTRV. The control system has also been used very successfully for numerous research projects spanning a number of years. A design incorporating the dynamic load component of the system developed here has since been successfully tested on a standard 62kW tractor operating under field conditions (Lecler, Lyne, Hansen and Meiring, 1990).

6 CONCLUSIONS

The major limitation in optimizing tractor operation is the inability of the tractor operator to obtain maximum tractive efficiency. Although tractive efficiency can be optimized by selecting the appropriate values of dynamic load and inflation pressure, in practice this is difficult to achieve.

Within the recommended operating range of the tyre, optimum tractive efficiency varies with the net traction demand, the soil type and the soil condition. There are prediction systems available to assist the operator achieve optimum efficiency, but, these rely on the operator being able to quantify net traction demand, the soil type and the soil condition. It has been shown that it is not practical for the operator to achieve this with any degree of accuracy and an ideal solution for the operator would be an automatic control system to optimize traction during field operations.

This research has shown that an algorithm operating with hardware available today can successfully vary the dynamic load and inflation pressure of a drive wheel and determine the optimum levels of these parameters to ensure maximum tractive efficiency. During an operation maximum tractive efficiency could be achieved within approximately 20s and allow the system to correct the inflation pressure and

dynamic load as conditions changed in a field.

The safety checks built into the system operated flawlessly. This indicates that careful design can ensure that an automatic control system will be safe to use.

During the evaluation of the system excellent agreement was achieved between the actual tractive efficiency measured at the estimated maximum point and that estimated for the same point. This was accomplished while simulating a range of field conditions which covered those that could be expected on a farm. A system using the dynamic load component of the algorithm developed here has since been successfully tested on an agricultural tractor under field conditions.

Tractive efficiency can be increased by up to 30% under some operating conditions by selecting the dynamic load and inflation pressure for optimum efficiency. This shows that substantial savings in time and energy could be achieved by using such a system.

The largest difference between optimum and minimum tractive efficiency occurred at low levels of net traction and the highest tractive efficiency levels occurred at high levels of net traction. These results indicate firstly, that the operator has to be particularly careful at low levels of net traction where large losses can occur and secondly, to make optimum use of the tractor, he should at all times strive to

load the tractor to as high a level of net traction as possible.

It should be feasible to incorporate such a system on a normal tractor. Weight transfer hitches and ballasting of the implements would make the implementation of such a system a practical option. It would relieve the operator of the difficulty of attempting to quantify the soil parameters, the net traction required, the required wheel slip and the inconvenience of ballasting and inflating the tyres correctly.

When developing a system it would be necessary to begin all optimization routines at maximum inflation pressure and maximum load and to reduce the dynamic load to a minimum level determined by a maximum wheel slip level. The optimization routine could then be completed by lowering the inflation pressure and cycling the dynamic load. This procedure would solve the limitation in the existing system of possibly losing traction at high inflation pressures and low dynamic loads.

This system used in conjunction with an expert system to provide the operator with feedback of tractor operating parameters and of what adjustments should be made would dramatically reduce the management skills required to optimize performance.

7 REFERENCES

Ashmore, C. 1986. Personal communication concerning logging truck trafficability using central tire inflation pressure systems, U.S. Forest Service, Auburn, Alabama, USA.

Ashmore, C., Burt, E.C. and Turner, J.L., 1987. An empirical equation for predicting tractive performance of log-skidder tires. Trans. ASAE 30(5), 1231-1236.

ASAE Standards., 1988. The standards, engineering practices and data adopted by the ASAE.

Bekker, M.G., 1956. Land locomotion, the mechanics of vehicle mobility. The Univ. of Mich. Press, Ann Arbor, Michigan, USA.

Bekker, M.G., 1960. Off-road locomotion : Research and development in terramechanics. The Univ. of Mich. press, Ann Arbor, Michigan, USA.

Brixius, W.W., 1987. Traction prediction equations for bias ply tires. ASAE Paper No. 87-1622.

Burt, E.C. and Bailey, A.C., 1985. Determining thrust from wheels and tires. International conference on soil dynamics, Auburn, Alabama, USA. 4, 643-655.

Burt, E.C., Bailey, A.C. and Wood, R.K., 1987. Effects of soil and operational parameters on soil-tire interface stress factors. J. Terramechanics 24(3), 235-246.

Burt, E.C. and Lyne, P.W.L., 1985. Velocity effects on tractor performance. Trans. ASAE 28(6), 1729-1730.

Burt, E.C., Lyne, P.W.L.L., Meiring, P. and Keen, J.F., 1983. Ballast and inflation effects on tire efficiency. Trans. ASAE 26, 1352-1354.

Burt, E.C., Reaves, C.A., Bailey, A.C. and Pickering, W.D., 1980. A machine for testing tractor tires in soil bins. Trans. ASAE 23(3), 546-547, 552.

Burt, E.C., Reaves, C.A. and Taylor, J.F., 1977. The NTML single-wheel agricultural tire tester. ASAE Paper No. 77-1056.

Burt, E.C., Wood, R.K. and Bailey, A.C., 1987. Tangential-to-Normal stress ratios for Pneumatic Tires. Trans. ASAE 30(6), 1591-1594.

Chancellor, W. and Zhang, N., 1987. Automatic wheel-slip control for tractors. ASAE Paper No. 87-1502.

Charles, S.M., 1983. Effects of ballast and inflation pressure on tractor tire performance. Agric. Eng. 65(2), 11-13.

Clark, R.L., 1984. Tractive modelling and field data requirements to predict traction. ASAE Paper No. 84-1055.

Clark, R.L. and Vande Linda, G., 1986. A rapid automatic ballast system. ASAE Paper No. 86-1550.

Czako, T.F., 1974. The influence of inflation pressure on cross-country performance. J. Terramechanics 11(3&4), 13-23.

Della-Moretta, L.B. and Hodges, H.C., 1986. A practical approach to road healing. ASAE Paper No. 86-1545.

Dwyer, M.J., 1982. Agricultural engineering - state-of-the-art report. J. Terramechanics 19(1), 9-29.

Dwyer, M.J., 1984. Tractive performance of wheeled tractors. J. Terramechanics 21(1), 19-34.

Dwyer, M.J., 1985. Predicting tractor performance. International conference on soil dynamics, Auburn, Alabama, USA. 4, 679-692.

Dwyer, M.J., Comely, D.R. and Evernden, D.W., 1975. Development of the NIAE handbook of Agricultural tyre performance. ISTVS, 5th International conf. Detroit, Michigan, USA.

Dwyer, M.J., Evernden, D.W. and McAllister, M., 1976. Handbook of Agricultural Tyre Performance. (2nd Edition). NIAE Report No. 18.

Evans, M.D., Clark, R.L. and Manor, G., 1989. A traction prediction and ballast selection model. ASAE Paper No. 89-1054.

Freitag, D.R., 1966. A dimensional analysis of the performance of pneumatic tires on clay. J. Terramechanics 3(3), 51-68.

Freitag, D.R., 1985. Soil dynamics as related to traction and transport systems. Proc. International conference on soil dynamics, Auburn, Alabama, USA. 4, 605-629.

Freitag, D.R. and Smith, M., 1966. Center-line deflection of pneumatic tires moving in dry sand. J. Terramechanics 3(1), 31-46.

Gee-Clough, D., McAllister, M., Pearson, G. and Evernden, D.W., 1978. The empirical prediction of tractor-implement field performance. J. Terramechanics 15(2), 81-94.

Gee-Clough, D., Pearson, G. and McAllister, M., 1982. Ballasting wheeled tractors to achieve maximum power output in frictional-cohesive soils. J. Agric. Eng. Res. 27(1).

Gill, W.R. and Vanden Berg, G.E., 1967. Soil dynamics in tillage and traction. U.S. Govt Printing Office.

Göhlich, H., 1984. The Development of Tractors and Other Agricultural Vehicles. J. Agric. Eng. Res. 29, 3-16.

Grogan, J., Morris, D.A., Searcy, S.W., Wiedeman, H.T. and Stout, B.A., 1984. Microcomputer-based information feedback systems for improving tractor efficiency. ASAE Paper No. 84-1594.

Hansen, A.C., Meiring, P. and North, R.P., 1978. An efficiency meter for optimizing the performance of diesel tractor engines. Agric. Eng. in RSA 12, 34-42.

Ismail, S.M.Md., Singh, G. and Gee-Clough, D., 1981. A preliminary investigation of a combined slip and draught control for tractors. J. Agric. Eng. Res. 26, 293-306.

Jahns, G., 1983. A method of describing diesel engine performance maps. ASAE Paper No. 83-103.

Janosi, Z., 1962. Theoretical analysis of the performance of tracks and wheels operating on deformable soil. Trans. ASAE 5, 133-134, 146.

Janosi, Z. and Hanamoto, B., 1961. The analytical determination of drawbar pull as a function of slip for tracked vehicles in deformable soils. Paper No. 41. 1st Int. Conf. on Mechanics of Soil-Vehicle Systems, Torino, Italy.

Johnson, C.E., Grisso, R.D., Nichols, T.A. and Bailey, A.C., 1987. Shear Measurement For Agricultural Soils - A Review. Trans. ASAE 30(4), 935-938.

Kacigin, V.V. and Guskov, V.V., 1968. The Basis of Tractor Performance Theory. J. Terramechanics 5(3).

Kaumbutho, P.G., Rosenberg, R.C., Burkhardt, T.H. and Srivastava, A.K., 1987. Tractor performance simulation model using bond graphs. ASAE Paper No. 87-1503.

Lecler, N., Lyne, P.W.L., Hansen, A.C. and Meiring, P., 1990. On line optimisation of the dynamic load on the drive wheels of a tractor. Agric. Eng. in S. Afr. 22(1), 191-299.

Lyne, P.W.L., Bremner, M.H., Hansen, A.C. and Meiring, P., 1988. A tractor gear selection aid. Agric. Eng. in S. Afr. 20(1), 134-146.

Lyne, P.W.L. and Burt, E.C., 1989. Real-time optimization of tractive efficiency. Trans. ASAE 32(2), 431-435.

Lyne, P.W.L., Burt, E.C. and Jarrell, J.D., 1983. Computer control for the National Tillage Machinery Laboratory single-wheel tester. ASAE Paper No. 83-1555.

Lyne, P.W.L., Burt, E.C. and Meiring, P., 1984. Effect of tire and engine parameters on efficiency. Trans. ASAE 27(1), 5-7, & 11.

Lyne, P.W.L., Jacobs, L.M. and Meiring, P., 1980. Optimization of tractive efficiency and field performance. ASAE Paper No. 80-1520.

Lyne, P.W.L. and Meiring, P., 1977. A wheel slip meter for traction studies. Trans. ASAE 20, 238-242.

MacLaurin, E.B., 1987. Soil-vehicle interaction. J. Terramechanics 24(4), 281-294.

Meiring, P. and Rall, M.G., 1979. An operator assist system to optimize tractor efficiency. ASAE Paper No. 79-1048.

Meiring, P., Rennie, A.R., Hansen, A.C. and Lyne, P.W.L., 1987. Tractor performance improvements via power demand mapping. ASAE Paper No. 87-1052.

Meiring, P., Walker, A.J., Hansen, A.C. and Lyne, P.W.L., 1985. Power demand mapping of tractor operations. ASAE Paper No. 85-1050.

NTML., 1984. Unpublished test data, test file No's TE01-2 & TDATA 2 at NSDL, Auburn, Alabama, USA.

Onafeko, O. and Reece, A.R., 1967. Soil stresses and deformations beneath rigid wheels. J. Terramechanics 4(1), 59-80.

Otterman, R.W., 1985. Voorspellingsmodelle vir dir werkverigting van trekkers. Unpublished M. Sc. Thesis, Univ. of Pretoria, RSA.

Persson, S.P.E., 1969. Gaps and Limitations in existing traction theories. ASAE Paper No. 69-134.

Perumpral, J.R., Liljedahl, J.B. and Perloff, W.H., 1971. The finite element method for predicting stress distributions and soil deformation under tractive devices. Trans. ASAE 14(6), 1184-1188.

Plackett, C.W., 1985. A review of force prediction methods for off road wheels. J. Agric. Eng. Res. 31, 1-29.

Schrock, M.D., Matteson, D.K. and Thompson, J.G., 1982. A gear selection aid for agricultural tractors. ASAE Paper No. 82-5515.

Siddall, J.N., 1982. Optimal engineering design. Marcel Dekker, New York, USA.

Spoor, G. and Godwin, R., 1979. Soil deformation and shear strength characteristics of some clays soils at different moisture contents. J. Soil Science 30, 484-498.

Taylor, J.H., 1980. Energy savings through improved tractive efficiency. Proc. Energy symposium, ASAE, Kansas City, Kansas, USA.

Taylor, J.H. and Vanden Berg, G.E., 1966. Role of displacement in a simple traction system. Trans. ASAE 9(1), 10-13.

Tire and Rim Association Yearbook., 1988. Tire and Rim Association, Inc. Akron, Ohio, USA.

Turnage, G.W., 1972a. Using dimensionless prediction terms to describe off-road wheeled vehicle performance. ASAE Paper No. 72-634.

Turnage, G.W., 1972b. Tire selection and performance prediction of off-road wheeled vehicle operations. Proc. 5th Int. Conf. Int. Soc. for Terrain-Vehicle Systems, Stockholm, Sweden.

Wang, K. and Zoerb, G.C., 1988. A farm tractor drivers information system. ASAE Paper No. 88-3020.

Wertz, K. and Grisso, R.D., 1988. Tractor tire pressures and ballast in Lancaster County. ASAE Paper No. 88-1515.

Wismer, R.D. and Luth, H.J., 1972. Off-road traction prediction for wheeled vehicles. ASAE Paper No. 72-619

Wood, R.K. and Burt, E.C., 1987. Thrust and motion resistance from soil-tire interface stress measurements. Trans. ASAE 30(5), 1288-1292.

Yavnai, A. and Wolf, D., 1979. Tractor slip control under variable drawbar pull. ASAE Paper No. 79-1553.

Yong, R.N., 1985. Application of finite element methods for traction prediction. Proc. Int. Conf. on Soil Dynamics, Auburn, Alabama, USA. 4, 827-847.

Yong, R.N., Boonsinsuk, P. and Fattah, E.A., 1980. Tyre flexibility and mobility in soft soils. J. Terramechanics 17(1), 43-58.

Yong, R.N. and Fattah, E.A., 1976. Prediction of wheel-soil interaction and performance using FEM. J. Terramechanics 13(4).

Yong, R.N., Fattah, E.A. and Boonsinsuk, P., 1978. Analysis and prediction of tyre-soil interaction and performance using finite elements. J. Terramechanics 15(1), 43-63.

Yong, R.N., Fattah, E.A. and Skiadas, N., 1984. Vehicle Traction Mechanics. Elsevier, New York, USA.

Zhang, N., Liljedahl, J.B. and Miles, G.E., 1984. Slip control of hydrostatically driven wheels. ASAE Paper No. 84-1053.

Zhang, N. and Perumpral, J.V., 1987. Engine and slip control for improving tractor operating efficiency. ASAE Paper No. 87-1062.

Zoz, F.M., 1972. Predicting tractor field performance. Trans. ASAE, 15(2), 249-255.

Zoz, F.M., 1987. Predicting tractor field performance (updated). ASAE Paper No. 87-1623

8 APPENDICES

Appendix A Description of the control and optimization routine.

The optimization routine was started by activating a latched switch known as the "Tire" switch on the console in the instrument car. The switch caused a supervisory programme running on the computer to down-load the control programme from the host computer to the mini computer.

The initial section of the programme consisted of an interactive editor which displayed default values of the various variables and limits. If any of the controlled variables deviated from their set points by more than a set limit the programme was automatically terminated, a partial list of these with typical values used is presented below:

Variables:	
DL min	12kN
DL max	15,5 + 0,139 * IPr
IPr min	110kPa
IPr max	166kPa
NU STEP	5 steps
DL RATE	1,5kN/s
PUMP RATE	6kPa/s

limits:	
SWTRV velocity	0.05m/s
TR	± 40%
DL	6kN
NT	5kN.

Once the above values had been edited to those required for the current test, the programme began cycling through the control and optimization routine. A flow chart of the control and optimization routine is given in Figure A1,

various blocks of the programme are labelled and descriptions of these blocks are given below:

(a) Once a ramp-down cycle had been enabled a number of the checks were bypassed.

(b) Once the initial target shown in Figure 16 in section 3.5 and the test zone had been reached the "Data" switch on the console was activated to start the optimization routine. This was a check to determine whether the data switch had been activated.

(c) A flag was used to indicate whether the tire switch was activated. This was the switch which started the main programme and was used to terminate the programme once the optimization routine was complete.

(d) A flag was set to indicate whether the data switch had been activated.

(e) Similarly a control flag was set once the control switch had been activated.

(f) Once control had been disabled for whatever reason a flag was set to prepare the programme for a ramp-down cycle.

(g) The data acquisition routines.

(h) During the ramp-down cycle, control was returned to the ramp-down block (h) via the connector (3). Once the ramp-down cycle was complete the flags and outputs were reset to zero and the programme was terminated.

(i) The various limits were checked and if any fault was detected at this stage a ramp-down cycle was executed and the programme terminated.

(j) This is the stage where the various set points were computed and a description of this stage is given in Appendix B.

(k) If control was not enabled, the set point signals were reset to zero.

(l) The analogue signals to the meters on the SWTRV and for the analogue controllers were transmitted from the instrument car. The pulse train for the computer integrity check was also transmitted to the SWTRV at this stage.

(m) A data point was saved for every 50mm distance travelled along the bin. This was only saved as a data point if data acquisition was enabled.

(n) This was the ramp-down routine which gradually reduced the dynamic load, the net traction and the vehicle velocity to zero over a two second period. This was achieved by ramping the set points from the current values to zero.

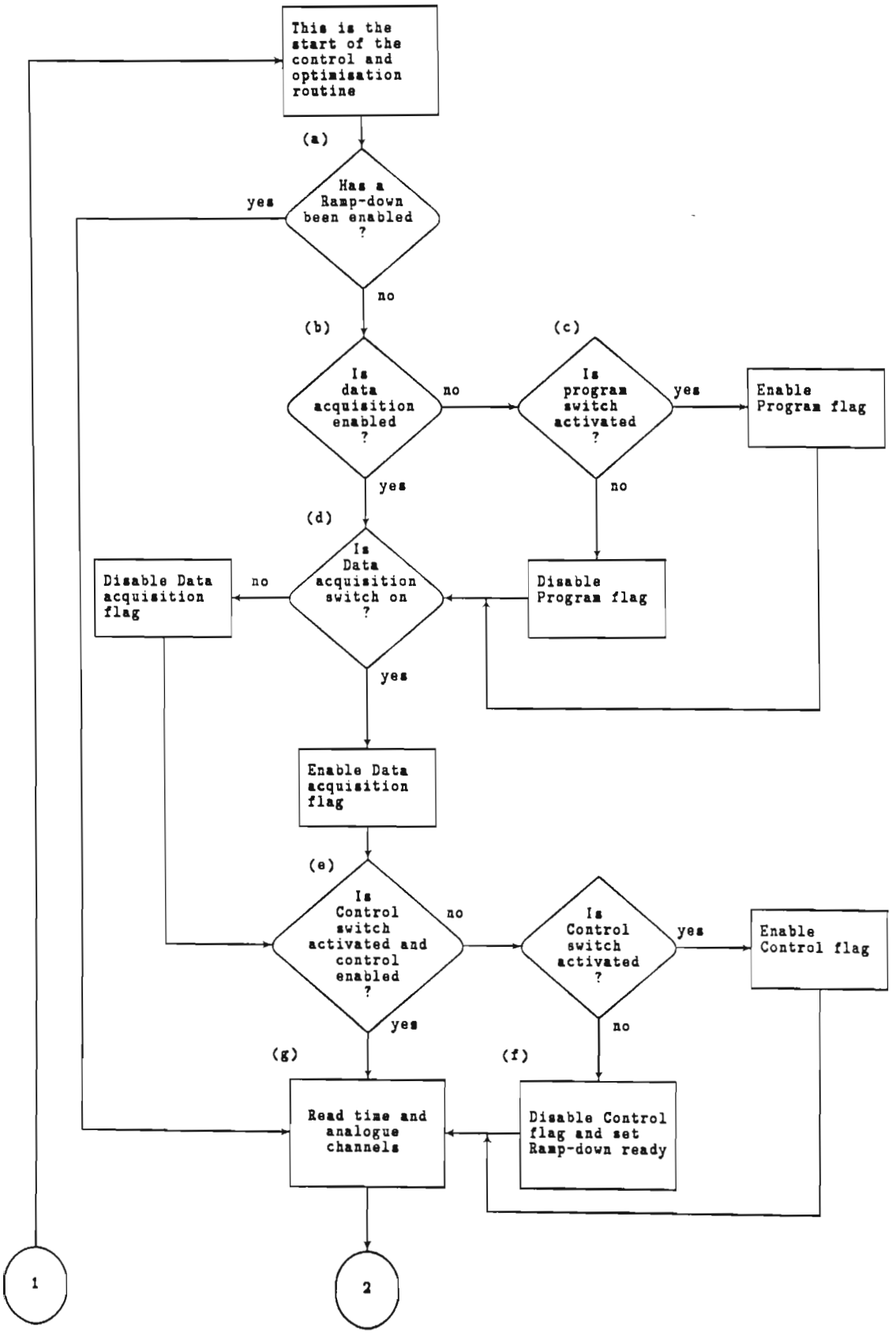
This is the start of the control and optimisation routine
(a)
Has a Ramp-down been enabled ?
yes
no
(b)
Is data acquisition enabled ?
no
(c)
Is program switch activated ?
yes
Enable Program flag
yes
no
(d)
Is Data acquisition switch on ?
Disable Data acquisition flag
no
Disable Program flag
yes
Enable Data acquisition flag
(e)
Is Control switch activated and control enabled ?
no
Is Control switch activated ?
yes
Enable Control flag
yes
no
(g)
(f)
Read time and analogue channels
Disable Control flag and set Ramp-down ready
1
2

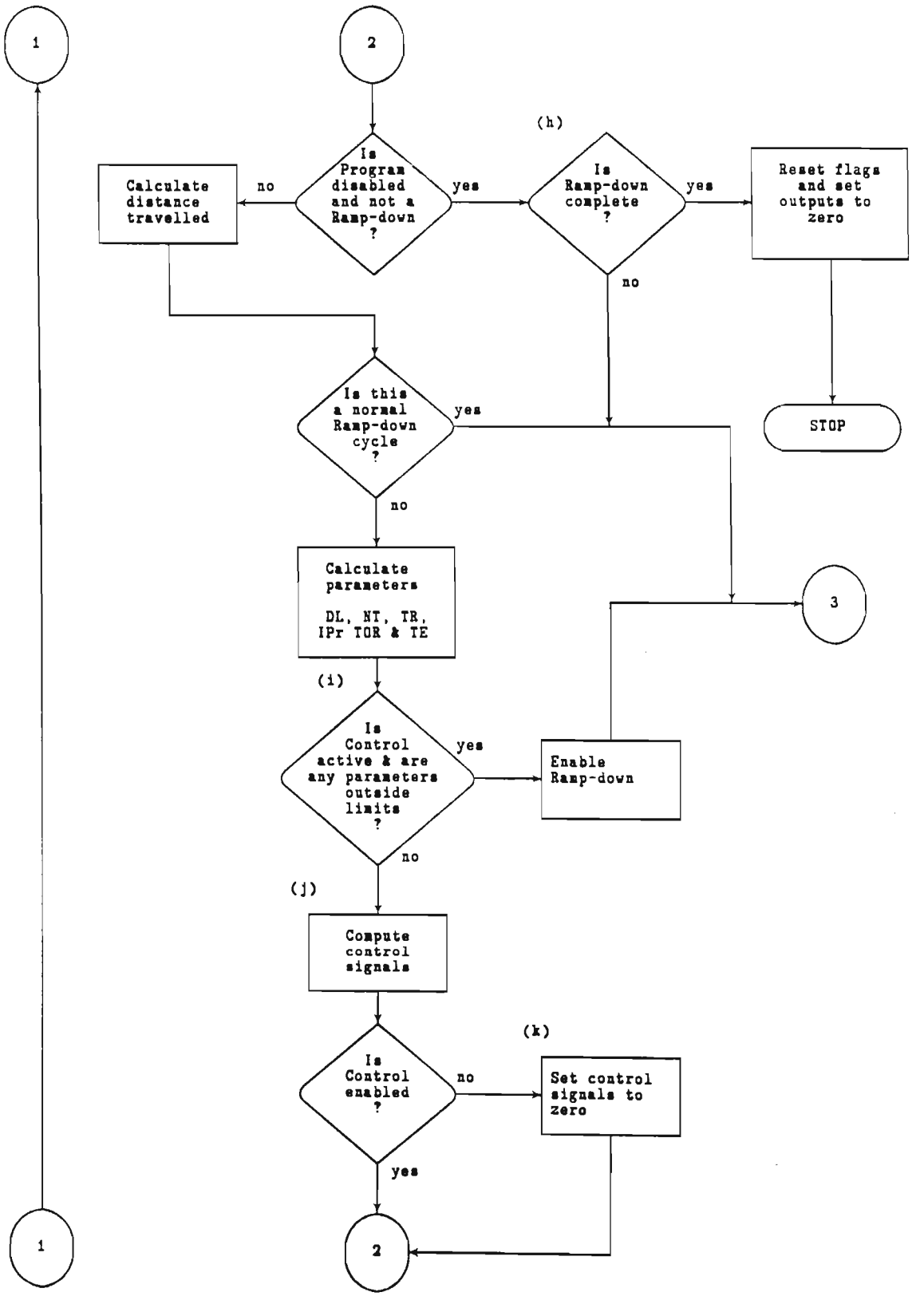
1
2
(h)
Is Program disabled and not a Ramp-down ?
no
yes
Calculate distance travelled
Is Ramp-down complete ?
yes
Reset flags and set outputs to zero
no
STOP
Is this a normal Ramp-down cycle ?
yes
no
Calculate parameters
DL, NT, TR, IPr TOR & TE
3
(i)
Is Control active & are any parameters outside limits ?
yes
Enable Ramp-down
no
(j)
Compute control signals
(k)
Is Control enabled ?
no
Set control signals to zero
yes
2
1

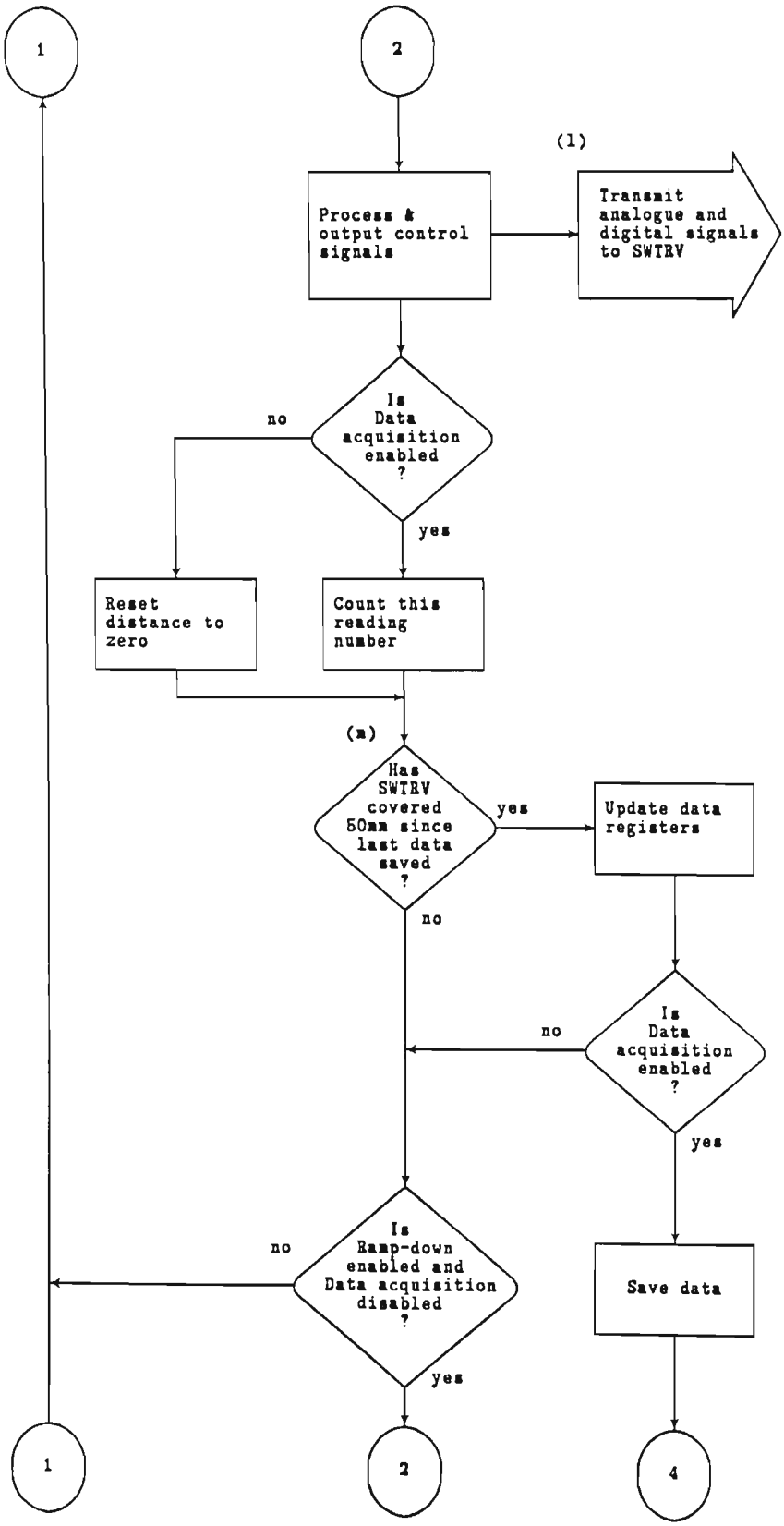
1
2
(1)
Process & output control signals
Transmit analogue and digital signals to SWTRV
Is Data acquisition enabled ?
no
yes
Reset distance to zero
Count this reading number
(a)
Has SWTRV covered 50mm since last data saved ?
yes
Update data registers
no
Is Data acquisition enabled ?
no
yes
Is Ramp-down enabled and Data acquisition disabled ?
no
yes
Save data
1
2
4

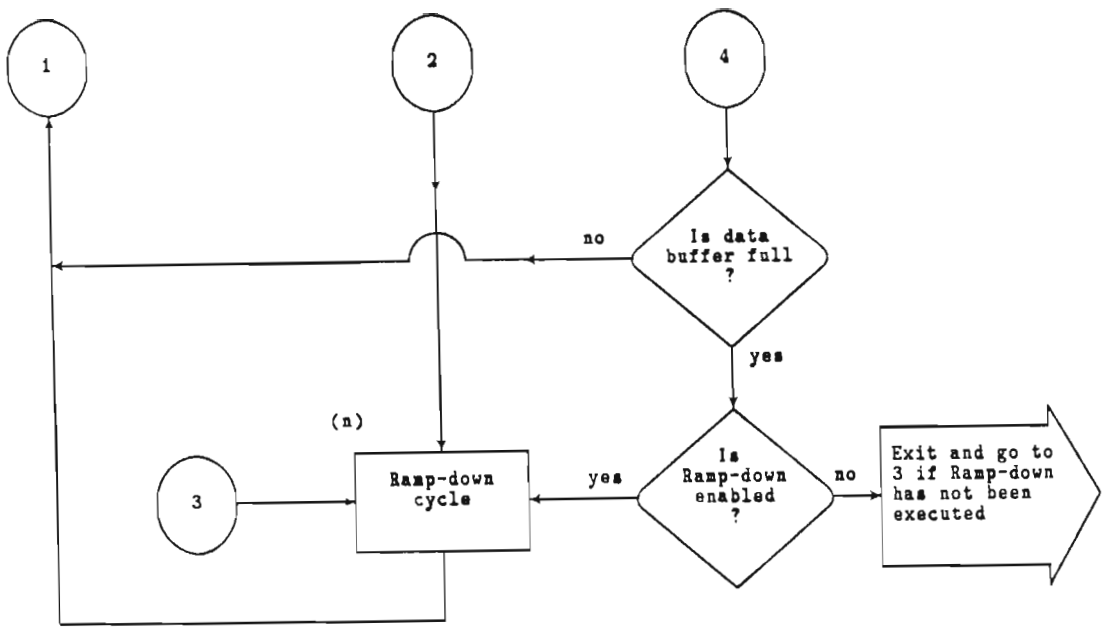

Figure A1 Flow chart of the control programme for the optimization routine.

APPENDIX B Description of the procedure to determine the set points for the controller.

A flow chart showing the process to determine the actual set point values for the controller on SWTRV is shown in Figure B1. This describes the logic used to vary the dynamic load and inflation pressure to the initial target and once the data acquisition had been activated to ramp it down to the minimum dynamic load DL min and to then set the intermediate targets to reach the final target.

Once the final target had been reached the coefficients for the tractive efficiency response surface coefficients were computed. The surface was then searched for the maximum tractive efficiency point. The maximum TE point was then set as a target and the DL and IPr ramped to it. When the maximum TE point was reached the programme indicated that this had been achieved and that the programme could be terminated.

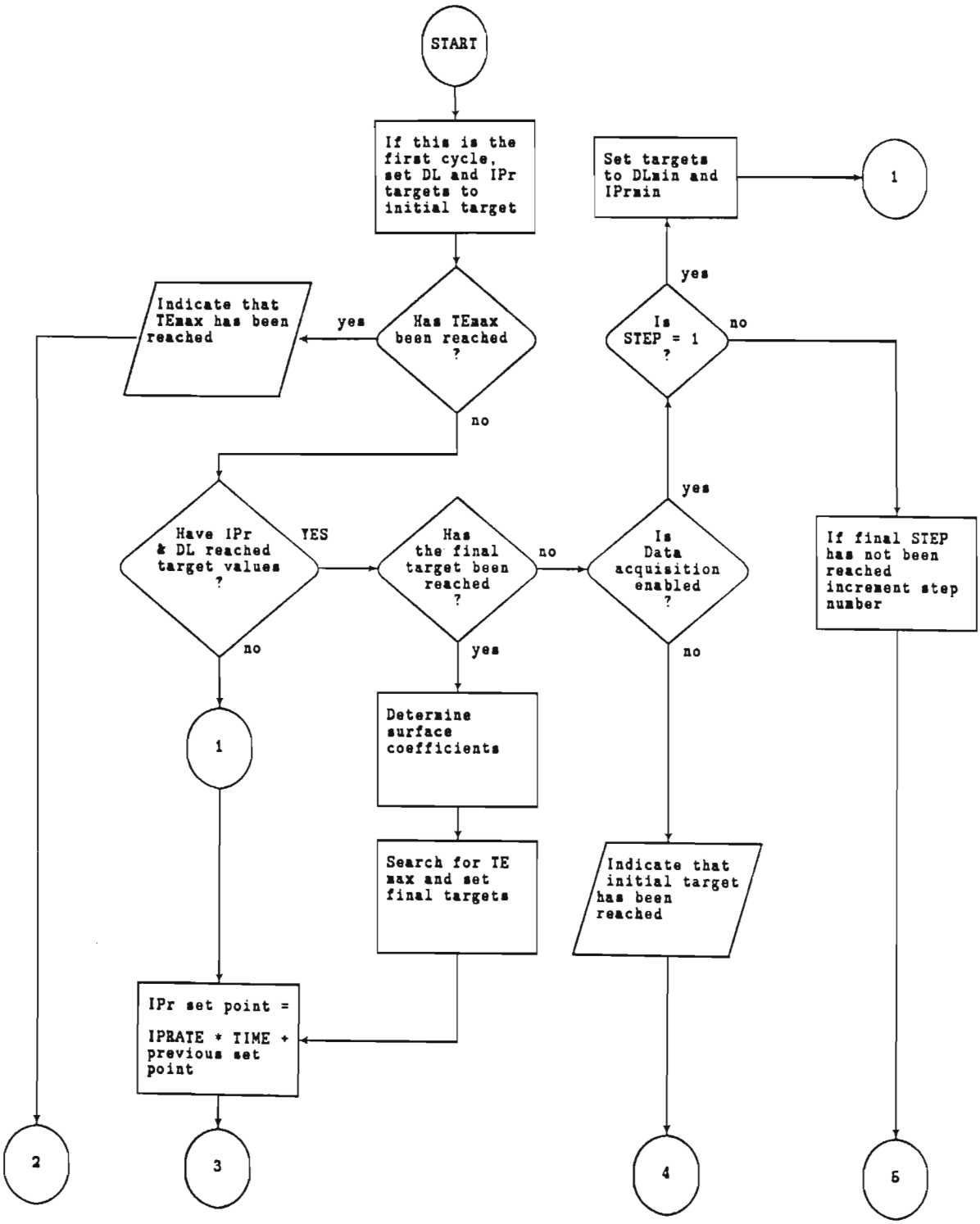
START
If this is the first cycle, set DL and IPr targets to initial target
Has TEmax been reached ?
yes
Indicate that TEmax has been reached
no
Have IPr & DL reached target values ?
YES
no
Has the final target been reached ?
no
yes
Is Data acquisition enabled ?
yes
no
Is STEP = 1 ?
yes
no
Set targets to DLmin and IPrmin
1
If final STEP has not been reached increment step number
Determine surface coefficients
Search for TE max and set final targets
Indicate that initial target has been reached
1
IPr set point =
IPRATE * TIME + previous set point
2
3
4
5

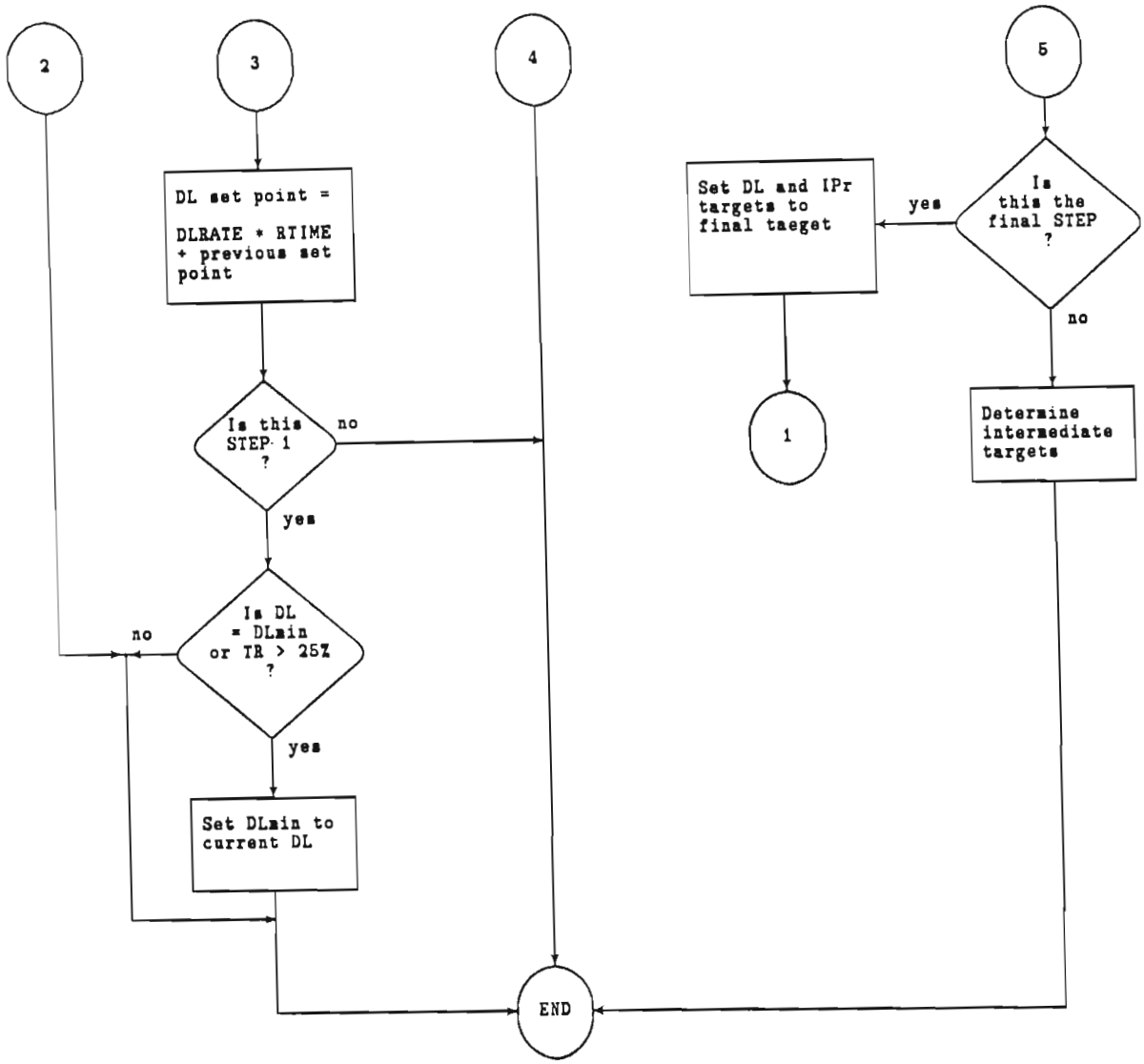

Figure B1 Flow chart of the process used to set the targets for the control programme during the optimization routine.

Appendix C Search technique to determine the optimum tractive efficiency.

The Hook and Jeeves strategy of direct search is one of the earliest and most successful methods of numerical optimization (Siddall, 1982). The direct search avoids the use of derivatives, making instead local exploratory searches to determine the slope of the surface.

Siddall (1982) provides a suite of optimization subroutines and a selection of these were used to implement the search process. The subroutines were written to locate the minimum point on a concave surface and therefore had to be modified to locate the peak on the convex profile of the tractive efficiency response surface. The steps involved in the search were as follows:

(a) The optimization function was calculated using the coefficients determined during the optimization routine.

(b) Constraints were set up to limit the search to within the dynamic load-inflation pressure area.

(c) The search was initiated within the dynamic load-inflation pressure area.

(d) Once the optimum point was located, 100 random points of tractive efficiency within the dynamic load-inflation pressure area were compared with the located optimum. This was carried out to verify that a global rather than a local optimum had been located. If a local optimum had been found the search was restarted from the higher tractive efficiency point.

This routine required approximately 400ms to locate the maximum tractive efficiency point. A test run showing the steps taken from the start to the optimum is shown in Figure C1.

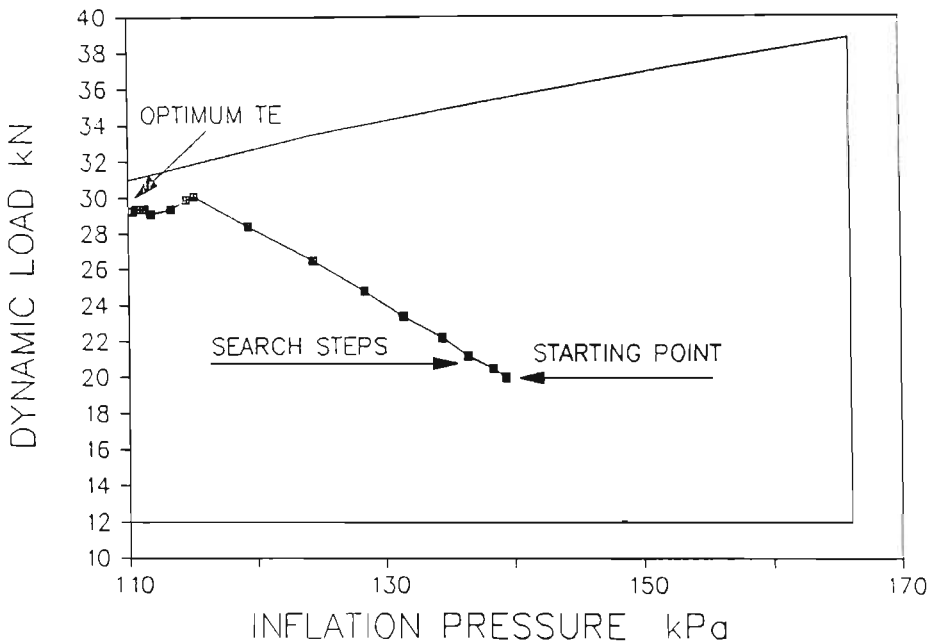

Figure C1 The steps taken to locate the optimum tractive efficiency during a 9kN test run.

Appendix D Penetrometer curves of the four soil conditions used for the evaluation tests.

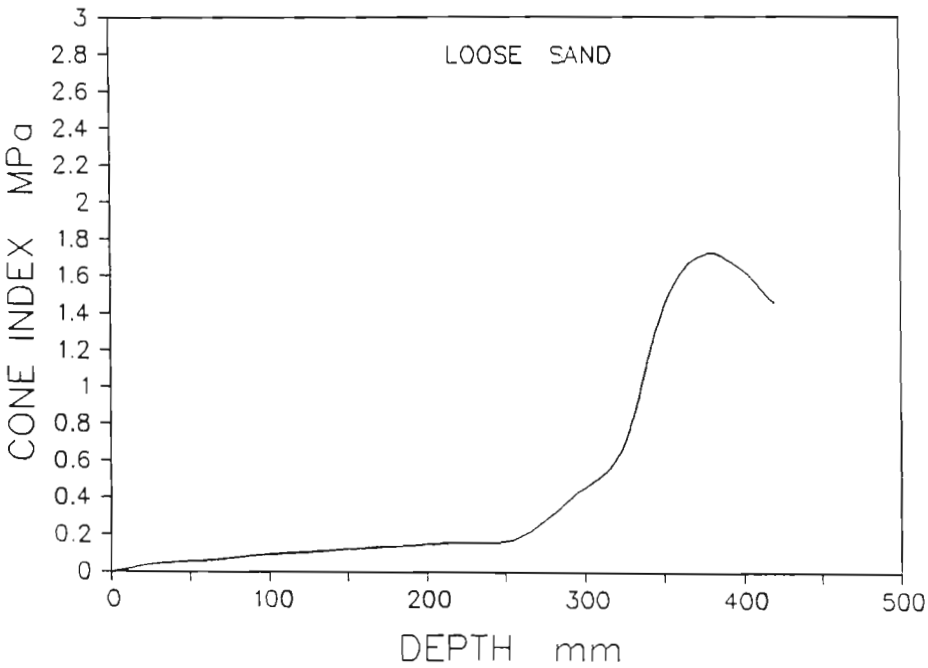

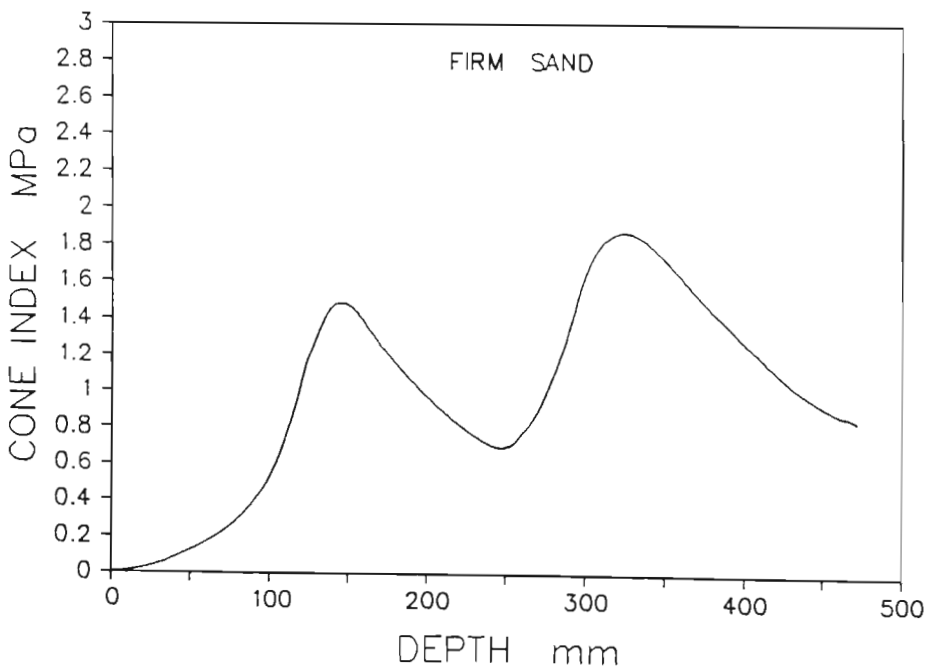

Figure D1 Average penetrometer curves for the Norfolk sandy loam soil in a loose and a firm condition.

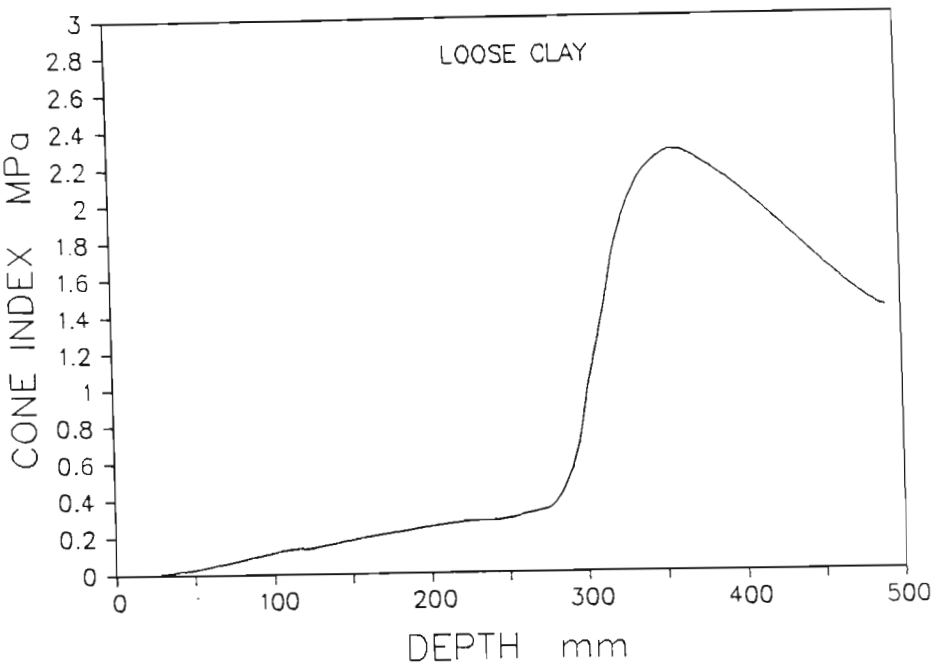

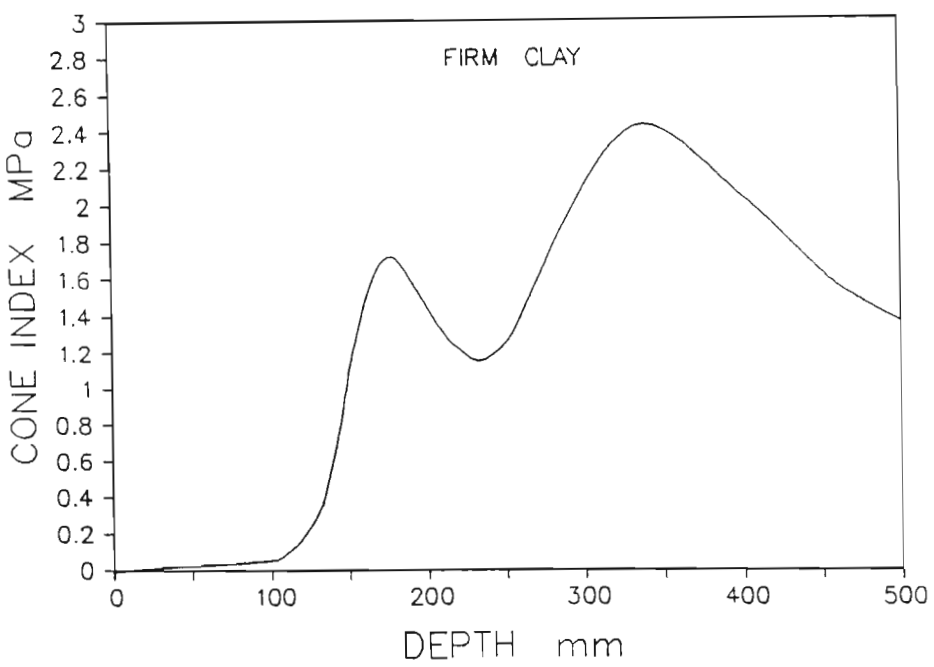

Figure D2 Average penetrometer curves for the Decatur clay loam soil in a loose and a firm condition.

Appendix E Test plans for the evaluation of the optimization routine.

Table E1 shows the test plan for the Norfolk sandy loam in a firm condition and Tables E2 and E3 show the test plans for the Decatur clay loam in a loose and firm condition respectively. The test code shown in Table E1 was used for all the tests.

Table E1 Test plan for the Norfolk sandy loam in a firm condition.

Soil: Norfolk sandy loam Fitting: Firm North				
Lane				
1 (1,27m)	2 (2,11m)	3 (2,95m)	4 (3,78m)	5 (4,62m)
F21121	F22031	F23091	F24061	F25122
F21092	F22032	F23094	F24062	F23123
F21RR1	F22063	F23033	F24093	F22063
		F23123		
South				

Test Code				
Fitting	Soil	Lane	NT	Rep
F S	1 2	1 2 3 4 5	03 06 09 12	1 2 3 P

Table E2 Test plan for the Decatur clay loam in a loose condition.

Soil: Decatur clay loam Fitting: Loose North				
Lane				
1 (1,27m)	2 (2,11m)	3 (2,95m)	4 (3,78m)	5 (4,62m)
S21066	S23065	S23064	S24092	S25093
S21RR1	S22091	S23122	S24123	S25063
S21062	S22032	S23061	S24033	S25121
S21062				
South				

Table E3 Test plan for the Decatur clay loam in a firm condition.

Soil: Decatur clay loam Fitting: Firm North				
Lane				
1 (1,27m)	2 (2,11m)	3 (2,95m)	4 (3,78m)	5 (4,62m)
F11129	F1212P	F13RR1	F14123	F15063
F11093	F12124	F13062	F14032	F15033
F11091	F12122	F13031	F14061	F15092
	F12121			
South				

Appendix F Summary of the estimated maximum TE and the measured TE at the estimated maximum TE point.

Table F1 Results for the test runs on a Norfolk sandy loam soil in a loose (S) and a firm (F) condition. The averages for the three replications and the percentage difference between the estimated and measured TE are also given.

Test	Maximum TE from				%	NT
Number	Regression	Avg.	Measured	Avg.	Diff.	kN
S13031	59		56		-5	
S14032	58	58,0	59	57,3	2	3
S15033	57		57		0	
S15061	58		61		5	
S11062	61	59,0	63	60,7	3	6
S15063	58		58		0	
S11091	64		65		2	
S14092	64	64,3	65	64,7	2	9
S12093	65		64		-2	
S12121	64		63		-2	
S13122	63	63,0	65	64,0	3	12
S14123	62		64		3	
F13031	66		66		-1	
F14032	67	65,3	63	63,8	-6	3
F15033	63		63		-0	
F14061	67		69		2	
F13062	68	66,8	65	66,7	-4	6
F15063	66		66		1	
F11091	74		71		-4	
F15092	69	72,4	66	70,0	-5	9
F11093	74		73		-2	
F12121	79		78		-1	
F14123	70	73,8	70	74,0	1	12
F12124	73		74		1	

Table F2 Results for the test runs on a Decatur clay loam soil in a loose (S) and a firm (F) condition. The averages for the three replications and the percentage difference between the estimated and measured TE are also given.

Test	Maximum TE from				%	NT
Number	Regression	Avg.	Measured	Avg.	Diff.	kN
S21031	63		60		-5	
S22032	64	63,7	62	61,3	-3	3
S24033	64		63		-2	
S25063	63		0			6
S23065	68	65,5	0	0,0		
S22091	65		65		0	
S24092	66	65,7	69	66,7	4	9
S25093	66		66		0	
S25121	66		65		-2	
S23122	68	67,0	67	66,0	-1	12
S24123	67		66		-2	
F22031	80		73		-9	
F22032	79	78,0	74	75,0	-6	3
F23033	75		77		3	
F24061	82		81		-1	
F24062	76	76,6	76	75,7	0	6
F22063	72		70		-3	
F21092	85		85		0	
F24093	76	78,6	75	77,3	-1	9
F23094	75		72		-4	
F21121	74		78		5	
F25122	81	76,7	78	76,3	-4	12
F23123	75		73		-3	